International PhD Program in Neuroscience

XXXIV Cycle

The Role of Lactate and Insulin – Like Growth Factor Binding Protein 6 in Glioblastoma Multiforme

---

PhD thesis

Lucia Longhitano

Coordinator: Prof. Claudio Bucolo

Tutor: Prof. Giovanni Li Volti

Department of Biomedical and Biotechnological Sciences

Section of Biochemistry

University of Catania – School of Medicine

2021

Al 13 marzo 2020, 12:03, che ha portato con sé
un pezzo del mio cuore
ma che allo stesso tempo
mi ha ridato la vita.
Ai miei due più grandi guerrieri...
... V & L

Ai miei genitori,
i miei angeli,
la mia salvezza.
Devo tutto questo a loro.
Devo tutto a loro...
... E & R.

A mia nonna,
alla compagnia che
ci siamo sempre fatto
fino alla fine...
... L

TABLE OF CONTENTS

RINGRAZIAMENTI

Non è la fine, ma l'inizio di qualcosa che sperò sarà bellissimo, come lo sono stati questi anni.

Grazie a chi ha permesso tutto questo, il mio tutor Prof. Giovanni Li Volti e il Prof. Daniele Tibullo. Credo sia doveroso, ancor prima di ringraziarvi, scusarmi con voi per non esser stata l'allieva modello che meritate, per tutte le volte che vi ho fatto perdere la pazienza.

Grazie Prof. Li Volti, per essere stato, oltre che un grande professore, un amico, un fratello ed un supporto. Grazie per avermi aiutata nei momenti peggiori, per avermi capita e per avermi trattata come una figlia. Grazie per essersi sempre dimostrato, prima che un professore, un grande uomo dal cuore immenso e con una bontà d'animo che pochi hanno.

Grazie Prof. Tibullo, per avermi guidata in tutto e per tutto. Grazie per avermi donato il tuo tempo, il tuo sapere e la tua esperienza, e per tutta la pazienza che hai avuto. Grazie per avermi insegnato il valore del lavoro di gruppo, e grazie per esser stato un fratello con il quale poter parlare, ridere, scherzare ed anche litigare.

Grazie ad entrambi per avermi fatto amare ancor di più questo lavoro e per avermi dato la possibilità di vivere tutto questo. "Da grande" vorrei essere anche solo l'1% di ciò che siete voi. Grazie per esser stati, e spero sarete, la mia seconda famiglia.
"La scelta di un giovane dipende dalla sua inclinazione, ma anche dalla fortuna di incontrare un grande maestro." (R. L. M.)

Grazie ai miei genitori, i miei angeli, per tutto ciò che mi hanno insegnato e per ciò che mi hanno messo a disposizione nel corso della vita permettendomi di arrivare fin qui.

Grazie Mamma, per essere il mio faro, la mia guida, la mia migliore amica e la mia miglior insegnante. Grazie per esser sempre stata la migliore, per avermi coccolata, "viziata" e aiutata in ogni istante.

Grazie Papà, il mio primo grande amore, il mio primo sostenitore, il mio punto di riferimento. Grazie anche a te per esser sempre stato il migliore, per aver sempre fatto il possibile e l'impossibile pur di esaudire ogni mia richiesta ed ogni mia necessità.

Grazie ad entrambi perché senza voi non sarei quella che sono, perché senza la vostra forza ed il vostro amore, oggi non sarei qui. Grazie per non avermi mai lasciata sola.

Grazie al guerriero più forte che io conosca, mio fratello.

Grazie per l'amore incondizionato, per la nostra vita insieme, per tutte le volte che abbiamo litigato, per tutte le volte che mi fai arrabbiare come nessun'altro al mondo. La vita ci ha messo alla prova, anzi ha provato a metterci con le spalle al muro, ma noi siamo sempre stati più forti di tutto. Grazie per aver sempre CAMMINATO al mio fianco.

LIST OF ABBREVIATIONS

AKT	Serine/Threonine Kinase
ALS	Acid Labile Subunit
AMPK	AMP-Activated Protein Kinase
ARG-1	Arginase-1
ATP	Adenosine Triphosphate
ATRX	Alpha thalassemia/X-linked Mental Retardation Syndrome
α-KG	α-Ketoglutarate
B7-H1	B7 Homolog 1
BCNU	1,3-bis (2-chloroethyl)-1-nitrosourea
CCL17	C-C Motif Chemokine Ligand 17
CCL2	C-C Motif Chemokine Ligand 2
CCL22	C-C Motif Chemokine Ligand 22
CCr2	C-C Motif Chemokine Receptor Type 2
Chi3l3	Chitinase 3 - like 3
CNS	Central Nervous System
CT	Computed Tomography
CX3CL1	C-X3-C Motif Chemokine Ligand 1
CX3CR1	C-X3-C Motif Chemokine Receptor 1
D-2-HG	D-2-Hydroxyglutarate
DC	Dendritic Cell
EEG	Multi-Channel Electroencephalogram
EGF	Epidermal Growth Factor
EGFR	Epidermal Growth Factor Receptor
EGR-1	Early Growth Response 1
ErbB2	Erb-B2 Receptor Tyrosine Kinase 2
FGF	Fibroblast Growth Factor
Fiz-1	FLT3 Interacting Zinc Finger 1
fMRI	Functional Magnetic Resonance Imaging
fNIRS	Functional Near Infrared Spectroscopy
G-CIMP	Glioma CpG-Island methylator Phenotype
GAM	Glioma-Associated Microglia
GBM	Glioblastoma Multiforme

GH	Somatotropic Hormone
GLS	Glutaminase
GPR81	G Protein-Coupled Receptor 81
GSCs	Glioblastoma Stem Cells
HCAR	Hydroxycarboxylic Acid Receptor
HIF-1α	Hypoxia Inducible Factor-1α
ICAM-1	Intracellular Adhesion Molecule 1
IDH	Isocitrate Dehydrogenase
IFNɣ	Interferon ɣ
IGF	Insulin-like Growth Factor
IGF-1R	Insulin-like Growth Factor 1 Receptor
IGF-2R	Insulin-like Growth Factor 2 Receptor
IGFBPs	Insulin-like Growth Factor Binding Proteins
IL-10	Interleukin-10
IL-12	Interleukin-12
IL-13	Interleukin-13
IL-1β	Interleukin-1β
IL-1β	Interleukin-1 β
IL-4	Interleukin-4
IL-6	Interleukin-6
IL-8	Interleukin-8
iNOS	Inducible Nitric Oxide Synthase
KRAS	Kirsten's Rat Sarcoma
LDHA	Lactate Dehydrogenase A
LDHB	Lactate Dehydrogenase B
LMP-1	LIM Mineralization Protein-1
LOH	Loss of Heterozygosity
M-CSF	Macrophage Colony-Stimulating Factor
MAPK	Mitogen-Activated Protein Kinase
MCTs	Monocarboxylate Transporters
MDSC	Myeloid-Derived Suppressor Cells
MEG	Magnetoencephalography
MEG	Malic Enzyme
MGMT	O-6-Methylguanine-DNA Methyltransferase
MIF	Macrophage Inhibitory Factor

MMP-2	Matrix Metalloproteinase-2
MMP-9	Matrix Metalloproteinase-9
Mrc1	Mannose Receptor C-Type 1
MRI	Magnetic Resonance Imaging
MT1-MMP	Type 1 Membrane Metalloprotease
NADP+	Nicotinamide Adenine Dinucleotide Phosphate
NADPH	Nicotinamide Adenine Dinucleotide Phosphate
NF1	Neurofibromatosis Type 1
NK	Natural Killer
NKT	Natural Killer T
NLS	Nuclear Localization Sequence
NMR	Nuclear Magnetic Resonance
NO	Nitric Oxide
NRP1	Neuropilin 1
OAA	Oxaloacetate
OXPHOS	Oxidative Phosphorylation
PDGFR	Platelet-Derived Growth Factor Receptor
PET	Positron Emission Tomography
PGE2	Prostaglandin E2
Phb-2	Prohibitin 2
PI3KA	Phosphoinositol 3 Kinase A
PPP	Pentose Phosphate
PTEN	Phosphatase and tensin homolog
PTN	Pleiotrophin
PTPRZ1	Protein Tyrosine Phosphatase Receptor Type Z1
RAF	Rapidly Accelerated Fibrosarcoma
ROS	Reactive Oxygen Species
RT	Radiotherapy
RTK	Receptor Tyrosine Kinases
RTK	Tyrosine Kinase Receptor
SLC	Solute Transporter
Socs2	Suppressor of Cytokine Signaling 2
SPECT	single-photon emission computerized tomography
STAT-3	Signal Transducer and Activator of Transcription 3
STI1	Cochaperone Stress Inducible Factor 1

TAM	Tumor-Associated Macrophages
TCA	Tricarboxylic Acid
TGFβ	Transforming Growth Factor-β
TIL	Tumor Lymphocytes
TKI	Tyrosine Kinase Inhibitor
TLRs	Toll-Like Receptors
TM	Transmembrane
TME	Tumor Microenvironment
TMZ	Temozolomide
TNFα	Tumor Necrosis Factor-α
TP53	Tumor Protein p53
VEGF	Vascular Endothelial Growth Factor
Wnt	Wingless-related Integration Site

ABSTRACT

Glioblastoma Multiforme (GBM) is the most common and most malignant primary brain tumor of the Central Nervous System (CNS) in the adults. It represents half of the newly diagnosed gliomas, and despite the aggressive therapeutic regimen, the median patient survival is about only 14-17 months after diagnosis. Tumor microenvironment (TME) plays a pivotal role in establishing malignancy and it is associated with high glycolytic metabolism and increased lactate production, which accumulates in the TME through monocarboxylate transporters (MCT1-4) modulating tissue metabolic activity through proton-coupled transport of monocarboxylates, specifically L-lactate, ketone bodies, and pyruvate. However, lactate can act as both a metabolite and a signal molecule through the activation of its GPR81 receptor, encoded by the HCAR1 gene. In the first part of the PhD project, we investigated the role of lactate in GBM progression and metabolic reprogramming both *in vitro* and in an *in vivo* model. The *in vitro* study was carried out in three human glioblastoma cell lines treated with lactate (20 mM) and 3,5-dihydroxybenzoic acid (150 µM), a well-established pharmacological lactate receptor agonist. Cell proliferation, migration, colony formation capacity, and the expression of genes involved in mitochondrial metabolism were evaluated. Lactate metabolism was assessed by the expression of its transporters MCT1 and MCT4, and GRP81. The results were validated in patient-derived GBM biopsies, by comparing MCT1 expression in high (H-) versus low (L-) proliferative index (PI) GBM samples. The in vivo study was carried out in a zebrafish model of GBM,

and the energy phenotype was assessed by Seahorse XFp, gene expression was evaluated by NGS sequencing, qPCR analysis and immunofluorescence. Effects of 20 mM lactate exposure on proliferation of developing brain tumors was assessed by counting phospho-histone 3 positive cells. Our results show that lactate significantly increased cell proliferation, migration, and colony formation capacity of GBM cells, both *in vitro* and *in vivo*. We also found that cells respond to high levels of extracellular lactate increasing MCT1 transporter expression in all three cell lines. In a Zebrafish model of GBM, altered metabolism and increased expression of MCT1 and GPR81 generate high levels of extracellular lactate, which in turn supports increased proliferation of tumor cells. Interestingly, 3,5-DHBA stimulation was able to increase significantly MCT1 in all tested cell lines. Furthermore, our results showed that both lactate and 3,5-DHBA exposure induced a significant increase in the expression levels of tested genes, confirming that lactate is involved in the metabolic switch of GMB cell lines. Finally, immunohistochemistry analysis on GBM biopsies demonstrated that High-PI GBM showed a significant increase in MCT1 and Ki67 expression levels when compared to Low-PI GBM. Furthermore, lactic acidosis has been reported in various solid TME including GBM. In particular, in TME various signaling molecules, growth factors and metabolites have been identified in sustaining GBM immune escape and inducing resistance to chemotherapy. During the early phases of the disease, microglia infiltrate TME thus contributing to tumorigenesis. Among various growth factors, insulin-like growth factor binding protein 6 (IGFBP6), an inhibitor of IGF-II actions, has been reported to play an important role in survival and migration of tumor cells, but its effects on

tumor and immune system interaction is still poorly understood. Thus, in the second part of the PhD project we studied the crosstalk between lactate and IGFBP6 in microglial cells and how such interaction modulates TME and GBM progression. We tested our hypothesis in three human glioblastoma cell lines (i.e. U87-MG, A172 and U251) and a human microglia cell line (HMC3) treated with lactate (20 mM) and/or with IGFBP6 (400 ng/mL). Cell proliferation, migration and colony formation capacity were evaluated respectively by Xcelligence technology, clonogenic and wound healing assay. We also evaluated the expression of IGFBP6 mRNA levels of GBM cells and microglia cells treated with lactate. To further confirm the possible existence of a lactate-IGFBP6 axis, we evaluated the effect of lactate, IGFBP6 and the conditioned medium of IGFBP6 pre-treated GBM cells on microglia by immunocytochemical analyzes and RT-PCR to assess a potential M2 anti-inflammatory phenotype shift. Our results showed that microglia exposed to lactate significantly increased mRNA and protein expression of MCT1, and genes involved in mitochondrial metabolism. We also showed an increase in the M2 marker, Arg-1, and a reduction of iNOS suggestive of an M1-proinflammatory state. Furthermore, lactate treatment in microglia cells, induced a significant increase in IGFBP6 expression. Consistently, IGFBP6 treated GBM cells showed a significant increase in cell proliferation, migration, and colony formation capacity. Interestingly, our data showed that IGFBP6 treatment also resulted in an increase in marker M2, Arg-1, and a reduction of iNOS expression levels. These results were further confirmed by evaluating the expression of mRNA levels of M1 and M2 markers on microglia cells cultured with conditioned media from IGFBP6 pre-treated GBM cells.

Finally, our results were further confirmed in patient-derived GBM biopsies and by transcriptome analysis. In conclusions, our results suggest that lactate and its transporter (MCT1) and receptor (GPR81) play a major role in GBM proliferation and migration, and it may represent a potential target to develop new strategies to counteract tumor progression and recurrencies and that there is a crosstalk lactate/IGFBP6 in microglial cells and that this relationship modulate TME impacting on tumor progression and resistance to therapy.

GLIOBLASTOMA MULTIFORME

General Introduction

Gliomas are a heterogeneous group of neoplasms that differ in localization within the central nervous system [1]. The growth potential, the extent of invasiveness, the morphological characteristics, the tendency to progress and the response to treatments vary according to the diagnosed cases. Furthermore, gliomas are classified according to their presumed cell of origin [2]. These include astrocytic tumors (astrocytoma, anaplastic astrocytoma and glioblastoma), oligodendrogliomas, ependymomas and mixed gliomas. [3–6]. They are the most common central nervous system (CNS) tumors, accounting for nearly 80% of all primary malignant brain tumors [5–7].

Glioblastoma multiforme (GBM) is the most common of the gliomas [8]. GBMs can arise de novo in the brain or evolve from a lower-grade astrocytoma and in adults, GBM most often occurs in the cerebral hemispheres, particularly the frontal and temporal lobes of the brain [9]. All GBM tumors present abnormal and numerous blood vessels, a common feature of a rapidly growing tumor. These blood vessels provide the oxygen and nutrients needed by tumors, helping them to grow and spread. Additionally, these blood vessels easily integrate with normal brain tissue and move away from the main tumor making GBM tumors a challenge to treat. In addition, several features including localization of tumors in the brain, resistance to therapy, migration of cancer cells to adjacent brain tissue, variously disrupted blood supply to the tumor which inhibits effective drug delivery, loss tumor capillary with consequent accumulation of fluid around the tumor (peritumoral edema) and intracranial hypertension also contribute to GBM therapy. Therefore, despite the

variety of modern GBM therapies, it is still a fatal disease with an extremely poor prognosis. Patients usually have a median survival of approximately 14-15 months from diagnosis [2,10,11].

Epidemiology

GBM is a rare tumor with an overall incidence of less than 10 per 100.000 people; despite this, the prognosis is poor with an average survival rate of only 14-15 months from diagnosis and this still makes it a crucial public health problem [11,12]. It accounts for about 50-60% of all gliomas [13] and can occur at any age, but the greatest incidence occurs between 55 and 60 years of age [14]. They are also the cause of 2.5% of cancer deaths and are the third leading cause of cancer deaths in people aged 15 to 34 [15,16]. The Western world has a higher incidence of gliomas than less developed countries [11], which may be due to poor reporting of gliomas,

limited access to health care, and differences in diagnostic practices [2,5]. Few studies have shown that blacks are less prone and the incidence of GBM is higher in other ethnic groups, including Asians, Latinos and whites [12] (Figure 1).

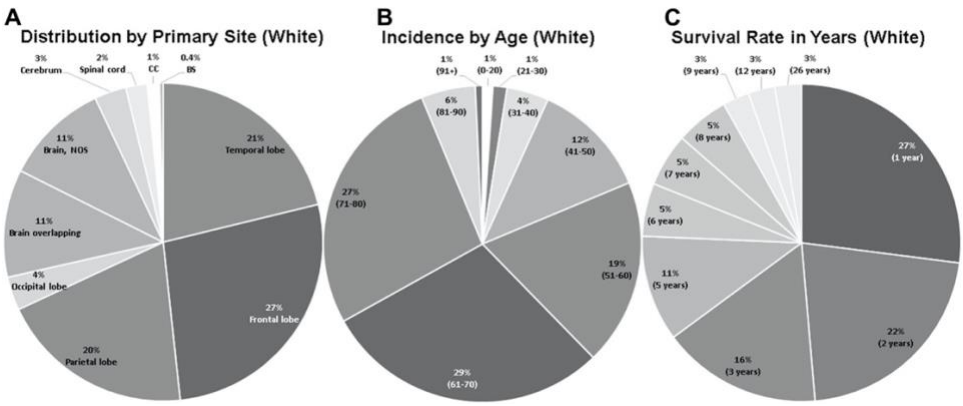

Figure 1. **Distribution, prevalence, and survival among white patients diagnosed with glioblastoma**. (**A**) Tumor site; (**B**) Prevalence by age. (**C**) Survival in years since first diagnosed. (Nizamutdinov, Damir et al. "Prognostication of Survival Outcomes in Patients Diagnosed with Glioblastoma." World neurosurgery vol. 109 (2018): e67-e74. doi:10.1016/j.wneu.2017.09.104).

Etiology

The etiology of brain tumors is still unclear, and the underlying cancerous causes cannot be identified. Glioblastoma is thought to be a spontaneous tumor [17]. The familial form of this tumor is described in 1% of cases [5]. To date, the only confirmed risk factor is exposure to high-dose ionizing radiation [5,18] and it has been estimated that the risk of developing GBM at the follow-up of radiotherapy it is about 2.5% [19]. Glioblastoma multiforme can also occur in the course of genetic diseases: tuberous sclerosis [19], Turcot syndrome [20], multiple endocrine neoplasms of type IIA [21] and type I neurofibromatosis, NF1 [18,22,23]. Additionally, a 2003 study found that patients with acute lymphoid leukemia who received treatment were more prone to developing GBM and this could result from both leukemia and the use of chemotherapeutic agents [19].

Classification

The World Health Organization (WHO) since 1993 has proposed a classification system that divides brain tumors into 4 subgroups [24], based on the characteristics of anaplasia or the presence of nuclear atypia, mitosis, endothelial proliferation and necrosis. The 2016 World Health Organization (WHO) classification of central nervous system (CNS) tumors is contained in a version of the 2007 classification, rather than a new version [25].

According to the parameters mentioned above, CNS tumors are classified into four grades (Table 1):

Table 1. **Brain tumor classification system developed by the World Health Organization (WHO)**.
(http://www.neurosurgeryindia.co.in/mobile/109890braintumors.html).

World Health Organization (WHO) Brain Tumor Grades			
	Grade	**Characteristics**	**Tumor Types**
Low Grade	**WHO Grade I**	• Least malignant (benign) • Possibly curable via surgery alone • Non-infiltrative • Long-term survival • Slow growing	Pilocytic astrocytoma Craniopharyngioma Gangliocytoma Ganglioglioma
	WHO Grade II	• Relatively slow growing • Somewhat infiltrative • May recur as higher grade	"Diffuse" Astrocytoma Pineocytoma Pure oligodendroglioma
High Grade	**WHO Grade III**	• Malignant • Infiltrative • Tend to recur as higher grade	Anaplastic astrocytoma Anaplastic ependymoma Anaplastic oligodendroglioma
	WHO Grade IV	• Most malignant • Rapid growth, agressive • Widely infiltrative • Rapid recurrence • Necrosis prone	Gliobastoma Multiforme (GBM) Pineoblastoma Medulloblastoma Ependymoblastoma

- **Grade I**: Tumors do not meet any of the criteria. These tumors are slow-growing, non-malignant and associated with long-term survival [25].
- **Grade II**: tumors meet only one criterion, namely cytological atypia only. These tumors are slow growing but recur as higher-grade tumors. They can be malignant or non-malignant [25].
- **Grade III**: Tumors meet two criteria, namely anaplasia and mitotic activity. These tumors are malignant and often recur as higher grade tumors [25].
- **Grade IV**: Tumors meet three or four of the criteria, ie show anaplasia, mitotic activity with microvascular proliferation and / or necrosis. These tumors reproduce rapidly and are very aggressive malignant tumors [25].

Brain tumors are also classified according to the cell of the nervous system from which they derive and from which they are named. The main types are gliomas, pituitary adenomas, meningiomas, ependymomas, medulloblastomas, neuromas and primary central nervous system lymphomas [26]. Gliomas are the most common and represent about 40% of all primary brain tumors [27]. Histologically, they share the characteristics of normal glial cells and are generally named based on these similarities [28]. The most common types of gliomas are [28]:

- Astrocytomas
- Oligodendrogliomas
- Ependymomas
- Glioblastoma multiforme

The most common classification divides gliomas according to the degree of aggressiveness (Figure 2):

- **Grade I**: pilocytic astrocytoma, more frequent in young age also in the cerebellum [29,30]
- **Grade II**: diffuse astrocytoma, oligodendroglioma, oligoastrocytoma, ependymoma
- **Grade III**: anaplastic astrocytoma, oligodendroglioma or anaplastic oligoastrocytoma [31];
- **Grade IV**: glioblastoma multiforme, gliosarcoma [32].

Another type of classification is based on the molecular characteristics of the tumor; in fact, although morphologically identical, different glioblastoma tumors result in different clinical outcomes and this can be partially explained by different tumor molecular fingerprints [11,33,34]. Numerous genetic and epigenetic alterations have been identified in gliomas [35–37]. The most commonly altered signaling pathways are RTK/RAS/MAPK/PI3KA [38,39]. Primary glioblastomas are characterized by EGFR amplification, PTEN mutation and absence of IDH mutations, while

secondary glioblastomas are characterized by TP53 mutations, IDH mutations and lack of EGFR amplification [35,40]. However, none of these alterations is sufficiently specific to distinguish between primary and secondary GBMs. Recently Jiao et al described ATRX (Alpha thalassemia/X-linked Mental Retardation Syndrome) mutations in diffuse glioma associated with alternative telomere elongation [35].

The most clinically relevant genetic alterations are:

-*Isocitrate dehydrogenase (IDH) mutations.* The determination of isocitrate dehydroarenes 1 or 2 (IDH 1/2) status represents the first layer of the molecular diagnosis, and IDH1-R132H (G395A) is most common mutation (~ 90%) [41]; mutated IDH proteins converts α-ketoglutarate (α-KG) into D-2-hydroxyglutarate (D-2-HG) [42] which in turn acts as a competitive inhibitor of α-KG-dependent dioxygenase, including some DNA and histone demethylases [43]. This inhibition increases DNA and histone methylation leading to the

hypermethylation of CpG islands and glioma phenotype known as "glioma CpG-island methylator phenotype" (G-CIMP) [44–46]. The mutated IDH-R132H protein might be a potential target for drug development. And as shown by Olar A [33] the absence of IDH1-R132H protein expression in no enhancing diffuse glioma of older adults (> 50 years of age) predicted rapid progression (in less than a year) to glioblastoma;

-*1p/19q co-deletion*. This co-deletion defines oligodendrogliomas and is used as a biomarker to predict benefit from radiotherapy and chemotherapy with procarbazine and vincristine compared to radiotherapy alone in patients with anaplastic gliomas [47]. Combined loss of heterozygosity (LOH) on 1p and 19q is strongly correlated with classic oligodendroglioma morphology and associated with a proneural profile [36,48], IDH mutations [49–53], G-CIMP phenotype [45,54,55], increased MGMT promoter

methylation [54,56–58], and is also predictive of response to chemotherapy [40,59];

-*Epidermal growth factor receptor (EGFR) amplification*. EGFR amplification is a characteristic signature of the TCGA classical glioblastoma subtype [36] and of the Phillips proliferative and mesenchymal glioblastoma subtypes [40,60];

-*O-6-methylguanine-DNA methyltransferase (MGMT) promoter methylation status*. O6-methylguanine-DNA methyltransferase (MGMT) is a DNA repair protein which repairs DNA alkylation induces by alkylating agents like temozolomide (TMZ) [40,61–63]. Methylated CpG sites bind specific proteins, this complex causing altered chromatin structure and loss of transcription (MGMT silencing), ultimately interfering with DNA repair [64]. Interestingly, several studies showed that in glioblastoma MGMT methylation status does not correlate with the EGFR amplification status or IDH, TP53 mutation [65].

Based on this classification, glioblastomas are divided into two categories based on their IDH status: IDH-wild-type and IDH-mutant glioblastomas [66]. Wild-type IDH glioblastomas represent approximately 90% of cases, and clinically correspond to primary glioblastomas with a predominance in patients over 50 years of age [67]. IDH mutant glioblastomas account for approximately 10% and are related to secondary glioblastomas [68,69] (Figure 2).

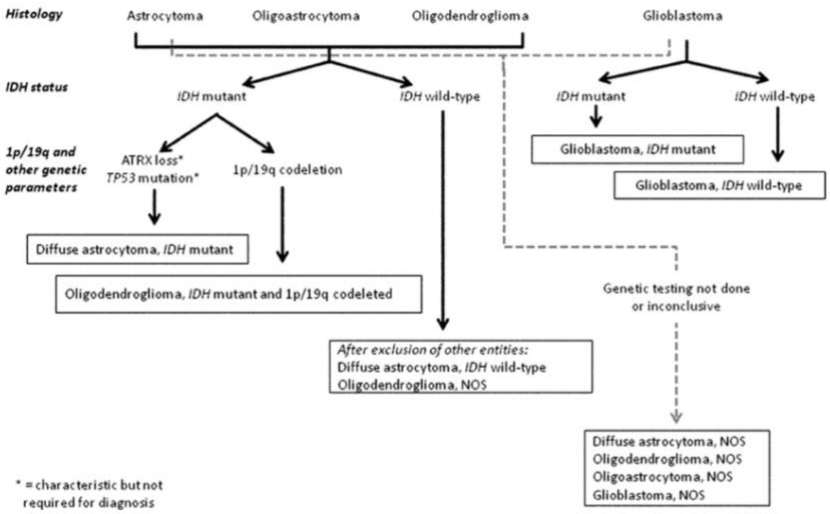

Figure 2. **Classification of the diffuse gliomas based on histological and genetic features**. (Louis, D.N., Perry, A., Reifenberger, G. et al. The 2016 World Health Organization Classification of Tumors of the Central Nervous System: a summary. Acta Neuropathol 131, 803–820 (2016). https://doi.org/10.1007/s00401-016-1545-1)

Morphological characteristics

GBM has typical features of malignant tumors such as the presence of atypical cells, nuclear hyperchromasia, increased mitotic figures, angiogenesis and necrotic areas [70]. GBM cells are spindle-shaped polygonal with acidophilic cytoplasm and indistinct cell edges [71]. In aggressive malignancies such as GBM, the vascularization is often excessive and facilitates tumor progression [70]. One of the most important features of GBM are necrotic foci which are distinguished according to the location and size of the necrotic area, surrounded by pseudopalized areas created by radially oriented glial cells observed in both primary and secondary glioblastomas [71–73]. Cells with a "pseudo-palisade" contour around central degeneration have long been recognized as both a distinctive feature of GBM and as a morphological finding that predicts aggressive behavior [74]. These cells are severely hypoxic in which hypoxia-induced factor-1 (HIF-1) is over-expressed and

secrete pro-angiogenic factors, such as vascular endothelial growth factor (VEGF) and interleukin 8 (IL-8) [75]. The micro-vascular hyperplasia that emerges in response promotes peripheral tumor expansion [76].

Among the various morphological alterations, angiogenesis is the key event in the progression of glioblastoma, in fact, among all solid tumors, glioblastoma multiforme has the highest degree of vascular proliferation and hyperplasia of endothelial cells [77,78]. The term angiogenesis refers to the formation of new blood vessels starting from a pre-existing circulatory network and also represents the key event in the progression of malignant gliomas [79,80]. VEGF is the main actor in the angiogenesis mechanism and plays a strategic role in the proliferation and migration of cancer cells, with a significant impact on survival and clinical outcome [81–83]. The process that leads to the vascular phase of the tumor is hypoxia which occurs when the tumor mass grows beyond the diameter of 1 mm [79].

Genetic and Molecular Pathogenesis

The activation of oncogenic factors and the inactivation of tumour suppressor factors combine to create one of the most aggressive tumours [84,85]. The amplification of oncogenes such as EGFR [86], as well as the loss of tumour suppressors such as PTEN on chromosome 10 [87] and p53 on chromosome 17 [88] are some of the most common genetic alterations in GBM (Table 2).

Table 2. Most common mutations in glioblastoma (From: Shahid Hussain Soomro, Li Rui Ting , Yang Yi Qing and Mingxin Ren. *Molecular biology of glioblastoma: Classification and mutational locations*. J Pak Med Assoc. 2017 Sep;67(9):1410-1414.)

Genetic alterations	Primary Glioblastoma (%)	Secondary Glioblastoma (%)
LOH 10q Mutation[8]	70	63
EGFR Amplification[8]	35	8
TP53 Mutation[8]	30	65
PTEN Mutation[8]	25	4
IDH Mutation[18]	5	80
MGMT promoter methylation[22]	42	79

GBM has a very complex pathogenesis involving mutations and alterations of several key cellular pathways involved in cell proliferation, survival, migration, and angiogenesis [38]. Genetic alterations have recently been discovered in the IDH genes, which code for isocitrate dehydrogenase 1 (IDH1) and 2 (IDH2) [89]. These are enzymes involved in the citric acid cycle that catalyze the oxidative decarboxylation of isocitrate to α-ketoglutarate while reducing $NADP^+$ to NADPH [90,91]. Although IDH1 is found within the cytoplasm and peroxisomes, IDH2 and IDH3 are located exclusively in the mitochondria [92]. IDH1 alterations are present in the secondary GBM but are rarely found in the primary GBM [93]; this difference made it possible to discriminate between these two types of tumour [94]. IDH1 mutation occurs early in glioma progression, with IDH1 amino acid residue R132 mutations identified in most (> 70%) grade II and III astrocytoma and oligodendrogliomas, as well as secondary GBMs that develop from

these lesions lower grade [35,93,95]. Furthermore, IDH2 mutation analysis revealed recurrent mutations of residual IDH2 R172 [96], with most mutations occurring in tumours lacking IDH1 mutations [93]. Epigenetic silencing of the O6-methylguanine methyltransferase (MGMT) gene by promoter methylation impairs DNA repair [63,97]. MGMT is the preferred point of attack for many carcinogens (e.g. Methylnitrosourea) and alkylating chemotherapeutic agents (e.g. BCNU, temozolomide, etc.) [97]. Hypermethylation of the CpG island located in the MGMT promoter region is primarily responsible for the loss of MGMT function in many tumour types [97,98].

It is known that cancer cells become cancerous due to the accumulation of mutations that lead to the activation of oncogenes and/or the inactivation of tumour suppressor genes [99–101]. In this way they escape the normal cell cycle regulation processes, proliferating indefinitely and uncontrollably.

Different genetic aberrations have been identified in GBM cells, some of which are present exclusively in either primary glioblastoma or secondary glioblastoma.

One of the first mutated oncogenes in GBM that has been identified is EGFR, the gene encoding the epidermal growth factor membrane receptor. This receptor, responding to its ligand, produces a signal of induction to mitosis. Since its discovery, many studies have analyzed aberrations on this gene and constant amplification of the gene has been found in GBM cells. However, it is still unclear whether this aberration is associated with longer or shorter patient survival [102].

ErbB2 belongs to the same family of receptors and several somatic mutations on the corresponding gene have been found in glioblastoma [103].

The TP53 gene, located on chromosome 17, is also particularly altered in GBM. The p53 protein is a transcription factor involved in

cell cycle regulation, DNA repair and integrity [104]. The goal of the activity of this protein is to counteract the proliferation of aberrant cells; in the first instance, in fact, it attempts to repair the damage to the DNA, but if this does not work, cell death is induced through the process of apoptosis [105]. Many alterations on TP53 are point mutations leading to amino acid substitution; the most frequent is G: C A: T on CpG islands [14]. Mutations on this gene lead to the expression of an abnormal protein or to its down regulation.

In secondary GBM, 57% of mutations are found in codons 248 and 273, while in primary GBM point mutations are more evenly distributed in the various exons [102].

Some hereditary syndromes can predispose to the risk of brain tumour, such as Li-Fraumeni syndrome: it is an autosomal dominant disease with a germline mutation on the TP53 gene and is characterized by multiple primary neoplasms, especially in children and young people [14]. Approximately 14% of neoplasms in families

with germline TP53 mutations are brain tumours and astrocytoma are predominant [106].

Another gene mutated in glioblastoma (especially primary) is PTEN, which expresses a protein that is part of a system that sends a stop signal to cell division, forcing the cells to undergo apoptosis. Deletion of this kind is frequent [107] even if the methylation of the promoter seems to be an alternative mechanism for the loss of PTEN expression [102].

Somatic mutations in the NF1 gene have been found in a few glioblastomas [108]. NF1 (Neurofibromatosis type 1) is an autosomal dominant disease characterized by neurofibromas, optic nerve gliomas, and other astrocytoma [109]. The gene normally encodes the neurofibromin protein which has a negative activity on the p21ras oncogene: therefore, the NF1 gene can be considered a tumour suppressor [110]. Mutations in this gene induce, therefore, a

cellular hyperproliferation with consequent formation of neurofibromas, glioblastomas and astrocytoma [14].

The mutations listed above often coexist within the same cell, making the therapeutic approach that aims to counter the tumour mechanism more complex.

Clinical presentation

As is the case with several types of brain tumors, the most common initial symptom of glioblastoma multiforme is headache. Since symptoms are often caused by the pressure of the tumor against adjacent brain structures, these can vary depending on the location of the tumor in the brain. They generally develop very quickly and as soon as the tumor sets in; however, in some cases, they appear when the disease has reached a very advanced stage. Symptoms of GBM include [2,111–113]:

- Nausea and vomiting (especially upon awakening)
- Seizures
- Tiredness and weakness
- Memory problems (amnesia etc.). They usually occur when the glioblastoma resides in the temporal lobe.
- Anomalies of the neuro-endocrine system. They occur in children, when glioblastoma has formed near the hypothalamus, pituitary, or epiphysis endocrine glands.
- Dizziness

Glioblastoma has a high infiltrative power, as it easily invades neighboring areas, reaches the meninges and/or spreads its cells in the cerebrospinal fluid [114]. It develops rapidly and its effects are devastating: without treatment, death occurs on average within 4 and a half months, due to cerebral edema and or to the increase beyond all limits of intracranial pressure [12]. Despite their very high malignancy, glioblastomas rarely spread to other parts of the

body: generally, they act exclusively at the level of the central nervous system.

Diagnosis

One of the main problems of glioblastoma management is related to the lack of effective diagnostic strategies [115]. Currently, the main diagnostic methods for the detection of gliomas are based on neurological tests and neuroimaging methods [15]. The definitive diagnosis is based on the histopathological examination of the tumor removed during surgery, using traditional histological, cytological and histochemical methods [116]. The formation of new blood vessels, or angiogenesis, is critical for the growth of malignant brain tumors [117]. Malignant gliomas with high neovascularization or vascular permeability are often associated with higher proliferation rates [118] and a higher degree of aggression. Due to this association, imaging techniques aimed at identifying abnormal vascularity or vascular permeability, including contrast computed tomography

(CT) and magnetic resonance imaging (MRI) are commonly used for diagnosis and clinical management of brain tumors [119]. Recent advances in imaging techniques and particularly MRI in recent years have also helped evaluate changes in tissue architecture and cellular metabolism of gliomas [2]. Neuroimaging remains the primary monitoring tool for glioblastoma, with assessments typically performed every 2-3 months during treatment [120].

Therapy

The goal of glioblastoma treatment is to slow and control tumor growth and help to live as comfortably and as well as possible. High grade glioma are very difficult tumors to treat due to the problems in completely removing the tumor and their resistance to radiotherapy and chemotherapy [121]. As there is no ideal treatment, patients are often treated on clinical trials investigating

new therapies [122]. Therefore, the treatment of patients with malignant gliomas remains palliative and encompasses surgery, radiotherapy, and chemotherapy [123].

The first treatment choice for accessible tumors is surgery. Accessible tumors are those that can be operated on without a high risk of causing severe neurological damage [124]. Depending on the tumor type surgery can accomplish many things including reduction of tumor burden, control seizures, reversal of neurological deficit, introduction of local therapeutic agent and improve quality of life [125]. The goal of surgery is to achieve gross total resection of the contrast enhancing component of the tumor, without compromising neurological function [126]. Radical resection may not be possible based on anatomic structures involved and the extent of surgical resection depends upon the site of the brain area involved [12,127].

Surgical treatment can be followed by radiotherapy (RT) to kill remaining tumor cells. Studies have shown that people live

longer when given the combination of surgery and radiation therapy compared with surgery alone [128]. Standard RT is delivered in 1.8-2 Gy fraction to a total dose of 54-60 Gy. A valid option for older patients or patients with limited life expectancy is a hypo-fractionated RT with a biologically equivalent dose of 40 Gy distributed in 15 fractions of 2.67 Gy [129]. If tumor exhibits MGMT promoter methylation or in case of elderly patients, the RT can be rejected, and temozolomide is administrated alone [130]. Several limitation and risk factors are associated with radiation therapy including the invasive nature of GBM, radiation necrosis, radiation-induced permanent neuronal damage, and radio-resistance of some tumors [12].

Temozolomide (TMZ) is the only standard chemotherapy for patients with GBM [131]. TMZ is a cytotoxic alkylating agent and the principal mechanism responsible for the cytotoxicity of TMZ is to methylate DNA at the N7 and O6 position on guanine which leads to

the failure of DNA miss match repair system to find a complementary base for methylated guanine thus resulting in long live nicks in DNA and consequently blocks the cell cycle at the G2-M boundary and triggers apoptosis [132]. Oral administration of TMZ, as adjuvant or concomitant with radiotherapy is becoming standard of care for patients of GBM, [133] and in 2005, a clinical trial demonstrated that concurrent RT and TMZ followed by adjuvant TMZ significantly prolonged the median survival more than that of radiation alone (14.6 months versus 12.1 months) [122]. At the 5-year analysis of this study, more patients treated with TMZ were alive [134]. These findings established the therapeutic benefit of TMZ in combination with RT, establishing the so-called "Stupp regimen" standard of care for GBM treatment [134,135]. Despite these advances, the median progression-free survival time is only 7 months [136]. However, it has been reported that high levels of Methyl Guanine Methyl Transferase (MGMT) activity in tumor cells is associated with poor

temozolomide response [62]. MGMT is a critical DNA repair protein that protects tumor cells against alkylating chemotherapeutic agents.

Other therapeutic strategies for GBM are molecularly targeted therapies designed to target tumor-specific recurrent genetic alterations as a novel approach to treating GBM, these include anti-angiogenic agents such as anti-VEGF monoclonal antibodies (Bevacizumab), anti -FGF, EGFR targeted monoclonal antibodies (Erlotinib and Gefitinib) and tyrosine kinase inhibitors

TUMOR MICROENVIRONMENT

Despite the aggressive therapeutic regimen described above, the median survival of patients with GBM remains only 15/17 months. This is mainly due to tumor-induced immunosuppression, which occurs through various mechanisms that create a complex network of mediators and cells that together limit the effectiveness of the therapy. In this process TME plays a fundamental role contributing to the heterogeneity of the tumor [137], and is strongly immunosuppressive since it contains different types of cells in addition to tumor cells, such as stromal cells, infiltrating inflammatory cells, immune cells, including microglia , endothelial cells, components of the extracellular matrix, which reprogram their metabolism according to the energy demand of the cancer cells [138]. The tumor microenvironment is, therefore, a unique environment that emerges during the progression of the tumor as a

result of the interaction with the host, and is dominated and modeled by the tumor to meet its energy demand [139]. TME is also composed of a complex network of cytokines, chemokines, growth factors and inflammatory and matrix remodeling enzymes [140].

TME promotes immune escape and tumor progression via the interaction between tumor cells and different cell populations which in turn influences tumor resistance, progression and metastasis [141].

Over the years, many studies have focused on understanding the various mechanisms responsible for immunosurveillance and immunosuppression.

It has been shown that inflammatory cytokines are present within TME including tumor necrosis factor-α (TNF-α), IL-6 and IL-8, which are often over-expressed and this promotes invasive properties of the tumor, such as angiogenesis and metastases [142,143]; but also cytokines such as IL-4, IL-13 and IL-10 which

promote an anti-inflammatory environment with consequent suppression of the adaptive immune response [144].

TME is also rich in immunosuppressive cells, a mixture of tumor-associated leukocytes, which are made up of myeloid cells, predominantly MDSC, macrophages and neutrophils at various stages of differentiation, as well as T lymphocytes [145] which are stimulated and act as promoters of carcinogenesis, metastasis and resistance to therapy [146,147], also influencing the activity of infiltrating effector tumor lymphocytes (TIL), which in turn influences the response to immunotherapy [148,149]. Furthermore, macrophages known as tumor-associated macrophages or TAM [150] are also abundant in TME, suppressing the functions of immune cells through the over-production of the enzyme arginase-1 (involved in the metabolism of l-arginine), which synergizes with iNOS to increase the production of superoxide and NO, by

attenuating the responses of lymphocytes [151] and by induction of iNOS in the surrounding cells [152].

Glioblastoma Multiforme Tumor Microenvironment

Within and surrounding brain tumors, there is substantial presence of microglia and macrophages, which acquire an alternatively activated phenotype with potent tumor-tropic functions that contribute to glioma growth and invasion [153].

The glioblastoma immune microenvironment is recognized as highly immunosuppressive, posing a major hurdle for inducing immune-mediated destruction of cancer cells [154] (Figure 3). Microglia, critical effector cells of the immune response in the CNS, are found intermingled with tumor-associated macrophages (TAMs) as a major component (30–50%) of the non-neoplastic cell population in gliomas [155,156]; microglia play key roles under both normal and pathological conditions [157] and contribute to tissue

homeostasis by actively surveying the brain, and by promoting the development of healthy neural networks by removing apoptotic cells, eliminating synapses and enhancing the production and survival of neuronal precursor cells [158]. In particular, Glioma-associated microglial cells (GAMs) are functionally similar to that of tumor-associated macrophages in the peripheral system and interact with GBM cells intimately via intracellular communications [159]. Although GAMs have a few innate immune functions intact, their ability to be stimulated via TLRs, secrete cytokines, and upregulate co-stimulatory molecules is not sufficient to initiate antitumor immune responses [160]. However, in malignant gliomas, there is M2-polarization of microglia [161] acquiring immunosuppressive and tumor-supportive properties and it occurs under the influence of tumor cytokines, such as transforming growth factor-β, interleukin-10, and prostaglandin E2 [162].

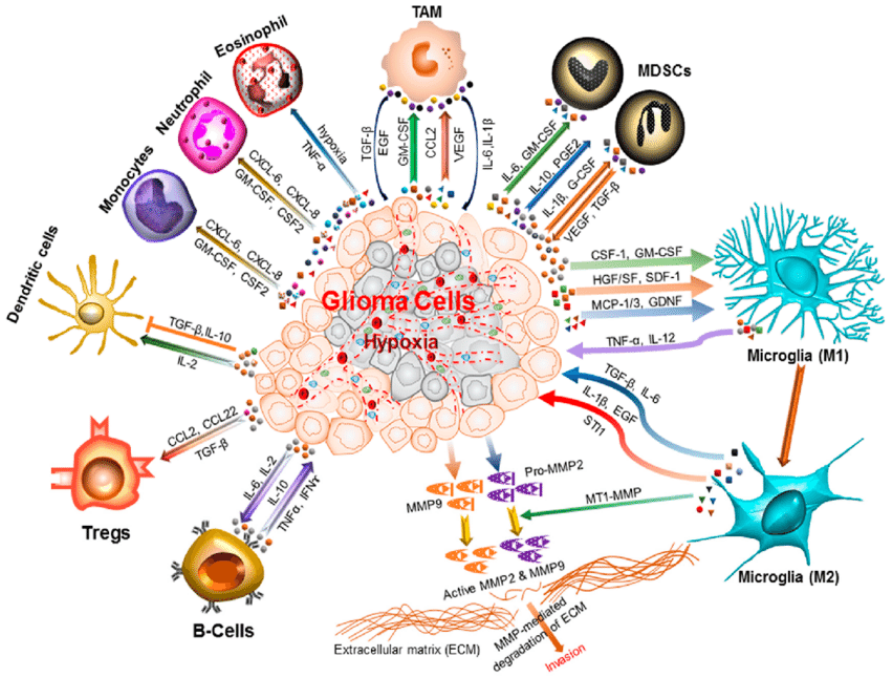

Figure 3. **Inflammatory microenvironment in brain cancers**. (Mostofa, A G M et al. "The Process and Regulatory Components of Inflammation in Brain Oncogenesis." Biomolecules vol. 7,2 34. 27 Mar. 2017, doi:10.3390/biom7020034).

Glioma – Associated Microglia (GAMs)

TME exhibits a complex structure and includes neoplastic cells as well as host and infiltrating immune cell varieties [163]. Microglia are part of the glioma microenvironment and are the

macrophages resident in the central nervous system (CNS) [155] that are involved in signaling tumorigenesis by producing chemokines and cytokines that promote tumor progression [164,165]. These cells are called glioma associated microglia/macrophages (GAM), which are abundant in the tumor mass and promote tumor growth [166,167]; in fact, they represent about 10-15% of the cells of the central nervous system (CNS) [168], and are distinguished from other cells by various characteristics, including the “ramifications” that emerge from the cell body [169]. Microglia are fundamental cells in the central nervous system, as they deal with the first and main immune defense. In fact, they respond quickly to traumatic and/or infectious stimuli by assuming the "amoeboid" phenotype, producing a set of cytokines, chemokines, reactive oxygen species and other pro-inflammatory mediators, designed to eliminate the pathogen [170]. However, the prolonged activation of these cells results in a pathological

inflammatory state, which in turn favors and promotes tumor progression [171].

Microglia show a remarkable degree of plasticity [172]. Following various stimulations, microglia can polarize into functional states classified as pro-inflammatory M1 activation (characterized by inflammatory and antitumor responses) [173] or cytoprotective and immunosuppressive M2 activation (shown by macrophages involved in tissue repair and resolution of inflammation) [174]. The M1/M2 continuum has been applied to CNS infiltrating macrophages/monocytes in the context of inflammation or tumor [175]. Classically activated macrophages assume an M1 phenotype characterized by the expression of the signal transducer and activator of transcription 1 (STAT-1) [176,177] and the overexpression of iNOS. While the alternatively activated pathway, M2, is characterized by CD163 and CD204 [178,179] surface expression, intracellular STAT-3 expression [180]

and arginase production [166,181] (Figure 4). Indeed, several markers have been proposed to distinguish between M1 and M2-like states, for example, the expression of Arg1, Mrc1, Chi3l3, Socs2, CD163, Fizz-1 and Ccl2 mRNA marks the activation of M2, while macrophages M1 express Nos2, IL12b [160,182]. During an acute phase of brain injury, microglia mainly adopt the M1 phenotype and release chemical mediators such as nitric oxide (NO) [183], reactive oxygen species (ROS) [184], amino acids and proinflammatory cytokines: interleukin-1β (IL-1β), IL-12, TNF-α and interleukin-6 (IL-6); while, high levels of Arginase-1 (Arg1) [183], CCL17, CCL22, mannose receptors and scavengers and production of anti-inflammatory cytokines such as: IL-4, IL-10 and TGF-β and low amounts of IL-12 and NO were found in microglia and M2-activated macrophages [173,185,186].

Glioma cells secrete a wide variety of immune cell suppressing factors, such as IL-10, IL-4, IL-6, M-CSF, macrophage

inhibitory factor (MIF), TGFβ, and prostaglandin E2 (PGE2) [187–189]. These factors promote the M2 phenotype and/or and suppress the M1 phenotype [177]. For example, TGFβ inhibits microglia cell proliferation and proinflammatory cytokine production in vitro [190]. IL-4, IL-6 and IL-10 have also been shown to polarize microglia to an M2-like phenotype [191].

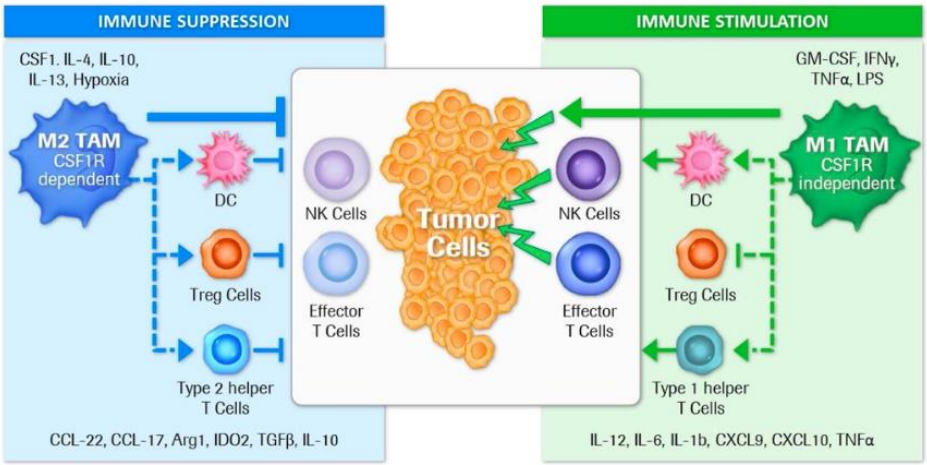

Figure 4. Direct and indirect regulation of immune suppression or stimulation by tumor associated macrophage subtypes. (Cannarile, Michael A et al. "Colony-stimulating factor 1 receptor (CSF1R) inhibitors in cancer therapy." Journal for immunotherapy of cancer vol. 5,1 53. 18 Jul. 2017, doi:10.1186/s40425-017-0257-y).

Interplay between GAMs and Gliomas

There exists an increasing body of evidence suggesting a cross-talk between GAMs and brain cancer cells [192]. Gliomas promote recruitment, proliferation and M2 polarization of microglia/macrophages into the TME [193] (Figure 5); these, in turn, are activated, polarized and reprogrammed to meeting their phenotype by facilitating survival, growth and above all the spread of glioma cells. Hence, tumor cells and cells of the tumor microenvironment work in synergy, involving numerous signaling pathways. For example, glioma-secreted factors, involving toll-like receptors and the p38 MAPK pathway, promote the expression and activity of type 1 membrane metalloprotease (MT1-MMP) on GAMs, which in turn activates glioma-derived pro-MMP-2 which in turn promotes glioma invasion [177,194]. Another mechanism associated with GAM is the CX3CR1/CX3CL1 interaction; this can also induce the production of MMP with consequent invasion of the glioma [195].

STI1 (cochaperone stress inducible factor 1) secreted by microglia has been shown to promote tumor growth and invasion through the participation of MMP-9 [196]. Thus, glioma cells stimulate microglia to increase the degradation of the extracellular matrix, thus promoting the invasion of glioma cells [177]. Yet another mechanism involves CD200, which is a type I transmembrane glycoprotein that interacts with its CD200R receptor [197], which in turn inhibits the activation of central nervous system microglia; CD200 downregulation in CD200-rich glioma cells could promote the formation of an activated microglia-associated tumor microenvironment, leading to glioma progression [198]. However, GAMs also have their role on GBM. GAMs of human GBM, express CCR2 to varying extents [199]. Lacking CCR2 solely on tumor microenvironmental cells leads to enhanced tumor progression, whereby high numbers of GAMs infiltrate gliomas independently of the CCR2/CCL2 signal [199]. Furthermore, CD11b+/CD163+ GAMs

secrete abundant pleiotrophin (PTN) to stimulate GSCs through its receptor PTPRZ1, promoting GBM malignant growth [200]. Furthermore, the expression of neuropilin 1 (NRP1) is related to poor prognosis and grade of glioma and is associated with the mesenchymal GBM subtype [201]. In human GBM, NRP1 expression is highly correlated with monocyte/macrophage markers, as well as with genes that contribute to the pro-tumorigenic phenotype of these cells [201].

Basically, it is still unclear whether microglia initiate or participate in early gliomagenesis, however, it is clear that neurodegeneration, neurotoxicity and neuroinflammation are associated with the chronic activation of microglia which has been hypothesized to contribute to gliomagenesis [202,203].

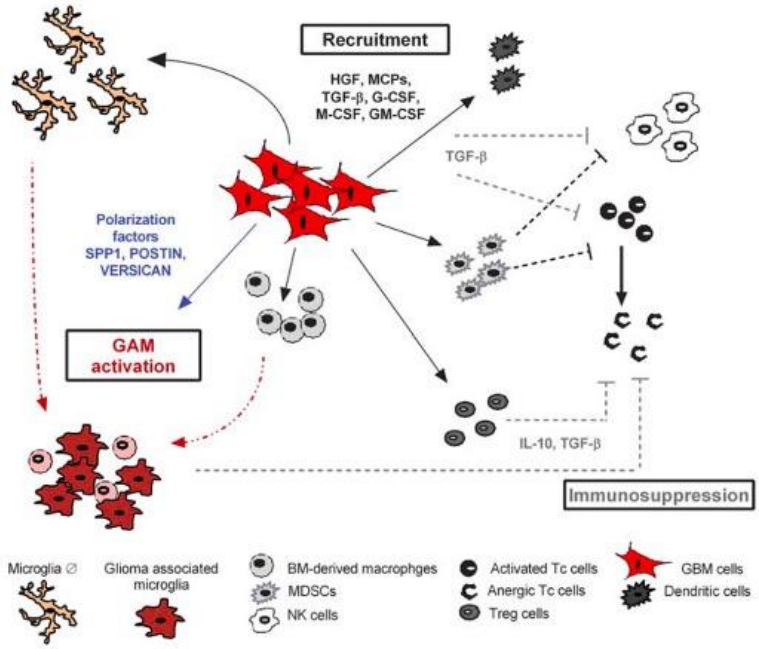

Figure 5. **Glioblastoma-immune system interactions**. The expression of all presented factors/cytokines is upregulated in GBMs and inversely correlates with patient survival. (Gieryng, Anna et al. "Immune microenvironment of gliomas." Laboratory investigation; a journal of technical methods and pathology vol. 97,5 (2017): 498-518. doi:10.1038/labinvest.2017.19).

LACTATE

Tumor cells must generate sufficient ATP and biosynthetic precursors in order to maintain cell proliferation requirements [204]. Several recent studies have further confirmed the importance of metabolic reprogramming in various cancers [205]. Glioblastoma TME includes different types of cells including tumor cells, stromal cells, and infiltrating immune cells (such as microglia and peripheral macrophages, granulocytes, myeloid-derived suppressor cells (MDSCs), and T lymphocytes) continuously interact and exchange signals through various secreted factors including cytokines, chemokines, growth factors, and metabolites, through which they are able to evade the immune response, [206,207]; TME plays vital roles in establishing malignancy [189,208,209] and exhibits high glycolytic metabolism with increased lactate production that is extruded to the tumor microenvironment through MCTs [210]. In

fact, most tumor cells use glycolysis rather than oxidative phosphorylation (OXPHOS) to produce ATP [211] and the excessive conversion of Glucose to Lactate is called Warburg effect. Moreover, the increased glycolysis leads, in turn, to an increase in lactate levels of up to 40 mM in tumors, while in normal conditions lactate levels are around 1.8 - 2 mM [212]. Consistently, clinical studies have demonstrated that patients with high levels of lactate showed poor prognoses and bad overall survival rates of head and neck cancer and non-small cell lung cancer [213].

Lactate accumulation results is an acidification of the extracellular pH of TME, ranging between 6.0 and 6.5 [204]. In turn, acidosis promotes angiogenesis, metastasis, and immunosuppression, which has been associated to a worse clinical prognosis. Hence, lactate is considered an important and fundamental oncometabolite in the metabolic reprogramming of cancer.

Lactate Metabolism

For many years it was thought that lactate was a "hypoxic waste product" [214] to be cleared from the muscles and blood, preferably converted into glucose in the liver via the Cori cycle. However, in recent years, lactate has been shown to be both a powerful fuel and a signaling molecule [215]. Furthermore, whenever glycolysis is active, lactate is formed which balances itself mainly by spreading through membranes via MCTs [216]. Several studies have shown that lactate can easily replace glucose as a fuel for almost any cell in the body (any cell with mitochondria), including the heart, liver, muscles, and even the brain [217], and that it is a powerful signaling molecule which triggers the stabilization of hypoxia-inducible factor-1α (HIF-1α), increasing the expression of VEGF and promoting angiogenesis; this has led scientists to study it in cancer models.

Lactate is the end product of glycolysis and is produced and secreted in high quantities by innate immune cells after inflammatory activation [218]. Moreover, high lactate concentrations in tumor microenvironments alter the phenotype of monocytes and macrophages by decreasing cytokine production and migration [219,220].

Several cell types, including cancer cells and immune cells, detect intracellular lactate concentrations via the membrane receptor GPR81, but it can also be taken up by cells via MCTs, affecting the cell's metabolism and it could help modulate the functions of immune cells [221].

Cancer cells are programmed to preferentially use aerobic glycolysis to meet their energy demand and consequently to support their proliferation and anabolic growth, an observation known as the Warburg effect [222–224]. Aerobic glycolysis rapidly generates ATP and glucose is preferably catabolized into lactate rather than

completely metabolized into carbon dioxide via mitochondrial oxidative phosphorylation (OXPHOS) [225,226]. This, therefore, leads to a greater production of lactate. In particular, glutaminase (GLS) promotes the conversion of glutamine into glutamate, which is then converted into α-ketoglutarate (αKG) by glutamate dehydrogenase which enters the TCA cycle [227]. The malate which is then generated from αKG can exit the TCA cycle and be converted into pyruvate by the malic enzyme (ME) [228], which contributes to redox homeostasis via the production of NADPH. An alternative use of glutamine in pancreatic ductal carcinomas involves the transamination of glutamate and oxaloacetate (OAA) into αKG and aspartate [229]. Aspartate exits the mitochondria and is transaminated back into OAA and glutamate; the OAA is then converted into malate and later into pyruvate. Finally, pyruvate is converted into lactate by the enzyme lactate dehydrogenase A (LDHA) [225]. In fact, a central enzyme in the metabolism of lactate

is lactate dehydrogenase (LDH). There are two different isoforms LDHA and LDHB [230]. LDHA has a higher affinity for pyruvate than lactate, thus converting pyruvate to lactate and NAD^+, while LDHB preferentially converts lactate to pyruvate by fueling oxidative metabolism [231,232]. Furthermore, the activity of this enzyme is also very important in immune cells; in fact it has been shown that LDHA promotes both the production of IFNγ by T lymphocytes [233] and the antitumor activity of macrophages [234], while the function of LDHB in immune cells remains to be clarified.

Lactate Transporters

Lactate cannot cross the plasma membrane by free diffusion; a specific transport mechanism provided by proton MCTs is required [235,236]. MCTs are critical regulators of intracellular lactate. Glycolytic cells use MCT transporters to export the lactate produced

by LDH; however, MCT functions are also required for lactate import into cells that use lactate as an oxidative metabolite [225].

MCTs belong to the family of solute transporter (SLC), consisting of 52 families of membrane transport proteins; in particular, the SLC16 family encodes 14 MCT isoforms and plays a significant role in the absorption, tissue distribution and clearance of both endogenous and exogenous compounds [235]. All family members are expected to have 12 transmembrane (TM) helices with intracellular C- and N-terminals and a large cytosolic ring between TM 6 and 7 [237,238]. As in other members of the superfamily of major facilitators, TM regions are more conserved of the loops and C-terminal [237,239]. Among all MCTs, only MCT1-4 have been confirmed to serve as proton-bound MCTs. MCTs 1-4 are known lactate transporters, but can carry other monocarboxylates such as pyruvate and ketone bodies such as acetoacetate, hydroxybutyrate and acetate [240].

Excessive expression of lactate transporters is a common feature of some tumors with a high metabolic rate [241], in fact the expression of MCT1, MCT2 and MCT4 has been widely characterized in tumor cell lines and in multiple tumor types of patients. Furthermore, MCT1 and MCT4 overexpression is associated with poor prognosis in different cancers [242,243]. Hypoxia can induce gene expression of MCT1/SLC16A1, MCT2/SLC16A7 and MCT4/SLC16A3 directly via HIF-1 activation for MCT4/SLC16A3 [244], or indirectly for the other two isoforms [210]. MCT1/SLC16A1 is also a direct target gene of Wnt, which couples Wnt activation to increased lactate export in glycolytic colon cancer cells [245]. NFkB signaling and p53 loss of function may further trigger MCT1/SLC16A1 transcription [246].

Furthermore, MCTs are expressed not only in cancer cells but also in the tumor microenvironment, suggesting that they exert numerous roles in the tumor including metabolic exchanges,

metabolic signaling and cancer metastases. First, they facilitate lactate exchanges in tumors. Indeed, oxidative tumor cells express MCT1 and are able to absorb lactate secreted by glycolytic tumor cells expressing MCT4 [247–249], and since oxidative tumor cells preferentially use lactate as an oxidative fuel over glucose, they spare glucose which becomes more available for glycolytic tumor cells [250] (Figure 6). This relationship has been called "metabolic symbiosis" [251]. In the cytosol of oxidative tumor cells, lactate is oxidized to pyruvate by LDHA, resulting in a reduction of NAD+ to NADH+ and H+. Pyruvate and NADH (via the malate-aspartate shuttle) can therefore feed the TCA cycle [250,252].

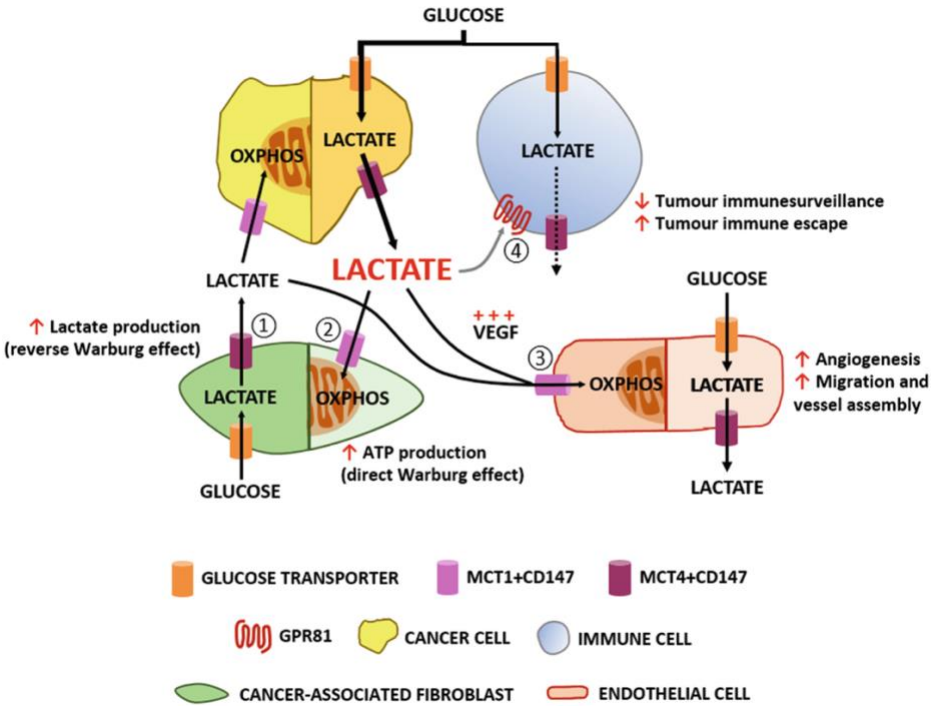

Figure 6. **Lactate shuttles between cancer cells and other cells in tumor microenvironment**. (Pereira-Nunes, Andreia et al. "Lactate and Lactate Transporters as Key Players in the Maintenance of the Warburg Effect." Advances in experimental medicine and biology vol. 1219 (2020): 51-74. doi:10.1007/978-3-030-34025-4_3).

Furthermore, MCTs, together with the lactate receptor GPR81, control lactate signaling; in fact, it has been shown that lactate in addition to being a metabolite is also a signaling molecule that regulates gene expression and the activation of various proteins,

influencing tumor angiogenesis, amino acid metabolism, histone deacetylases and immune tolerance.

The Lactate Receptor GPR81

Lactate was generally regarded as a waste product of metabolism. However, lactate has been shown to act as a signaling molecule [253,254]; in fact, lactate carries out its pro-tumor activity also independently of MCTs, by binding to its receptor, GPR81, on the cell surface [255]. This reporting via GPR81 does not require H^+ or MCT, nor a conversion to pyruvate or an alteration of the intracellular NADH/NAD^+ ratio [256].

GPR81 belongs to the hydroxycarboxylic acid receptor subfamily (HCAR), which is composed of three members: HCAR1 (GPR81), HCAR2 (GPR109A) and HCAR3 (GPR109B) [257]. This receptor belongs to the class of Gi-coupled receptors and is mainly expressed

in adipocytes but has also been found in skeletal muscle and brain [254,258–261].

GPR81 has been shown to contribute to the growth and proliferation of cancer cells by responding to lactate in the extracellular environment in an autocrine or paracrine manner [256].

In the case of the autocrine response, the lactate released by the tumor cells is taken up by the GPR81 expressed on these cells. Instead, in the case of the paracrine response, lactate acts on GPR81 expressed on non-cancerous cells located in the TME that support tumor growth [262], including immune cells (dendritic cells and macrophages), adipocytes and endothelial cells [263]. Although lactate signaling via GPR81 does not require H^+ or MCT, that silencing of GPR81 in pancreatic cancer cell lines significantly decreased expression of the lactate transporters MCT1 and MCT4, and their chaperone protein CD147. Surprisingly, knockdown of GPR81

resulted in a significant reduction in mitochondrial activity and a marked increase in cell death.

Furthermore, the presence of a high concentration of lactate in the extracellular environment of the tumor is associated with a poor prognosis; therefore, autocrine or paracrine GPR81 signaling is likely to be involved in promoting tumor growth and/or metastasis [264].

Metabolic Switch in Tumorigenesis

Through the activation of oncogenes and tumor suppressor mutations, defects in cellular respiration and overexpression of glycolytic enzymes and metabolite transporters [265], tumor cells in glycolytic tumors undergo metabolic reprogramming transforming into highly glycolytic and poorly oxidative cells with the formation of lactate as a product final despite normoxic conditions. The

proliferating tumor cells, therefore, convert most of the glucose into lactate, even in the presence of high quantities of oxygen [266]. This phenomenon is called the "Warburg effect" [267]. It is well known that the Warburg effect is a key feature of all hypoxic cells as well as highly proliferating cells, such as activated effector T cells [268]. There are numerous oncogenes and tumor suppressor genes involved in the metabolic passage from oxidative phosphorylation (OXPHOS) towards an altered glycolysis of tumor cells; among them myc, NFκB, Akt/protein kinase B, epidermal growth factor (EGF), insulin growth factor I, phosphoinositol 3 kinase (PI3K), mTOR, homolog of the viral oncogene of Kirsten's rat sarcoma (KRAS), AMP-activated protein kinase (AMPK) and hypoxia-inducible factor 1α [214,223,269–274] (Figure 7).

Cancer cells that have undergone this metabolic reprogramming possess an "inefficient" mechanism for producing ATP which therefore promotes aerobic glycolysis and lactate

production in the cytosol instead of glucose oxidation which progresses through mitochondrial oxidative phosphorylation [275]. To date, it is still unclear why cancer cells move away from an "efficient" metabolic mechanism and "choose" an inefficient pathway by producing two cytosolic ATPs per glucose molecule instead of ~ 36-38 ATP via coupled mitochondrial respiration [275]. Furthermore, due to the enhanced expression of LDH-A, the enzyme that converts pyruvate into lactate, NAD^+ is generated, which allows for continuous glycolysis and the production of ATP. Despite the high conversion rate of pyruvate to lactate at the end of the glycolytic pathway, some pyruvate remains to be used in the tricarboxylic acid (TCA) cycle for bioenergetic and biosynthetic purposes [276,277]. The TCA cycle and the pentose phosphate (PPP) pathway can maintain a high pool of precursors to maximize tumor cell proliferation at the expense of surrounding normal tissue or the host

in general [278]. Furthermore, PPP generates NADPH as a mediator of antioxidant reactions to protect cells from oxidative damage [279].

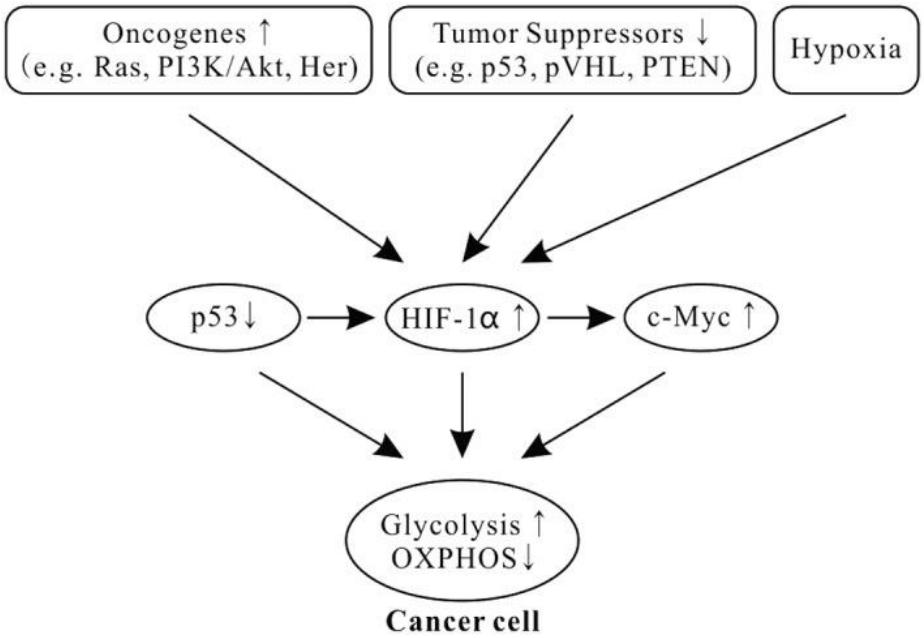

Figure 7. **Alterations of oncogene and tumor suppressor and hypoxia drive cancer cells to aerobic glycolysis**. (Zheng, Jie. "Energy metabolism of cancer: Glycolysis versus oxidative phosphorylation (Review)." Oncology letters vol. 4,6 (2012): 1151-1157. doi:10.3892/ol.2012.928).

Lactate as a Key Molecule in the "Immune Scape"

TME is highly dynamic and constantly changing environment as the tumor grows. The innate and adaptive immune cells present

within it are responsible for the detection and elimination of tumor cells [280]. However, given the ability of tumor cells to secrete anti-inflammatory cytokines, chemokines and various growth factors, there is the recruitment of immunosuppressive cell populations into TME, which directly inhibit immune responses [281,282]. Since cancer cells with an elevated glycolytic phenotype, in addition to creating demanding metabolic environments that invade the function of tumor-infiltrating immune cells, they also release immunosuppressive metabolites and by-products, such as lactate, form a metabolic symbiosis with immune cells and lead to the formation of an acid TME, which has a strong impact on immune cells (Figure 8). Paradoxically, immune cells also contribute to the production of intratumoral lactate [283]. In fact, in TME the lactate concentration can reach 40 mM, thus contributing to the immune escape, through various mechanisms. Lactate inhibits the migration of monocytes and the release of cytokines, tumor necrosis factor and

IL-6 [219]. Furthermore, lactate strongly inhibits the activation of T cells (173) and the differentiation of monocytes into dendritic cells [284–286]. Furthermore, it induces apoptosis of natural killer (NK) and natural killer T (NKT) cells, both of which have antitumor activity [287,288]. It also blocks the production of interferon (IFN)-γ and interleukin (IL) -4 by antitumor NKT cells in TME by inhibiting mTOR signaling, thus preventing the activation of these immune cells [288]. Furthermore, lactate prevents DC differentiation leading to an increase in the production of IL-10, a potent immunosuppressive cytokine [289] which inhibits the production of proinflammatory cytokines such as IFNγ, TNFα, IL-1β and IL-6; moreover, IL-10 prevents DC maturation and T cell activation [290]. Lactate also promotes the development of myeloid suppressor cells (MDSCs), capable of suppressing both innate and adaptive immunity. Finally, the lactate in TME is absorbed by TAMs through their MCTs, resulting in the transcription of VEGF factor HIF-α and the

metabolizing enzyme arginase-1 (ARG1), which promote polarization TAM [291] towards the M2 phenotype, known as the immuno-suppressive phenotype.

Hence lactate is an important component of TME, promoting tumor growth and immunosuppression and thus carcinogenesis.

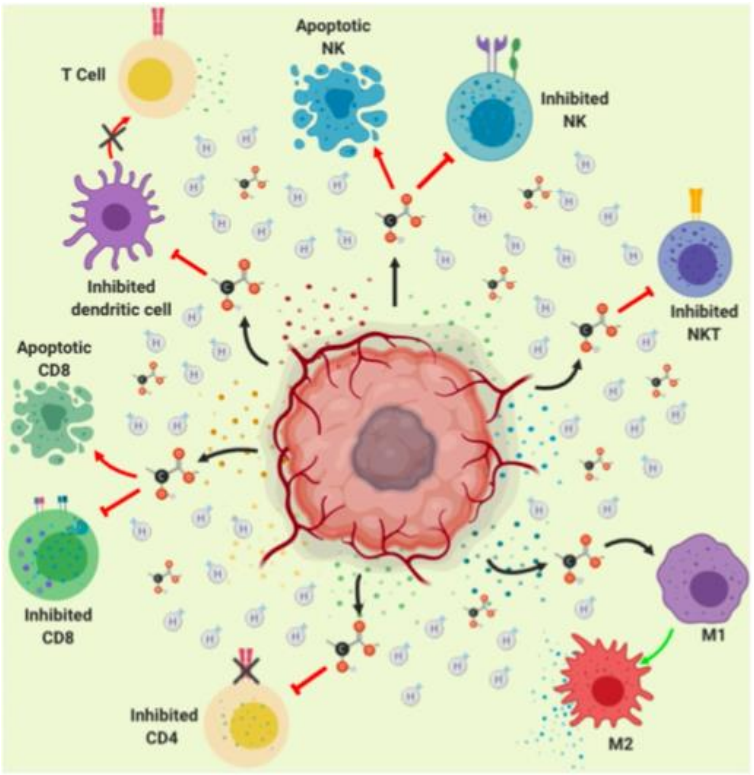

Figure 8. **Role of lactate in immune suppression**. (de la Cruz-López, Karen G et al. "Lactate in the Regulation of Tumor Microenvironment and Therapeutic Approaches." Frontiers in oncology vol. 9 1143. 1 Nov. 2019, doi:10.3389/fonc.2019.01143).

IGFBP6

The Insulin-like Growth Factor System

The IGF system plays an essential role in the regulation of various cellular processes, such as proliferation, survival, migration and differentiation [292]. The Insulin-like Growth Factor (IGF) family includes three ligands (IGF-1, IGF-2 and insulin), three membrane receptors (IGF-1R, IGF-2R and IR), IGF-binding proteins (IGF- binding proteins, IGFBPs) and IGFBP proteases [293] (Figure 9). Insulin-like growth factors IGF-1 and IGF-2 are low molecular weight (7 KDa) peptides produced mainly by hepatocytes under the influence of somatotropic hormone (GH), but also by other tissues, even independently of GH [294]. Their name derives from the high structural homology with insulin, with which they share 50% of the amino acid sequence. Once produced, the IGFs are released into the circulation, and act with both autocrine, paracrine and endocrine

mechanisms [293]. Only 1% of IGFs circulate in free form [293], most form a ternary complex with the IGFBPs and the ALS (Acid Labile Subunit) [292]. Once the ALS subunit has been dissociated, the IGFBP-IGF complex leaves the vascular district, crosses the endothelium to reach the target tissues, at the level of which the IGFs interact with their specific membrane receptors [295]. The type 1 receptor, IGF-1R, is the receptor that most mediates the effect of IGFs, it is a receptor with tyrosine kinase activity identified in most tissues, and in particular in striated muscle, cartilage, bone, liver, kidney and hematopoietic system [296]. This receptor is capable of binding both IGF-1 and IGF-2, and following the binding of the ligand there is the activation of the receptor and the modulation of numerous biological processes important both at the physiological and pathological level, in fact it has now been widely demonstrated its role in neoplastic development and progression [297]. Specifically, the binding of IGF-1 or IGF-2 with IGF-1R leads to the

auto-phosphorylation of the receptor, the recruitment of multiple adapter proteins (IRS, Shc and others) and the subsequent activation of multiple signaling pathways. Two well characterized pathways are the RAS/RAF/MAPK pathway and the PI3K/AKT pathway, pathways involved, respectively, in the stimulation of cell proliferation and survival [298]. On the contrary, the binding of IGF-2 to the IGF type 2 receptor does not produce signaling events, but induces the degradation of IGF-2 itself, thus reducing its functionality. For this reason, IGF-2R is considered a tumor suppressor [299].

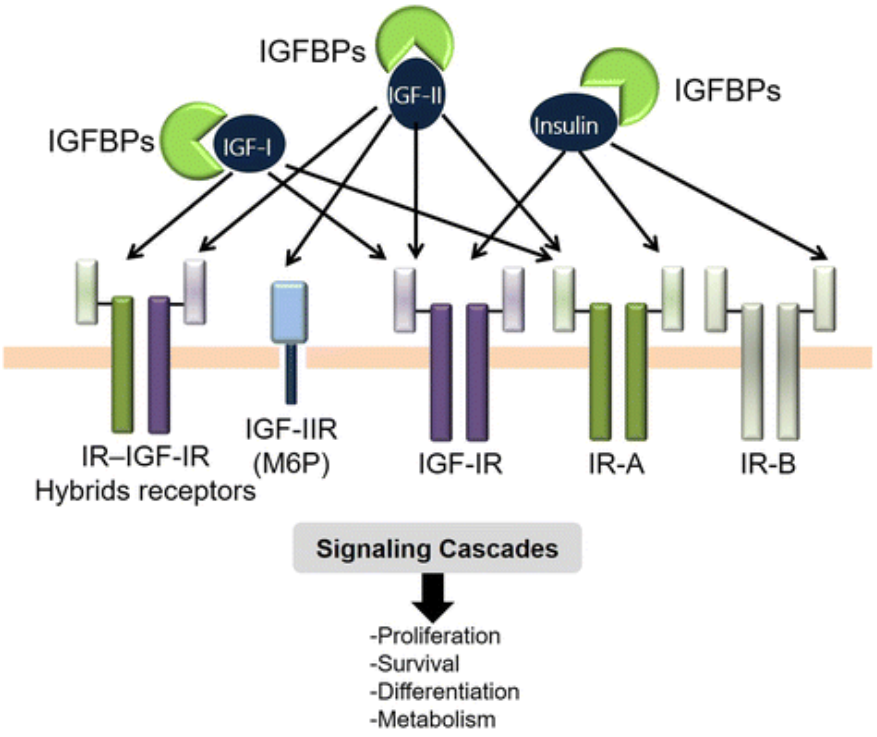

Figure 9. **Representation of the insulin and IGF receptor family**. (Li, Heming et al. "IGF-IR signaling in epithelial to mesenchymal transition and targeting IGF-IR therapy: overview and new insights." Molecular cancer vol. 16,1 6. 30 Jan. 2017, doi:10.1186/s12943-016-0576-5).

Insulin Growth Factor Binding Proteins (IGFBPs)

IGFBPs are a superfamily of six proteins (IGFBP 1-6) that are structurally related and expressed in a tissue-specific manner, mainly located in plasma and CSF [300]. All IGFBPs have a structure in which it is possible to distinguish two highly conserved domains

[301], namely the amino terminal domain and the carboxy-terminal domain, both containing amino acid residues involved in the binding with the IGFs, and finally a central domain of binding between the domain C- and N-terminal, containing sites of post-transductional modifications, such as glycosylation, phosphorylation and proteolysis [299,302]. There are also other subdomains, responsible for the binding of numerous proteins such as heparin, integrins, nuclear transport proteins, ALS and other ligands [303]. Post-translational modifications involving IGF-binding proteins can influence their cellular effects, glycosylation, for example, does not modify the interaction with IGF but can influence the association with the cell surface, phosphorylation influences the affinity of binding to IGFs and sensitivity to proteases and, finally, proteolysis influences both IGF-dependent and independent actions [303]. All circulating IGFBPs are able to bind and convey IGFs within the body, regulating their concentration and also their activity at the target

tissue level [304]. In plasma the most represented IGF binding protein is IGFBP-3, it binds 75% of the circulating IGFs forming heterotrimers with the ALS glycoprotein [304,305]; also IGFBP-5 can form similar ternary complexes, these complexes extend the half-life of circulating IGFs from 20-30 minutes to over 15 hours [306]. However, all IGFBPs can be found in plasma in free form or in the form of binary complexes with IGFs, and only in this condition are they capable of crossing the vascular wall [303]. The formation of IGFBP-IGF complexes, in addition to protecting the IGFs from degradation, regulates their interaction with the receptor, since the latter does not occur as long as the IGFs are complexed with the IGFBPs [302]. The release of IGFs can occur following the proteolysis of IGFBPs or following the association of the IGFBP with the cell membrane or with extracellular matrix proteins, this association reduces the binding affinity between IGFBPs (in particular IGFBP-1, IGFBP -2, IGFBP-3 and IGFBP-5) and IGF, resulting in their release

[307]. The variation in the concentration of IGFBPs is linked, in addition to a different rate of secretion, to the modulating action carried out by more or less specific proteases, which are able to cleave IGFBPs into forms that show greater or lesser affinity for IGFs [303]. The activity of proteases depends on numerous factors which include the amount of the proteases themselves, their concentration in the affected area and, finally, the presence of molecules capable of modulating the proteolytic activity; among the modulators of the action of proteases there are the same IGFs [307].

The roles of the six IGFBPs in modulating the action of IGFs in different cellular processes, such as proliferation, differentiation, survival and migration, have been studied in different cell lines, moreover it has been seen that, while IGFBP-4 and -6 inhibit the action of IGFs, IGFBP-1, -2, -3 and -5 can both inhibit and enhance the action of IGFs [306]. In recent years it has been shown that IGFBPs can act through IGF-independent mechanisms and their effects

include inhibition of apoptosis, modulation of cell adhesion and migration [308]. These are actions mediated by the binding of IGFBPs to ligands other than IGFs, including extracellular proteins and proteoglycans, cell surface proteins and receptors, intracellular proteins [309]. Another mechanism by which IGFBPs exert IGF-independent effects is linked to their translocation of the nucleus, due to their nuclear localization signal and the binding with importins, once these proteins have reached the nucleus, they modulate the transcription of target genes by interacting with transcription factors [307].

Insulin Growth Factor Protein Binding 6 (IGFBP6)

The IGFBP-6 protein is a member of the family of IGF-binding proteins [310], although it shares a good part of its properties with the other members, it is distinguished from these by some structural and functional characteristics. In the first instance, it is distinguished from other IGFBPs in that it is capable of binding the IGF-2 factor

with an affinity 20 to 100 times higher than the IGF-1 factor, which is why this protein is considered a relatively specific inhibitor of IGF -2 [309]. Other distinctive features of IGFBP-6 reside at the level of the N-terminal domain, in particular in the lack of the two adjacent cysteines in the conserved GCGCC motif [311], and in having a structure stabilized by three disulfide bonds, and not by four as all the other IGFBPs [312]; in fact this region of IGFBP-6 has a different three-dimensional structure [309]. The protein sequence is highly conserved, human IGFBP-6 shares 70-85% homology with mouse, rat and pig IGFBP-6 [312] (Figure 10).

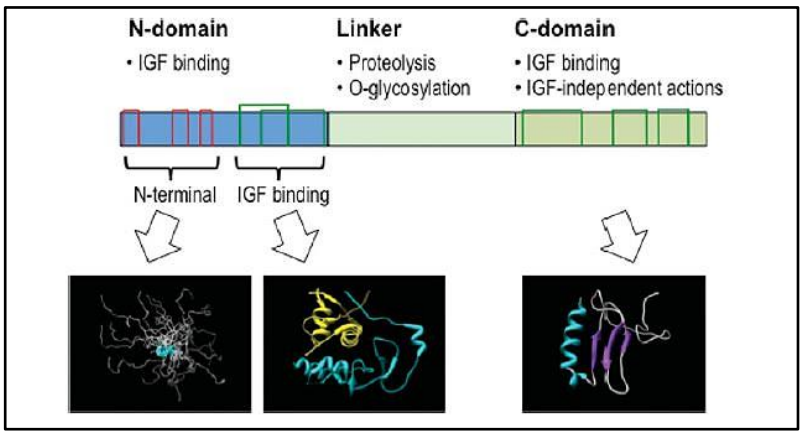

Figure 10. **IGFBP6 structure**. (Bach, Leon A et al. "Insulin-like growth factor-binding protein-6 and cancer." Clinical science (London, England : 1979) vol. 124,4 (2013): 215-29. doi:10.1042/CS20120343).

Like all IGFBPs, IGFBP-6 is also expressed in many tissues such as lung, liver, intestine and central nervous system [313], and expression is regulated by various factors including cAMP, IGF, retinoic acid, vitamin D [314], p53 and glucocorticoids [299]. The expression of the protein is also regulated by the Hedgehog and Wnt signaling pathways [309]. The main function of the IGFBP-6 protein is to inhibit the action of IGF-2, and consequently to inhibit the proliferation, differentiation, migration and cell survival induced by IGF-2 in different cell lines [299], this occurs both in cells normal than in cancer cells, so IGFBP-6 is considered a tumor suppressor [312]. The same cellular processes, including angiogenesis, however, can be regulated by IGFBP-6 also with mechanisms independent of IGF-2 [315] (Figure 11).

The IGFBP-6 protein can compromise cell survival by inhibiting the action of IGF-2, but also by increasing the transcription of EGR-1 (Early Growth Response 1), therefore in an IGF-

independent manner [316]. EGR-1 is a tumor suppressor gene and the binding of the IGFBP-6 protein to the promoter of the gene promotes its expression [309]. Clearly IGFBP-6 exerts intracellular actions through importin-mediated nuclear translocation mechanisms, although it has been shown that both the α-importin and the Ku80 protein can bind to the nuclear localization sequence (NLS) of IGFBP-6, competing for the same binding site [317]. Ku80 is a component of the Ku complex (heterodimer of two polypeptides, Ku70 and Ku80), involved in DNA repair processes and in the maintenance of telomere length [318]. It has been hypothesized that the interaction with IGFBP-6 compromises the transport of Ku80 from the cytoplasm to the nucleus, thus favoring the proapoptotic effect of IGFBP-6 through the interruption of DNA repair [309].

As far as cell migration is concerned, IGFBP-6 performs a double action, as in some cells it can inhibit migration, inhibiting IGF-2 and promoting the transcription of EGR-1 (independent

mechanism from IGF-2), but it is also true that IGFBP-6 can promote tumor cell migration through binding to Phb-2 protein (Prohibitin 2) and/or activation of MAP kinases [319]. The modulation of the activity of prohibitins occurs through phosphorylation, following the binding with IGFBP-6; however, the same prohibitins, in turn, can regulate several intracellular signaling pathways, including the MAP kinase pathway [320].

The IGFBP-6 protein is involved in the development and progression of various cancers and could be used as a prognostic biomarker in various cancers [321]. Numerous studies have shown that cancer cells have a lower level of protein expression than normal cells, which is why it is considered a tumor suppressor [299], although there are exceptions, as in certain circumstances it can stimulate cell migration [321].

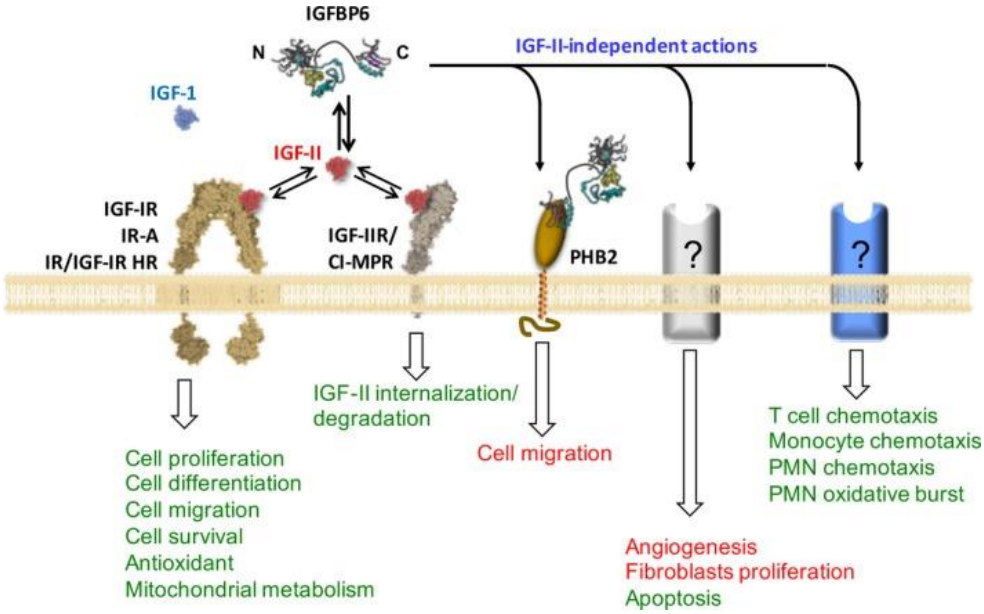

Figure 11. **Extracellular actions of IGFBP-6. IGFBP-6 presents both IGF-dependent and IGF-independent actions**. (Liso, Arcangelo et al. "From fever to immunity: A new role for IGFBP-6?." Journal of cellular and molecular medicine vol. 22,10 (2018): 4588-4596. doi:10.1111/jcmm.13738).

CHAPTER I

(Submitted) Journal of Experimental & Clinical Cancer Research

Lactate shapes mitochondrial fitness inducing MCT1 in glioblastoma

Lucia Longhitano[1,#], Nunzio Vicario[1,#], Daniele Tibullo[1,#], Cesarina Giallongo[2], Giuseppe Broggi[2], Rosario Caltabiano[2], Giuseppe Barbagallo[2], Marta Baghini[3], Michelino Di Rosa[1], Rosalba Parenti[1], Antonio Giordano[4], Maria Caterina Mione[3,*], Giovanni Li Volti[1,*]

[1]Department of Biomedical and Biotechnological Sciences, University of Catania, 95123 Catania, Italy;

[2]Department of Scienze Mediche Chirurgiche e Tecnologie Avanzate "G.F. Ingrassia", University of Catania, 95123 Catania, Italy;

[3]Department of Cellular, Computational and Integrative Biology (Cibio), University of Trento, 38123 Trento, Italy

[4]Sbarro Institute for Cancer Research and Molecular Medicine and Center of Biotechnology, College of Science and Technology, Temple University, BioLife Science Bldg, Suite 431-1900 N 12th Street, Philadelphia, PA 19122, USA

[#]These authors equally contributed to this work as co-first.

*Authors to whom correspondence should be addressed.

Abstract

Background: Glioblastoma represents the most malignant primary brain tumor. Tumor microenvironment plays a pivotal role in establishing malignancy and it is associated with high glycolytic metabolism and increased lactate production, which accumulates in the TME through monocarboxylate transporters (MCTs). MCTs are a group of transmembrane proteins encoded by the SLC16 gene family and two members of this group, MCT1 and MCT4, modulate tissue metabolic activity through proton-coupled transport of monocarboxylates, specifically L-lactate, ketone bodies, and pyruvate. The aim of the present study was to investigate the role of lactate in GBM progression and metabolic reprogramming in vitro and in an in vivo model.

Methods: The in vitro study was carried out in three human Glioblastoma cell lines treated with Lactate (20 mM). Cell proliferation, migration, colony formation capacity,was evaluated. Lactate metabolism was assessed by the expression of its transporters MCT1 and MCT4, and β-Catenin, E-Cadherin and GRP81. These results were confirmed using a well-established pharmacological lactate receptor agonist, the 3,5-dihydroxybenzoic acid (150 μM). The expression of genes involved in mitochondrial metabolism was also evaluated. The results were validated in patient-derived GBM biopsies, by comparing MCT1 expression in high (H-) versus low (L-) proliferative index (PI) GBM samples. The in vivo study was carried out in a zebrafish model of GBM (doi: 10.1242/dmm.026500). The energy phenotype was assessed by Seahorse XFp, gene expression was evaluated by NGS sequencing, qPCR analysis and immunofluorescence. Effects of 20 mM lactate exposure on proliferation of developing brain tumors was assessed by counting phospho-histone 3 positive cells.

Results: Our results show that lactate significantly increased cell proliferation, migration and colony formation capacity of GBM cells, both in vitro and in vivo. We found that cells respond to high levels of extracellular lactate increasing MCT1 transporter expression and in U-87 MG cells GPR81 stimulation increased β-Catenin protein levels and suppressed E-Cadherin, while in both A-172 and U-251

MG we observed an increase of MCT1, β-Catenin and E-Cadherin expression. In a Zebrafish model of GBM, altered metabolism and increased expression of MCT1 and GPR81 generate high levels of extracellular lactate, which in turn supports increased proliferation of tumor cells. Interestingly, 3,5-DHBA stimulation was able to increase significantly MCT1 in all tested cell lines. Furthermore, our results showed that both lactate and 3,5-DHBA exposure induced a significant increase in the expression levels of tested genes, confirming that lactate is involved in the metabolic switch of GMB cell lines. Finally, immunohistochemistry analysis on GBM biopsies demonstrated that High-PI GBM showed a significant increase in MCT1 and Ki67 expression levels when compared to Low-PI GBM.

Conclusions: Our results suggest that lactate and its transporter (MCT1) and receptor (GPR81) play a major role in GBM proliferation and migration and it may represent a potential target to develop new strategies to counteract tumor progression and recurrencies.

INTRODUCTION

Glioblastoma (GBM) represents the most common primary brain tumor in the adult population and is classified by WHO as a grade IV glioma. Current therapeutic approach for newly diagnosed GBM relies on surgical resection, radiotherapy and chemotherapy (i.e. temozolomide) [1]. However, despite aggressive therapeutic regimens, these tumors still have a dismal prognosis with medial overall survival of 12 to 15 months. Histologically, GBM is a highly cellular glioma composed by glial cells with significant pleomorphism and nuclear atypia [2]. Such cellular features are coupled with microvascular proliferation and palisading necrosis characterized by regular areas of necrosis and dense accumulation of GBM cells [2]. GBM characteristics are related to cell proliferation, usually assessed by evaluating KI-67 expressing cells classifying high proliferative index (HPI, KI-67 positive cells > 30%) and low proliferative index (LPI, KI-67 positive cells < 30%). Furthermore, GBM cell proliferation, migration and invasiveness are closely related to availability of blood-derived nutrients and oxygen. Indeed, two niches have been described in GBM in relation to availability of

oxygen, the so-called perivascular niches, in which GBM cell receive glucose and oxygen from blood stream and oxidative phosphorylation in these cells determines highly efficient metabolism, and the GBM hypoxic niches, for example tumor core, in which low oxygen levels shapes metabolisms towards a glycolytic state inducing lactate accumulation [3]. Indeed, such tumors have a rapid rate of glucose consumption and convert large amounts of glucose into lactic acid, even in the presence of oxygen [4]. This metabolic phenotype, known as Warburg effect contrasts sharply with that observed in normal tissues in which glycolysis occurs mainly in hypoxic conditions [5].

To maintain enhanced glycolytic flow, glioblastomas require rapid outflow of lactic acid into the tumor microenvironment (TME), facilitated by a series of plasma membrane transporters called monocarboxylate transporters (MCTs) [6]; among these only four (MCT 1-4) are known to play a role in lactic acid transport in mammalian tissues, including cancers [7] and MCT1 and MCT4 have been implicated in multiple aspects of GBM progression including angiogenesis, cell proliferation and immunity modulation [8]. Glycolytic cancer cells are known to upregulate lactate export by

increasing MCT4 expression to better adapt to lactate accumulation. In contrast, tumor cells of oxidative tumors have been reported to upregulate MCT1 expression to mediate lactate uptake from the extracellular environment to fuel metabolism [9]. A recent report suggests that this dynamic may create a metabolic symbiosis between the two GBM subpopulations maintaining a favorable environment for both subtypes [8,10].

Besides having a role as end-product metabolite of glycolysis and being utilized by cellular metabolic programs to produce energy, lactate also acts as signalling molecule through its receptor HCAR1 (GPR81) [11]. Therefore, extracellular lactate is not a simple bystander causing milieu acidification but it also serves as a paracrine and autocrine signalling molecule in TME [12]. Elevated expression of HCAR1/GPR81 was found in carcinomas of the breast, pancreas and cervix, despite negligible expression in the corresponding benign epithelium [12,13]. Several groups have identified autocrine roles for HCAR1/GPR81 in TME, where lactate produced by tumor cells activates HCAR1/GPR81 and confers cancer-promoting phenotypes [14], including upregulation of transporter MCT1 and MCT4 and the secretion of factors that

promote angiogenesis and tumor progression [15].

The aim of the present study was to assess the role of lactate metabolism in cancer growth and progression in several glioblastoma cell lines, in pathological specimens and in an in vivo model.

MATERIALS AND METHODS

GBM cell lines

Human glioblastoma cell lines (U87-MG, A172 and U251) were purchased from ATCC Company (Milan, Italy). Cells were suspended in DMEM (Gibco, cat. no. 11965092) culture medium containing 10% fetal bovine serum (FBS, Gibco, cat. no. 10082147), 100 U/mL penicillin and 100 U/mL streptomycin (Gibco, cat. no. 15070063). At 80% confluency, cells were passaged using trypsin-EDTA solution (0.05% trypsin and 0.02% EDTA, Gibco, cat. no. 25300054).

Lactate (Sigma–Aldrich, Milan, Italy) and 3,5-Dihydroxybenzoic acid (Sigma–Aldrich, Milan, Italy) were added to cell culture of all experiments at final concentrations of 20 mM and 150 uM, respectively, for 24, 48 and 72 hours.

Clonogenic assay

Colony assays performed by seeding cells in 6-well plates at low density (2000 cells/well) and allowing growth for 10 days. Colonies were fixed, stained with crystal violet and colonies were quantified

with Operetta high content screening (HCS) System (Perkin Elmer). The experiments were done in quadruplicates.

Real-Time Monitoring of Cell Proliferation

xCELLigence experiments were performed using the RTCA (Real-Time Cell Analyser) DP (Dual Plate) instrument according to manufacturers' instructions (Roche Applied Science, Mannheim, Germany and ACEA Biosciences, San Diego, CA). The RTCA DP Instrument includes three main components: (i) RTCA DP Analyser, which is placed inside a humidified incubator maintained at 37 °C and 5% CO2, (ii) RTCA Control Unit with RTCA Software preinstalled and (iii) E-Plate 16 for proliferation assay. First, the optimal seeding number was determined by cell titration and growth experiments. After seeding the optimal cell number (3000 cells/well), cells were treated and automatically monitored every 15 min for 24h. Optimal cell number was determined in a preliminary set of experiments (data not shown) to obtain a significant cell index value and a constant cell growth during the entire duration of the experiment.

Cell Migration

Cell migration was studied by employing the "wound healing" assay. Briefly, cells were seeded in 24 wells dishes and cultured until confluence. Cells were treated with vehicle, lactate or 3,5 - DHBA and were then scraped with a 200 µl micropipette tip and monitored at 0, 24, and 48 h. The uncovered wound area was measured and quantified at different intervals with ImageJ 1.37v (NIH).

Immunoblotting

Briefly, for western blot analysis, 30 µg of protein was loaded onto a 12% polyacrylamide gel MiniPROTEAN® TGXTM (BIO-RAD, Milan, Italy) followed by electrotransfer to nitrocellulose membrane TransBlot® TurboTM (BIO-RAD, Milan, Italy) using TransBlot® SE Semi-Dry Transfer Cell (BIO- RAD, Milan, Italy). Subsequently, membrane was blocked in Odyssey Blocking Buffer (Licor, Milan, Italy) for 1 h at room temperature. After blocking, membrane was three times washed in phosphate-buffered saline (PBS) for 5 min and incubated with primary antibodies against MCT1 (1:1000), MCT4 (1:1000), β-catenin (1:500), E-Cadherin (1:500) and β-actin (1:1000) (anti-mouse, Cat. No. 4967S, Cell Signalling Technology,

Milan, Italy), overnight at 4 °C. Next day, membranes were washed three times in PBS for 5 min and incubated with infrared anti-mouse IRDye800CW (1:5000) and anti-rabbit IRDye700CW secondary antibodies (1:5000) in PBS/0.5% Tween-20 for 1 h at room temperature. All antibodies were diluted in Odyssey Blocking Buffer. The blots were visualized using Odyssey Infrared Imaging Scanner (Licor, Milan, Italy), and protein levels were quantified by densitometric analysis. Data were normalized to β-actin expression.

Real-time RT-PCR for gene expression analysis

RNA was extracted by Trizol® reagent (Invitrogen, Carlsbad, CA, USA). First-strand cDNA was then synthesized with Applied Biosystem (Foster City, CA, USA) reverse transcription reagent. Quantitative real-time PCR was performed in Step One Fast Real-Time PCR System Applied Biosystems, using the SYBR Green PCR MasterMix (Life Technologies, Monza, Italy). The specific PCR products were detected by SYBR Green fluorescence. The relative mRNA expression level was calculated by the threshold cycle (Ct) value of each PCR product and normalized with that of actin by using

a comparative 2−ΔΔCt method. The sequence of primers used are presented in Table 1.

Table 1. List of qRT-PCR primers.

Gene of interest	Forward primer (5′ ⟶ 3′)	Reverse primer (5′ ⟶ 3′)
PGC1α	ATGAAGGGTACTTTTCTGCCCC	GGTCTTCACCAACCAGAGCA
SIRT1	AGGCCACGGATAGGTCCATA	GTGGAGGTATTGTTTCCGGC
TFAM	CCGAGGTGGTTTTCATCTGT	AGTCTTCAGCTTTTCCTGCG
ND4	CCAGTGGAATGCCTTGCCTA	TTGATCGCGGTGAGATTCCC
CyB	ACGAGCCACCGAAACAGAAT	ACGATTTTCGCCAGTCACCT
COX II	ACGACCTCGATGTTGGATCA	ATCATTTACGGGGGAAGGCG
COX IV	GCGGCAGAATGTTGGCTAC	AGACAGGTGCTTGACATGGG
ATPsynthase	CCGCCTTCCGCGGTATAATC	ATGTACGCGGGCAATACCAT
MCT1	TGTTGTTGCAAATGGAGTGT	AAGTCGATAATTGATGCCCATGCCAA
MCT4	TATCCAGATCTACCTCACCAC	GGCCTGGCAAAGATGTCGATGA
HCAR1	TTCGTATTTGGTGGCAGGCA	TTTCGAGGGGTCCAGGTACA
β-Actin	CCTTTGCCGATCCGCCG	AACATGATCTGGGTCATCTTCTCGC

Zebrafish model

Adult zebrafish (Danio rerio) were housed in the Model Organism Facility – Center for Integrative Biology (CIBIO) University of Trento and maintained under standard conditions [16]. All zebrafish studies were performed according to European and Italian law, D.Lgs.

26/2014, authorization 148/2018-PR to M. C. Mione. Fishes with somatic and germline expression of oncogenic HRAS were generated as described [17,18].

The following zebrafish transgenic lines were used in the course of this study:

Et(zic4:Gal4TA4, UAS:mCherry)$_{hzm5}$ called zic:Gal4 [17]

Tg(UAS:eGFP-HRAS_G12V)$_{io006}$ called UAS:RAS [18]

The characterization of the GBM model is described in detail in Mayrhofer et al., 2017 [17].

Gene expression analysis

The analysis of expression of genes involved in glycolysis in zebrafish brain tumors was performed on previously generated data (GSE74754, https://www.ncbi.nlm.nih.gov/geo/query/acc.cgi?acc=GSE74754). The heatmap was generated using the web application heatmapper (http://www.heatmapper.ca/) .

For gene expression analysis of further samples, total RNA was extracted from larval heads and brains/tumors with TRIzol reagent (Invitrogen). Total RNA was cleaned up using RNeasy Mini Kit

(Qiagen) following the manufacturer's instructions and treated twice with DNase I (1 unit/µg RNA, Qiagen). The RNA concentration was quantified using nanodrop2000 (Thermo Fisher) and VILO superscript KIT (Thermo Fisher) was used for First-strand cDNA synthesis according to the manufacturer's protocol. qRT-PCR analysis was performed using qPCR BIO Sygreen Mix (Resnova - PCR Biosystem) using a standard amplification protocol. The primers used for zebrafish mct1 were: forward 5'-AGCCAGGTGTCATGGATCTCC-3' and reverse 5'-CAACTAATCCCGTGCCTGACA-3'; for hcar1 zebrafish were: forward 5'- GACACGGCTTGGATCTCCTCTA-3' and reverse 5'-TGCCAAGACCATACCCAATGA-3'; for zebrafish rps11 (housekeeping): forward: 5'-ACAGAAATGCCCCTTCACTG-3' and reverse: 5'- GCCTCTTCTCAAAACGGTTG-3'. Real-time PCR was performed with a CFX96 Real-Time PCR Detection System (Bio-Rad) machine. Q-PCR analysis was performed with Microsoft Excel and Graphpad Prism. In all cases, each PCR was performed with triplicate samples and repeated with at least two independent samples.

Immunofluorescence in zebrafish

Adult zebrafish resulting from crosses between zic:Gal4 and UAS:RAS, or from somatic expression of UAS:RAS [19], were screened under a fluorescent stereomicroscope for the presence of GFP-HRAS^{G12V} brain masses. Positive fish (over 90% of screened fish) were sacrificed by MS222 overdose, their brains removed, fixed and sectioned as previously described.

Sections were then washed in PBS (pH 7.4) and incubated primary antibodies diluted in PBS containing 5% normal goat serum and 0.1% triton x-100 at 4°C overnight. The antibody used and their dilutions were as follows: MCT1(Abcam, 1:100) and HCAR (Abcam 1:100), Phospho Histone 3 (Abcam, 1:1000). A secondary antibody conjugated with Alexa 546 (1:250) was used for 2 hours at room temperature, and nuclei were counterstained with DAPI. Images were acquired using an inverted Leica TSP8 confocal microscope. For whole-mount immunofluorescence of 5 day postfertilization (dpf) zebrafish, larvae of the zic: Gal4 line (controls) or zic:Gal4 x UAS:RAS line (tumor) were treated with 20 mM lactate or 10 mM AZ3965 in 1% DMSO in E3, or with 1% DMSO alone. Solutions with the drugs were changed every day starting at 1dpf till 5dpf, when the

larvae were culled by anesthetic overdose, fixed in 4% PFA for 2 to 12 hrs at 4 C, their brains carefully removed under a stereomicroscope and processed with Ph3 antibody, diluted 1:1000 in 5% NGS, 0.5% Triton X100 in PBS overnight. A secondary antibody conjugated with Alexa 546 was used for 6 hours at room temperature. Images were acquired using an inverted Leica TSP8 confocal microscope, after equilibrating the brains in 100% glycerol.

Seahorse on zebrafish

For Seahorse analysis, tumors from adult fish or control brains were dissociated with a pipette tip in the assay medium provided by the manufactory, passed through a 40 mM sieve and counted. 50K cells were seeded on poly-L-Lysin coated Seahorse XFP plates and incubated for 20 min in the absence of CO2 before adding medium up to a final volume of 180 ul. XF mitostress test kit including oligomycin, carbonyl cyanide p-trifluoromethoxy-phenylhydrazone (FCCP), and Rotenone A were obtained from Seahorse Bioscience Inc. (Billerica, MA, USA). XFp cell culture plates, sensor cartridges and XF base medium were also purchased from Seahorse Bioscience Inc. The Agilent Seahorse XFp Sensor Cartridge is hydrated in

Agilent Seahorse XF Calibrant at 28 °C in a non-CO2 incubator overnight. Control and tumor zebrafish brain cells are plated in the Agilent Seahorse XFp Cell Culture Miniplate at the desired density (50 K per well) using the appropriate cell culture growth medium. PBS 1X is added to the chambers to prevent evaporation of the culture medium. Within 1 hour from plating the Agilent Seahorse XFp Cell Culture Miniplate is put into a 28 °C non-CO2 incubator for 1 hour prior to the assay.

Mito stress test assay

Assay medium is prepared by supplementing Agilent Seahorse XF Base Medium with 1 mM pyruvate, 2 mM glutamine, and 10 mM glucose bringing the pH to 7.4 with 0.1 N NaOH. Cells are placed in 28°C incubator with 5% CO2.

Injections of oligomycin, FCCP and Rotenone A were diluted in the assay medium following Agilent Seahorse XFp Mito Stress Test User Guide and loaded into ports A, B and C, respectively. The machine was calibrated, and the assay was performed using mito stress test

assay protocol as suggested by the manufacturer (Seahorse Bioscience, Billerica, MA, USA). ECAR was measured under basal conditions followed by the sequential addition of oligomycin, FCCP and Rotenone A.

Data analysis

The XF reports of mito stress data were analysed with the freeware Wave and exported to Excel and Prism for further analysis and visualization.

Human gene expression

Dataset selection

The NCBI Gene Expression Omnibus (GEO) database (http://www.ncbi.nlm.nih.gov/geo/) [20] was used to select transcriptomes datasets of interest. Mesh terms "human", "glioblastoma", and "tumor grade", were used to identify the datasets. We sorted the datasets by the number of samples (High to Low), age and sex of the participants and by the clinical data made available by the authors. We selected the GSE108474 dataset [21] over the others available for the number of subjects recruited (541),

for the availability of clinical data (tumor staging) and for the variety of tumors analyzed (glioblastoma, oligodendrocytoma, astrocytoma and normal subjects).

Data processing, experimental design and statistics

To process and identify Significantly Different Expressed Genes (SDEG) within the datasets, we used the MultiExperiment Viewer (MeV) software (The Institute for Genomic Research (TIGR), J. Craig Venter Institute, La Jolla, USA). In cases where multiple genes probes have insisted on the same GeneID NCBI, we used those with the highest variance. For GSE108474 we performed a statistical analysis with GEO2R, applying a Benjamini & Hochberg (False discovery rate) [22–24].

Table 2; Samples selected from GSE108474

Disease type	Number	Grade
NT	28	Negative
Astrocytoma	148	G2=65; G3=58; Na=25
Oligodendrocytoma	67	G2=30; G3=23; Na =14
Glioblastoma	221	G4=130; Na =91

G= tumor grade; Na= not assigned; NT= non tumor

Significant differences between groups were assessed using the Ordinary one-way ANOVA test, and Tukey's multiple comparisons test correction was performed to compare data between all groups. Correlations were determined using Pearson correlation. All tests were two-sided and significance was determined at adjusted p value 0.05. The dataset selected was transformed for the analysis in Z-score intensity signal. Z score is constructed by taking the ratio of weighted mean difference and combined standard deviation according to Box and Tiao (1992) [25]. The application of a classical method of data normalization, z-score transformation, provides a way of standardizing data across a wide range of experiments and allows the comparison of microarray data independent of the original hybridization intensities. The z-score it is considered a reliable procedure for this type of analysis and can be considered a state-of-the-art method, as demonstrated by the numerous bibliography [26–37]. The efficiency of each biomarker across the different tumor grade was assessed by the receiver operating characteristic (ROC) curve analyses [38–40]. The ROC curves analyzed brain biopsies of healthy subjects (NT) vs glioblastoma patients, astrocytoma vs glioblastoma, and oligodendroglioma vs

glioblastoma. The area under the ROC curve (AUC) and its 95% confidence interval (95% CI) indicates diagnostic efficiency. The accuracy of the test with the percent error is reported [41].

RESULTS

We first analysed the effects of lactate on 3 human GBM cell lines (i.e. U-87 MG, A-172 and U-251 MG) by performing a clonogenic assay on lactate exposed cells (**figure S1**). We observed that lactate induced an increase of about 2-fold of both number (78.3 ± 9.0 control versus 151.0 ± 17.1 lactate) and area (123.2 ± 8.2 control versus 215.0 ± 30.4 lactate) of colonies of U-87 MG cells (**figure S1**). Interestingly, analysis of clonogenicity on A-172 revealed that lactate reduced the total number of colonies (35.7 ± 0.3 control versus 21.0 ± 1.2 lactate, **figure S1**), but dramatically affected the area of colonies that was more than 4-fold increased as compared to control cultures (731.3 ± 0.5 control versus 3470.8 ± 30.3 lactate, **figure S1**). We also repeated our analysis on U-251 MG cell, that showed similar response to lactate as U-251 MG cells, with a significant increase of the total number of colonies (26.5 ± 0.9 control versus 38.0 ± 3.6 lactate) and mean colony area (700.0 ± 7.1 control versus 1409.4 ± 28.0 lactate, **figure S1**).

We then moved to compare the effect of increased levels of extracellular lactate with the selective stimulation of the lactate

receptor hydroxycarboxylic acid receptor 1 (HCAR1) mediated by 3,5-dihydroxybenzoic acid (3,5-DHBA). We observed in all tested cells a significant increase of normalized cell index after lactate exposure (**figure 1a-c**), confirmed by an increase of the total area under the curve for U-87 MG (76.5 ± 0.4 lactate versus 38.9 ± 0.2 control, **figure 1a**), A-172 (86.6 ± 0.8 lactate versus 64.4 ± 0.4 control, **figure 1b**) and U-251 MG (78.1 ± 1.1 lactate versus 40.5 ± 0.8 control, **figure 1c**). 3,5-DHBA stimulation was also able to induce similar effects on cell proliferation on U-87 MG, A-172 and U-251 MG cell line, showing increased normalized cell index in all tested cell lines (**figure 1a-c**), confirmed by an increase of the total area under the curve for U-87 MG (106.3 ± 2.4, **figure 1a**), A-172 (134.6 ± 1.1, **figure 1b**) and U-251 MG (122.9 ± 1.3, **figure 1c**). We then tested whether lactate affects cell migration of GBM cells. Interestingly, we observed a reduced % of wideness of scratch assay test at 24 and 48 hours in all tested cells lines (**figure 1d-g**). We also confirmed the effects of HCAR stimulation through 3,5-DHBA on cell migration, finding a significantly reduced % of wideness of scratch assay test at 48 hours in all tested cells lines (**figure 1d-g**).

In an effort to link lactate, as a positive modulator of cell proliferation and migration, to the underlying molecular mechanisms activated in GBM cell lines, we performed western blot analysis for lactate transporters MCT1 and MCT4, and for β-Catenin and E-Cadherin on control and lactate treated U-87 MG, A-172 and U-251 MG cells.

We found that U-87 MG cells responds to increased levels of extracellular lactate by increasing the levels of MCT1 transporter of about 2.5-fold as compared to control cultures and slightly, but significantly, reducing MCT4 expression levels (**figure 2a**).

Importantly, the β-Catenin protein levels were found to be significantly increase of about 6-fold in lactate exposed U-87 MG cells and such a modulation was coupled with reduced expression levels of E-Cadherin (**figure 2a**).

Notably, analysis of A-172 and U-251 MG exposed to increased extracellular lactate levels, revealed some differences in cellular responses as compared to U-87 MG cells. Indeed, we confirmed that exposure to lactate increased MCT1 and β-Catenin expression levels in both A-172 (**figure 2b**) and U-251 MG (**figure 2c**) but showed that both cell lines respond to lactate also inducing significantly higher MCT4, increased of about 1.2-fold in both cell lines, and E-Cadherin

expression levels (**figure 2b-c**).

Given the evidence on cellular modulation exerted by increased extracellular levels of lactate, we sought to link molecular mechanisms underlying these phenomena with the activation of lactate receptor HCAR1. We first investigated HCAR1 mRNA expression levels on U-87 MG, A-172 and U-251 MG cell lines after exposure to lactate, finding a significant increase of HCAR1 mRNA levels in all tested cells at 24 hours (**figure 2d**). We then moved to evaluate the effects of 3,5-DHBA, confirming a significant increase of HCAR1 mRNA levels at 24 hrs post 3,5-DHBA incubation in all tested cell lines (**figure 2e**).

To find whether HCAR1 selective stimulation was able to increase lactate transporters MCT1 and MCT4 we also checked the mRNA expression levels of these transporters, finding that 3,5-DHBA stimulation was able to significantly increase MCT1 expression of about 25-fold, 5-fold and 13-fold in U-87 MG, A-172 and U-251 MG, respectively (**figure 2f**). Such evidences were coupled with contrasting data on the other tested transporter MCT4. Indeed, we observed that U-87 MG cells respond to 3,5-DHBA stimulation by

increasing MCT4 mRNA expression of about 2-fold (**figure 2g**), but A-172 showed no significant changes in MCT4 expression and U-251 MG cells showed a significant reduction of MCT4 expression upon treatment with 3,5-DHBA as compared to untreated cells (**figure 2g**).

To further expand our evidences on molecular mechanisms induced by the increase of extracellular lactate, we analyzed a panel of mRNAs of genes involved in mitochondrial activity and energy metabolism. Our data show that U-87 MG significantly increase of about 4-fold the relative mRNA levels of transcription factor A mitochondrial (TFAM), PPARG coactivator 1 alpha (PGC1a) and sirtuin 1 (SIRT1) (**figure 3a-b**), coupled with an overall increase of ATP synthase (ATP syn), cytochrome c oxidase subunit 4 (COX IV) and COX II, mitochondrial Cytochrome b (CYTB) and mitochondrial NADH-ubiquinone oxidoreductase chain 4 (ND4, **figure 3a**), when exposed to lactate for 24 or 48 hours as compared with untreated cells (**figure 3a-b**). These observations were confirmed in A-172 (**figure 3c-d**) and U-251 MG cell lines (**figure 3e-f**). Specifically, we observed superimposable effects on A-172 as compared to U-87 MG cells, where U-251 MG showed an increase of about 15-fold of TFAM,

PGC1a and SIRT1 at 48 hours as compared to untreated cells (**figure 3f**), coupled with a slight reduction of COX IV mRNA at the same timepoint (-1.87 ± 0.1 log_2 fold change over control, **figure 3e**). We also performed a computer-assisted analysis of mitotracker fluorescence intensity on control versus lactate treated cells, finding that lactate was able to significantly increase cytoplasmic mitotracker intensity 18 hrs post treatment (**figure 3g-h**).

To link intracellular mediators of mitochondrial fitness with HCAR stimulation, we performed an mRNA expression level analysis of PGC1a, TFAM, SIRT1, ATP syn, COX II and COX IV on 3,5-DHBA stimulated cells. Our analysis revealed that U-87 MG cells exposed to 3,5-DHBA recapitulate the molecular mRNA activation observed with lactate (**figure 4a-b**). Indeed, all tested genes, except for TFAM, were significantly increased in cultures exposed to HCAR stimulation (**figure 4b**). These data were confirmed in A-172 cells that showed increased levels of all tested genes upon 3,5-DHBA stimulation (**figure 4c-d**). Finally, U-251 MG showed a very similar mRNA expression profiles, but we observed that HCAR stimulation through

3,5-DHBA did not modulate PGC1a expression at tested timepoint on this cell line (**figure 4e-f**).

To finally link HCAR stimulation with the effects on mitochondria observed on GBM cell lines exposed to increased extracellular lactate levels, we performed a mitotracker analysis, finding a significant increase of normalized intensity in 3,5-DHBA stimulated cells as compared to control cultures (**figure 4g**).

Given the capability of extracellular lactate to modulate β-Catenin and E-Cadherin expression levels, we performed a western blot analysis on 3,5-DHBA stimulated A-172 cells. Our analysis revealed that HCAR1 activation induces a significant increase of β-Catenin protein expression levels as compared to control cultures and this phenomenon was coupled with a significant reduction of E-Cadherin (**figure 4h**), revealing that lactate may also act via additional mechanisms that induce E-Cadherin not related to HCAR1 activation.

To investigate whether lactate accumulation, resulting from increased glycolysis, may have similar effects *in vivo*, we used a zebrafish model of glioblastoma [17] (**figure 5a**), and analysed the metabolic phenotype of these tumors. Comparison of the expression

levels of 29 genes encoding for enzymes and transporters involved in the glycolytic pathway acquired through RNA-Seq (GSE74754, https://www.ncbi.nlm.nih.gov/geo/query/acc.cgi?acc=GSE74754), revealed increased expression (log2 FC >1.2, P-value <0.001 or adjusted P-value <0.05) of 26 out of 29 genes, with *aldh1a3, hk2 and hcar1-3* being the most upregulated in tumors (**figure 5b**). We then performed a mitostress test on freshly dissociated zebrafish control and tumor brains using the Seahorse XFp apparatus. This test confirmed that upon blockage of energy production through mitochondrial respiration, zebrafish GBM cells experience a huge increase of the extracellular acidification rate (ECAR), indicating a prominent role of anaerobic glycolysis in energy production, accompanied by increased proton leak (leading to high ROS production) and lower ATP yield (**figure 5c**). Staining for MCT1 and HCAR1 in sections of zebrafish brain tumors revealed an increase in the number of both MCT1+ and HCAR1+ cells (**figure 5d**), whereas q-PCR analysis of mRNA expression for *mct1* and *hcar1* revealed a significant increase in expression for *mct1* in adult tumors compared to control brain, and a significant increase in expression of *hcar1* in

both adult brain tumors and in 5days post-fertilization (dpf) larvae expressing oncogenic RAS (**figure 5e**).

Then, we evaluated the effects of exposing to lactate or to the MCT1 inhibitor, AZ3965 (AZD), on the proliferation rate of control brains and brains expressing oncogenic RAS, using immunostaining for a mitotic marker (phospho-serine 10 on histone 3, PH3). Incubation of developing larvae from 1 to 5 dpf with 20 uM lactate induced a significant increase in proliferation in brains expressing oncogenic RAS, but not in control brains, while treatment with 10 uM AZD did not affect the proliferation rate in either control or RAS expressing brains (**figure 5f).**

MCT1 gene expression analysis as a diagnostic and prognostic marker of glioma

The MCT1 gene expression analysis obtained from the GSE108474 dataset showed that there were significant differences when the expression levels obtained from brain biopsies of glioblastoma patients were compared to the other brain tumors stages. (**figure 6**). Specifically, patients with glioblastoma expressed significantly higher levels of the MCT1 messenger in the brain than patients with oligodendrocytoma ($p<0.0001$), astrocytoma ($p<0.0001$), or healthy

subjects (p<0.0001) (figure 6a). This finding was confirmed by the significantly positive correlation between MCT1 expression levels and tumor grade (r = 0.4026; p = 0.0223) (figure 6b). According to these results, we investigatated the prognostic potential of MCT1 expression in the progression of main brain tumors. Currently the expression analysis of Isocitrate Dehydrogenase (NADP (+)) 1 (IDH1) and the identification of its main mutations (e.g. R132H) are used for glioma diagnosis and prognosis [42]. By carrying out a Pearson correlation analysis between MCT1 and IDH1 brain tumor expression levels, we highlighted that in glioblastoma patients the expression levels of the two genes were significantly closely inversely correlated (r = -0.4163, p <0.0001) (**figure 6c**). Furthermore, in order to evaluate the potential diagnostic ability of MCT1 gene expression to discriminate against the brain tumors stages, we performed a Receiver operating characteristic (ROC) analysis. We confirmed the diagnostic ability of MCT1 to discriminate the glioblastoma patients from healthy subjects (AUC=0.7558, p<0.0001) (**figure 6d**) or from the patients affected to astrocytoma (AUC=0.7775, p<0.0001) (figure 6e) or oligodendrocitoma (AUC=0.8104, p<0.0001) (**figure 6f**).

DISCUSSION

Cell metabolism and its related intercellular signalling has been shown to be of great importance in a number of physiological and pathological processes [43].

In the present study, we first evaluated the effects of lactate on three human GBM cell lines, finding that it increases both migration and cell proliferation. Such a phenomenon was linked to a potential lactate dependent HCAR1 activation, as observed using 3,5-DHBA, a selective HCAR1 agonist.

Several authors showed that stimulation of HCAR1 leads to the activation of cell survival signalling promoting cell proliferation via the inhibition of apoptosis and stimulates the secretion of several angiogenic factors in a PI3K/Akt-CREB signalling pathway-dependent manner [44]. Interestingly, an essential part of the repair process after a neonatal brain injury is the generation of new cells by increase of proliferation and differentiation of stem cells, Lauritz H. K. et al., by neurosphere assays, demonstrated that the cells lacking HCAR1 had reduced proliferation ability [45].

Moreover, MCT1 is mainly used by oxidative cells to intake extracellular lactate and MCT4 is mainly used to release accumulated lactate into the extracellular milieu, in many cases by hypoxic and/or highly glycolytic cells [46–48]. Our data support the hypothesis that lactate leads GBM cells to increase HCAR1, acting as a sensor, levels and MCT1, mediating lactate intake from the extracellular milieu. This phenomenon is coupled with increased mitochondrial content and fitness, thus prompting GBM cells towards oxidative metabolism. It is worth noticing that this mechanism is not related to the increased lactate level itself but is dependent on the agonism on HCAR1 receptor. Indeed, we were able to reproduce these metabolic reshaping using the selective HCAR1 agonist 3,5-dhba. Consistently, a study performed in GPR81-silenced pancreatic cancer cells led to reduced mitochondrial activity and survival in several cancer cell [49]. In particular, several cancer cell types, including colon, breast, lung, cervical, and pancreatic showed an increase of HCAR1 expression and functional studies indicated that it is important for lactate regulation of genes involved in lactate uptake and metabolism. Moreover, HCAR1 is critical for cancer cell survival only when glucose was absent and in the presence of lactate [50].

Interestingly, we observed critical differences in cell response to HCAR1 activation analyzing MCT4 levels. Indeed, we observed that 24 hrs of exposure to lactate mediated a reduction of MCT4 protein levels in U-87 MG, whether we found a significant MCT4 increase in both U-251 MG and A-172. Such differential response to lactate among tested cell lines, may be linked to the metabolic reshaping of these cells. Noteworthy, quantification of the main mitochondrial genes revealed that U-87 MG cells underwent a rapid increase of mitochondrial content, although less pronounced versus basal levels, as compare to that of A-172 and U-251 MG. Our data suggest that U-87 MG have a different response as compare to the other cell lines in terms of timing to repurpose their transporters and metabolism. Indeed, upon 3,5-DHBA stimulation of HCAR1 we observed a significant increase of MCT4 in U-87 MG, where we obtained contrasting results for A-172 and U-251 MG.

This set of experiments suggest that HCAR1 activation induces MCT1 increase, thus mediating lactate intake in stimulated cells. It is therefore conceivable that intercellular metabolism and mitochondrial content are closely related to HCAR1 activation by several pathways including lactate as a metabolite and other

receptor-mediated mechanisms. To this regard, Zaho Y., et al., showed that increasing lactate concentration in liver tumor microenvironment could activate HCAR1 receptor and facilitate MCT1-mediated uptake of lactate, leading to increased ATP production and decrease of the AMP:ATP ratio in the intracellular compartment [51]. Tumor cells stimulate mitochondrial biogenesis not only for proliferation but also for promoting malignant transformation, in migration and invasiveness and during tumor adaptation to hypoxia [52,53]. As previously mentioned, we observed an increase of mitochondrial biogenesis in GBM cell treated with lactate or HCAR1 inducer, this phenomenon could be due to the increase of lactate uptake after MCT1 overproduction. Moreover, we also showed that the increase of mitochondrial mass also induces an increase of OXPHOS gene expression. Exogenous treatment of lactate in various tumor cell lines induced an increase in ROS levels. We hypothesize that this latter increase in oxidative state determines an enhances of mitochondrial biogenesis such as showed by increase of PGC1a, SIRT1 expression and oxidative genes.

Interestingly, our results indicate also that HCAR1 activation promotes the modulation of b-catenin and e-cadherin expression

suggesting that lactate participates to the epithelial-mesenchymal transition (EMT) in GBM. Several studies have been conducted investigating the metabolic changes during EMT in breast, lung, and ovarian cancers, following an increased recognition of metabolic reprogramming as a hallmark of tumor development [54–56].

Lactate produced and exported by tumor cells can be also used by adjacent tumor cells, in the tumor microenvironment, including endothelial cells and stromal cancer-associated fibroblasts, reprogramming their functions, and contributing to tumor progression [57]. Consequently, several authors hypothesized that lactate might also modulate the same epigenetic mechanisms in adjacent normal cells modulating also EMT processes [58,59].

Given the insights coming from in vitro experiment on relevant human GBM cell lines, we enrolled a HRAS overexpressing zebrafish model of GBM to test whether similar metabolic changes are taking place in this model. Our data confirmed a widespread upregulation of glycolytic enzymes, with upregulation of HCAR1, thus indicating a prominent role for lactate signalling. In the tumor microenvironment HCAR1 upregulation was coupled with a significantly increased

proton leak and less efficient ATP production. The increased expression of lactate transporters (*mct1*) and sensor (*hcar1*) was already present at 5 dpf, when tumors start to grow.

Lactate exposure determined a significant increase in proliferating PH3 positive cells in RAS-overexpressing zebrafish brain, but not in control brains, and this was reverted by selective inhibition of MCT1. This evidence suggests that lactate intake support cell proliferation in cancer and that metabolic reshaping is a critical stimulus in GBM microenvironment. Thus, both cell culture and in vivo studies, using different approaches and different genes, converge toward the same conclusion, i.e. that glycolysis is prominent in GBM and leads to massive lactate production which shapes the microenvironment towards an aggressive phenotype and represent a valid therapeutic target.

Our data from human GBM biopsies were also consistent with preclinical evidence we are providing herein. We observed that in high proliferative GBM biopsies, KI67 negative cells were expressing significantly higher levels of MCT1 as compare to proliferative cells and low proliferative GBM cells. This indicates that GBM cells response to lactate, besides sustaining metabolic reshaping and

response, it favours proliferation of neighbourhood cells by cooperating with their glycolytic metabolism, sensing and removing extracellular lactate. Our data is consistent with other studies in patients with advanced cancer showing that MCT-1 inibition may provide a significant role in cancer growth and progression and may represent a druggable target for development of new therapeutic strategies (ClinicalTrials.gov identifier (NCT number): NCT01791595). Further confirmation of our study was obtained by analyzing the human GSE108474 dataset. The analysis allowed us to highlight that MCT1 is significantly modulated during the progression of the disease. In particular, significant expression changes were highlighted with the increase in the degree of malignancy. Furthermore, our results showed that MCT1 can potentially be used in order to discriminate patients with glioblastoma versus those with astrocytoma and oligodendrocytoma. These data are in agreement with the current bibliography which considers MCT1 a new prognostic biomarker and potentially target in human glioblastoma [60]. Interestingly, the correlation analysis between MCT1 and IDH1 brain expression levels in glioblastoma patients was inversely proportional, further

confirming recently obtained data in which mutant IDH1 expression is associated with down-regulation of monocarboxylate transporters [61].

In conclusion, we showed that lactate is involved in various mechanisms favoring tumor development and progression. In particular, lactate possesses a dual role being involved in the metabolic changes of tumor cells and acting as a molecule promoting cellular signaling through its membrane receptors. The ability to metabolically shift from glycolytic to oxidative metabolism and vice versa, is likely to confer an advantage in survival, progression and drug resistance. A glycolytic metabolism (Warburg effect) certainly in the first phase of disease expansion, determines an advantage in tumor proliferation. The lactate thus produced in the tumor microenvironment favors, on the one hand, the immune escape mechanisms, on the other, it may modify the metabolism of the adjacent tumor cells, becoming more oxidative and therefore more resistant also to antiblastic therapies. Therefore, lactate metabolism may be considered as a therapeutic target to develop novel pharmacological strategies to GBM therapy and improve the outcome and quality of life of such patients.

FIGURE LEGEND

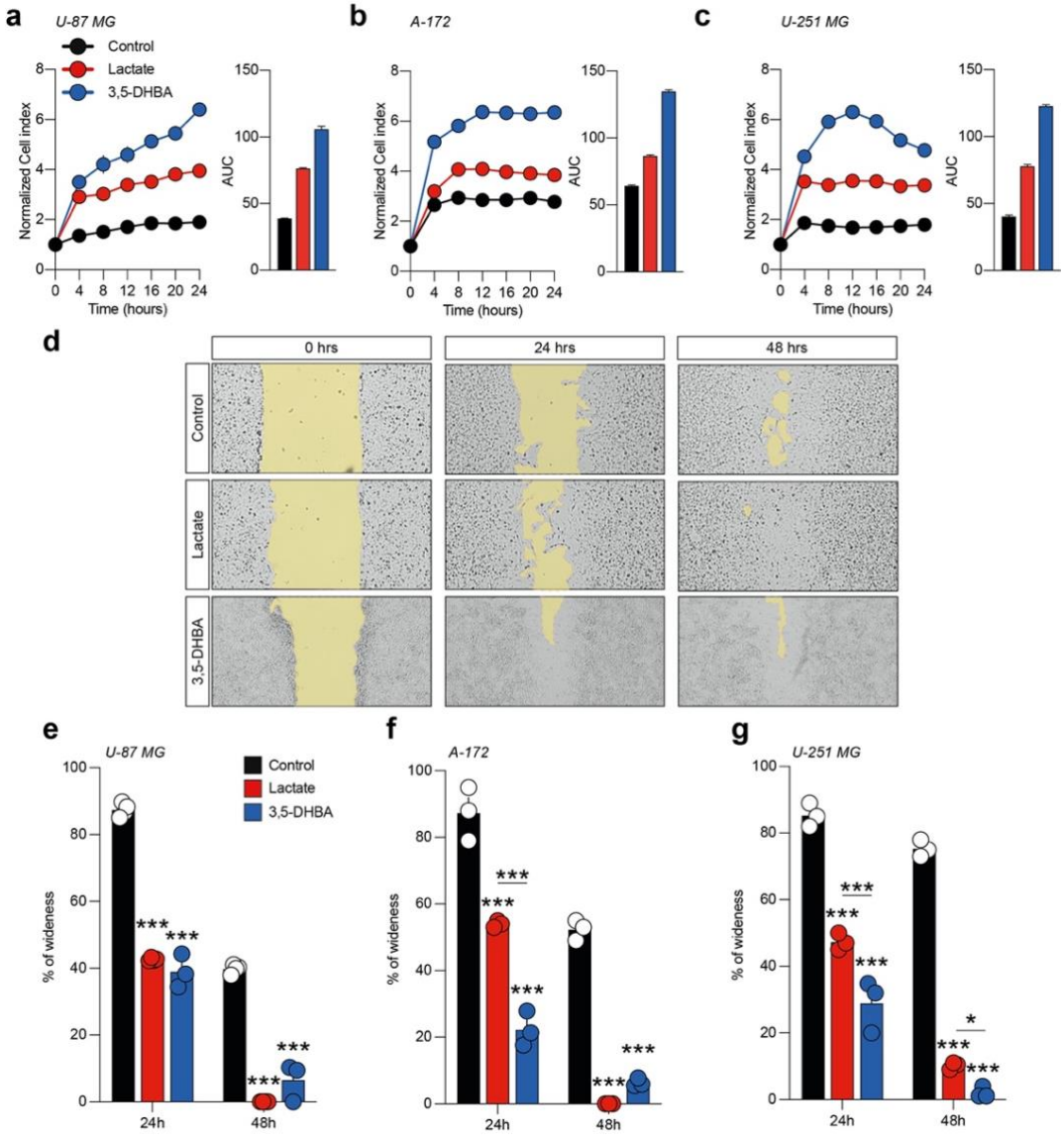

Figure 1.

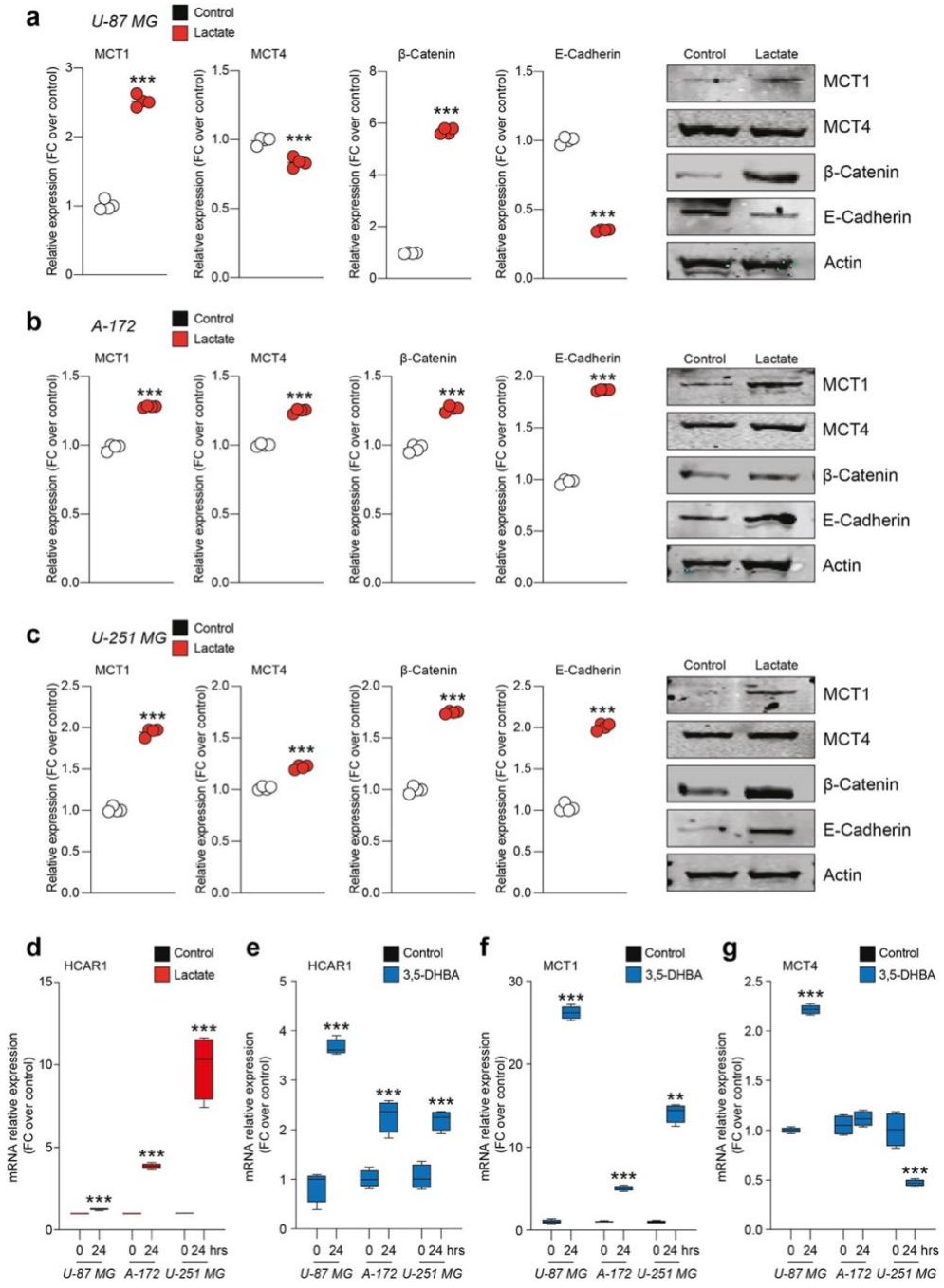
a
U-87 MG
Control
Lactate
MCT1
MCT4
β-Catenin
E-Cadherin
Relative expression (FC over control)
Control
Lactate
MCT1
MCT4
β-Catenin
E-Cadherin
Actin
b
A-172
c
U-251 MG
d
HCAR1
mRNA relative expression (FC over control)
0 24 0 24 0 24 hrs
U-87 MG
A-172
U-251 MG
e
HCAR1
3,5-DHBA
f
MCT1
g
MCT4

Figure 2.

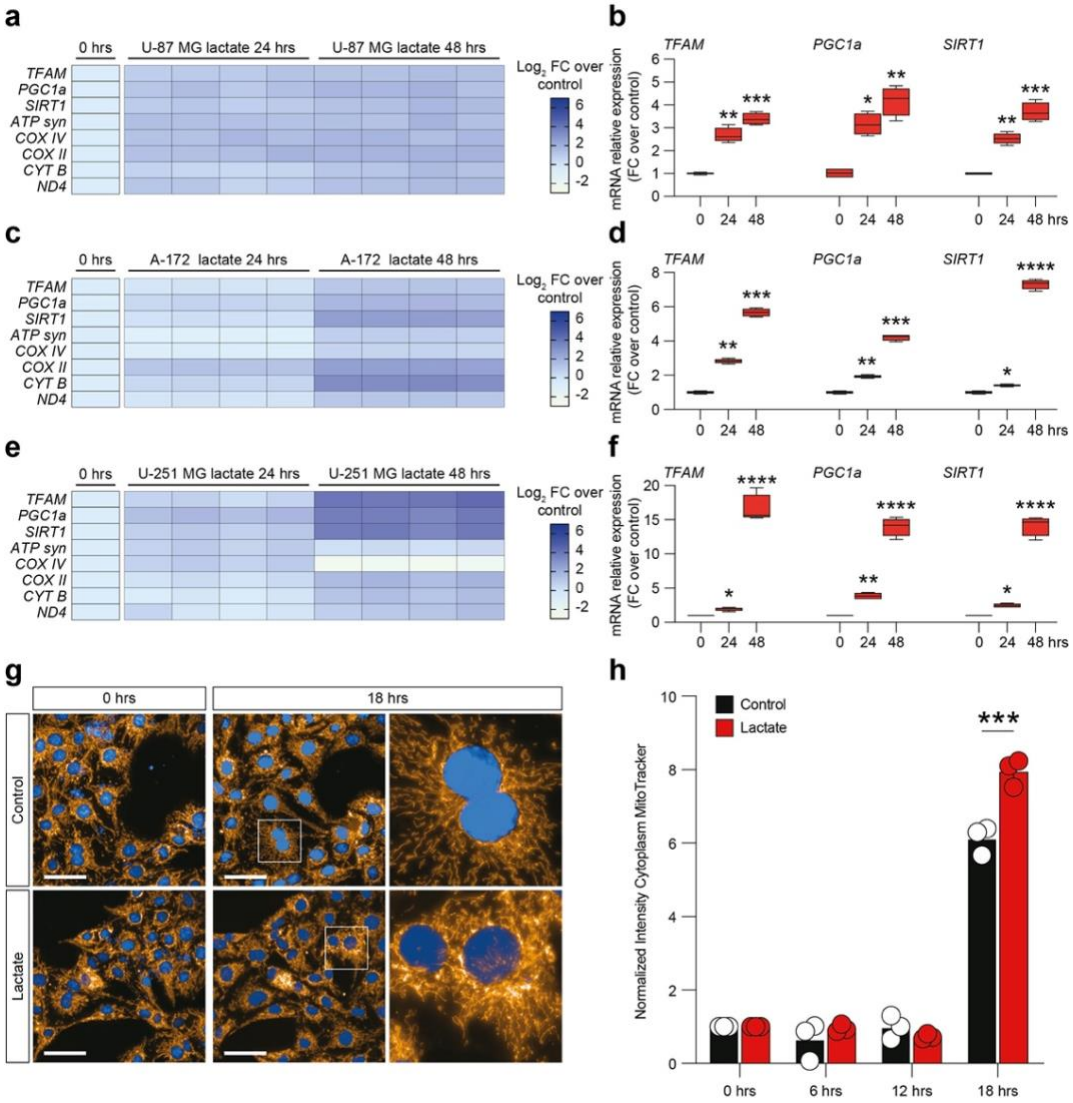
a
0 hrs
U-87 MG lactate 24 hrs
U-87 MG lactate 48 hrs
TFAM
PGC1a
SIRT1
ATP syn
COX IV
COX II
CYT B
ND4
Log2 FC over control
b
TFAM
PGC1a
SIRT1
mRNA relative expression (FC over control)
0 24 48 hrs
c
A-172 lactate 24 hrs
A-172 lactate 48 hrs
d
e
U-251 MG lactate 24 hrs
U-251 MG lactate 48 hrs
f
g
18 hrs
Control
Lactate
h
Control
Lactate
Normalized Intensity Cytoplasm MitoTracker
0 hrs
6 hrs
12 hrs
18 hrs

Figure 3.

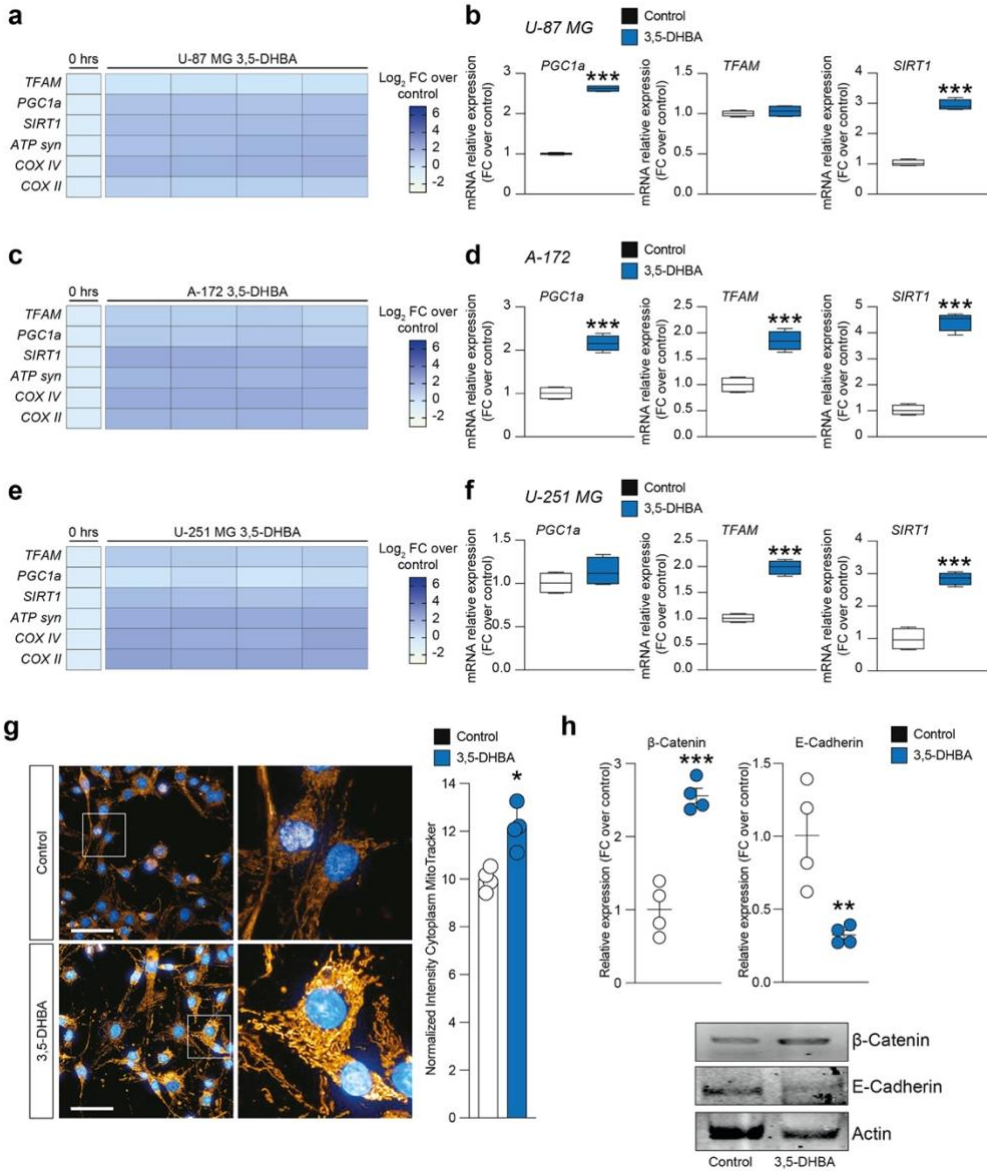
a
0 hrs
U-87 MG 3,5-DHBA
TFAM
PGC1a
SIRT1
ATP syn
COX IV
COX II
Log2 FC over control
b
U-87 MG
Control
3,5-DHBA
PGC1a
TFAM
SIRT1
mRNA relative expression (FC over control)
c
A-172 3,5-DHBA
d
A-172
e
U-251 MG 3,5-DHBA
f
U-251 MG
g
Control
3,5-DHBA
Normalized Intensity Cytoplasm MitoTracker
h
β-Catenin
E-Cadherin
Relative expression (FC over control)
Actin

Figure 4.

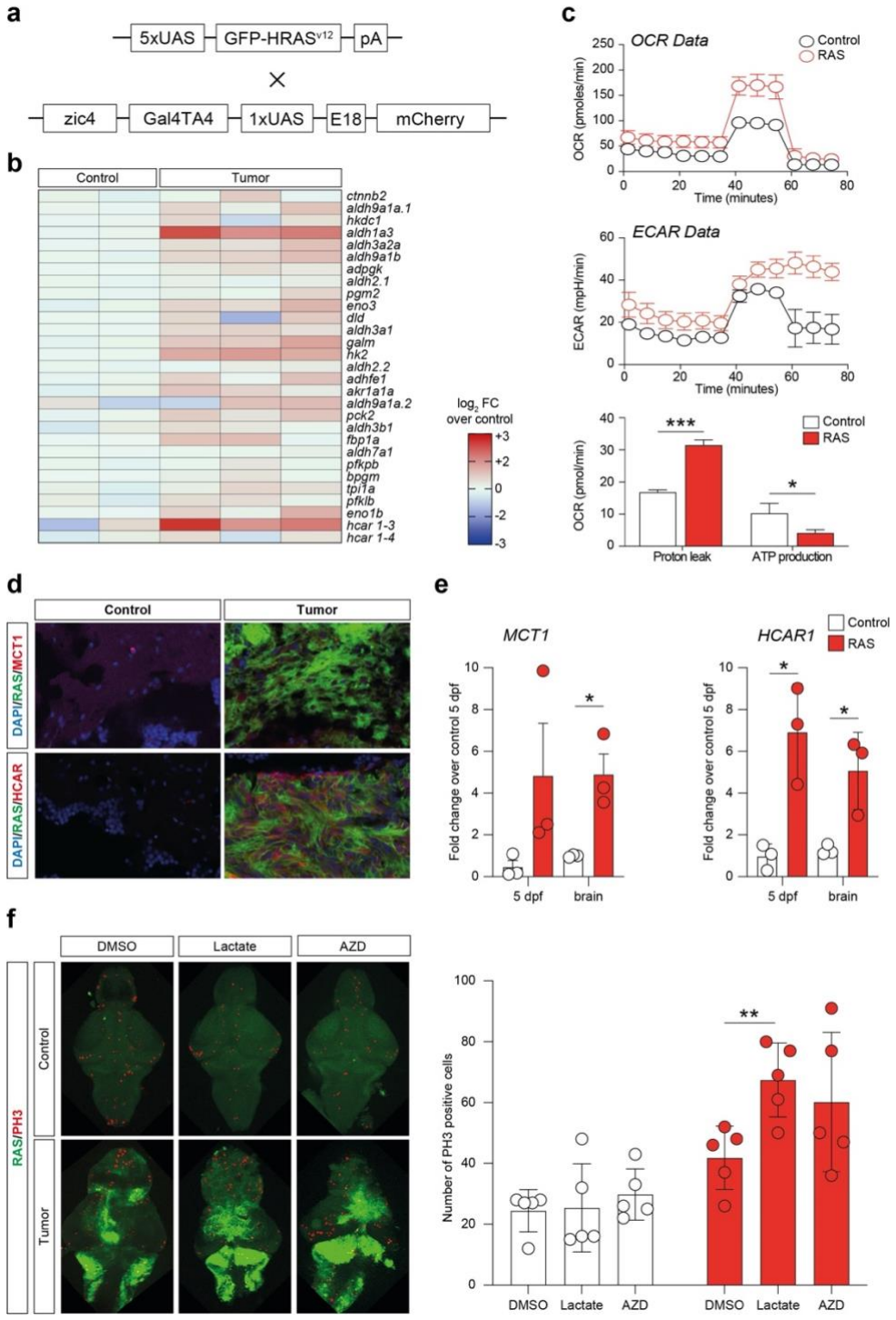
a
5xUAS
GFP-HRASv12
pA
×
zic4
Gal4TA4
1xUAS
E18
mCherry
b
Control
Tumor
ctnnb2
aldh9a1a.1
hkdc1
aldh1a3
aldh3a2a
aldh9a1b
adpgk
aldh2.1
pgm2
eno3
dld
aldh3a1
galm
hk2
aldh2.2
adhfe1
akr1a1a
aldh9a1a.2
pck2
aldh3b1
fbp1a
aldh7a1
pfkpb
bpgm
tpi1a
pfklb
eno1b
hcar 1-3
hcar 1-4
log2 FC over control
+3
+2
0
-2
-3
c
OCR Data
Control
RAS
OCR (pmoles/min)
Time (minutes)
ECAR Data
ECAR (mpH/min)
OCR (pmol/min)
***
*
Proton leak
ATP production
d
Control
Tumor
DAPI/RAS/MCT1
DAPI/RAS/HCAR
e
MCT1
HCAR1
Fold change over control 5 dpf
5 dpf
brain
f
DMSO
Lactate
AZD
RAS/PH3
Control
Tumor
Number of PH3 positive cells
**

Figure 5.

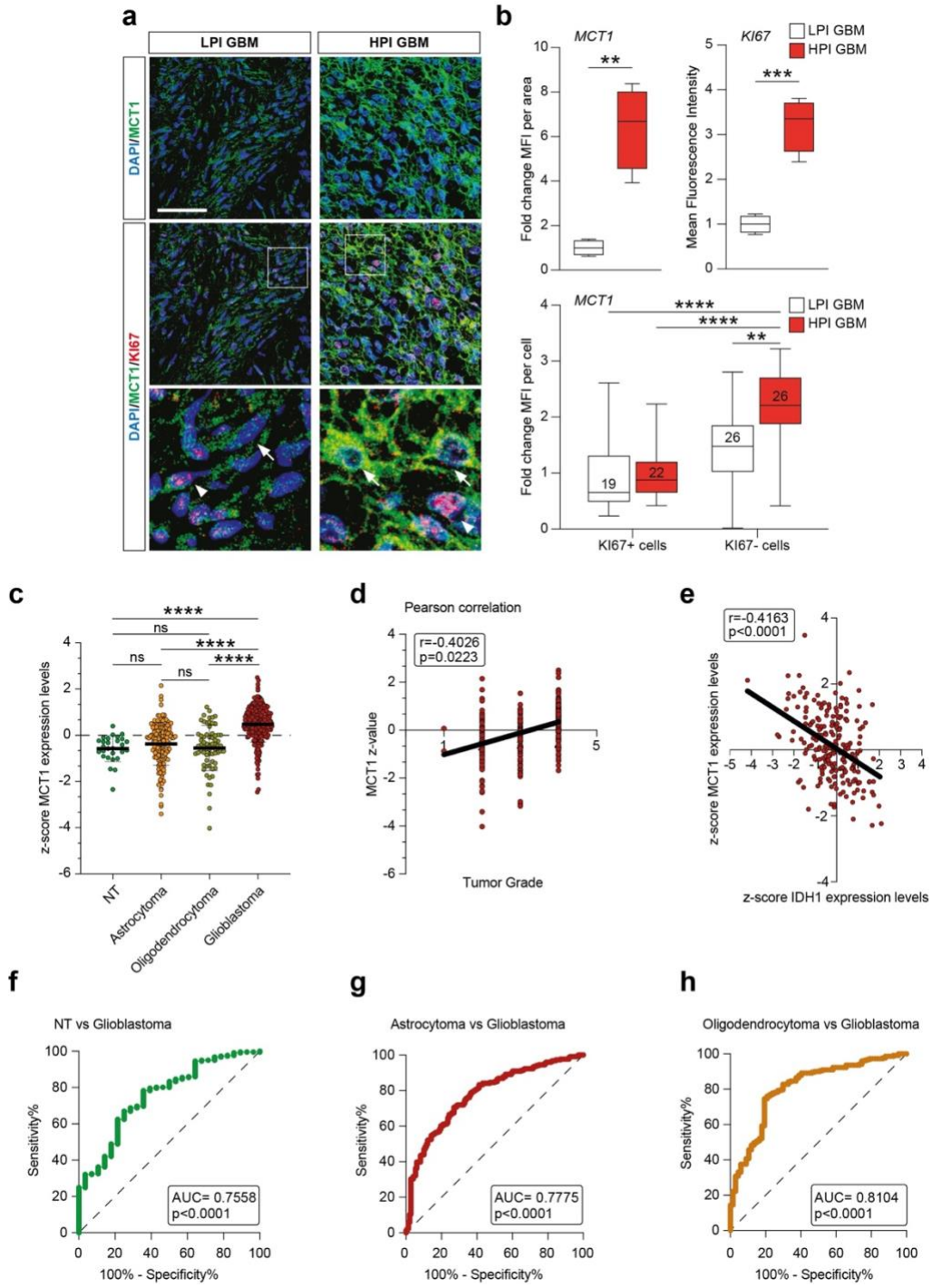
a
LPI GBM
HPI GBM
DAPI/MCT1
DAPI/MCT1/KI67
b
MCT1
KI67
LPI GBM
HPI GBM
Fold change MFI per area
Mean Fluorescence Intensity
Fold change MFI per cell
KI67+ cells
KI67- cells
c
z-score MCT1 expression levels
NT
Astrocytoma
Oligodendrocytoma
Glioblastoma
d
Pearson correlation
r=-0.4026
p=0.0223
MCT1 z-value
Tumor Grade
e
r=-0.4163
p<0.0001
z-score MCT1 expression levels
z-score IDH1 expression levels
f
NT vs Glioblastoma
AUC= 0.7558
p<0.0001
Sensitivity%
100% - Specificity%
g
Astrocytoma vs Glioblastoma
AUC= 0.7775
p<0.0001
h
Oligodendrocytoma vs Glioblastoma
AUC= 0.8104
p<0.0001

Figure 6.

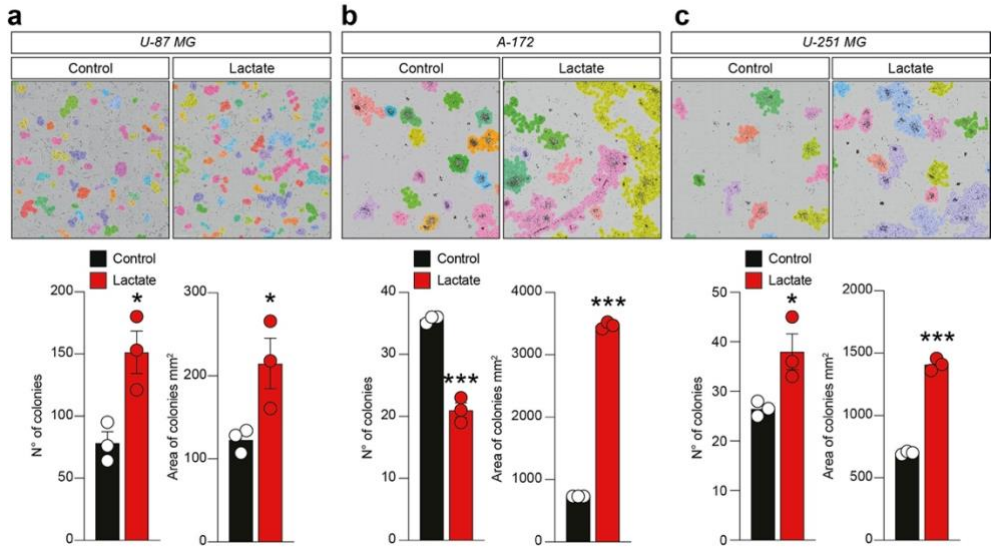

Supplementary Figure 1

FIGURE LEGENDS

Figure 1. Lactate and 3,5-DHBA promote glioblastoma cell proliferation and migration

Real-time cell proliferation monitoring by xCELLigence system following treatments with Lactate and 3,5-DHBA of U-87 MG cells (a), A-172 cells (b) and U-251 cells (c). Cell index values were normalized at the time of pharmacological treatments in order to obtain a normalized cell index. Each line is expressing the average of four different experiments.

Analysis of human glioblastoma cell migration through a wound healing assay following treatments of U-87 MG cells (e), A-172 cells (d-f) and U-251 MG cells (g) with Lactate and 3,5-DHBA. Figures presented are the representative of at least three independent experiments (means ± SEM). p values < 0.05 were considered to be statistically significant (*$p < 0.05$; **$p < 0.01$; ***$p < 0.001$).

Figure 2. Lactate regulates the expression of MCTs and EMT markers in Glioblastoma cells.

MCT1, MCT4, B-Catenin and E-Cadherin protein expression in U-87 MG cells (a), A-172 cells (b) and U-251 MG cells (c) following 72 h of lactate treatment. Figures presented are the representative of at least four independent experiments and values represent the means ± SEM of experiments performed in quadrupled.

HCAR1 gene expression (d) in U-87 MG, A-172 and U-251 MG cells following 24 h of lactate treatment. HCAR1 (e), MCT1 (f) and MCT4 (g) gene expression in U-87 MG, A172 and U-251 MG cells following 24 h of 3,5-DHBA treatment.

Values represent the means ± SEM of experiments performed in quadrupled. p values < 0.05 were considered to be statistically significant (*p < 0.05; **p < 0.01; ***p < 0.001 vs untreated).

Figure 3.

Lactate promotes up-regulation of Mitochondrial activity gene expression in Glioblastoma cells.

Effect of Lactate on Mitochondrial biogenesis and OXPHOS gene expression in U-87 MG cells (**a-b**), A-172 cells (**c-d**) and U-251 MG cells (**e-f**) following 24 and 48 h of treatment. Computerized analysis of mitotracker fluorescence intensity on the control versus lactate 18 hours after treatment (**g-h**). Figures presented are the representative of at least three independent experiments. Values represent the means ± SEM of experiments performed in quadrupled. p values < 0.05 were considered to be statistically significant (*p < 0.05; **p < 0.01; ***p < 0.001 vs untreated).

Figure 4.

HCAR1 selective stimulation promotes up-regulation of Mitochondrial activity gene expression and regulates the protein expression of EMT markers in Glioblastoma cells.

Effect of 3,5-DHBA on Mitochondrial biogenesis and OXPHOS gene expression in U-87 MG cells (**a-b**), A-172 cells (**c-d**) and U-251 MG cells (**e-f**) following 24 h of treatment. Computerized analysis of mitotracker fluorescence intensity on the control versus lactate 18 hours after treatment (**g**). Figures presented are the

representative of at least three independent experiments. B-Catenin and E-Cadherin protein expression in A-172 cells (**h**) following 72 h of HCAR1 stimulation. Figures presented are the representative of at least four independent experiments and values represent the means ± SEM of experiments performed in quadrupled. p values < 0.05 were considered to be statistically significant (*$p < 0.05$; **$p < 0.01$; ***$p < 0.001$ vs untreated).

Figure 5.

Metabolic changes in a zebrafish model of GBM leads to increased glycolysis and lactate transport and sensing.

(a) schematic representation of the genetic components of the zebrafish GBM model (Mayrhofer et al., 2017); (b) increased expression of several members of the glycolytic pathway in GBM. Heatmap representing 29 glycolysis genes and their relative expression levels. (c) Analysis of mitochondrial metabolism (mitostress test) of tumor cells by XP Seahorse technology. d) Increased levels of HCAR1 in tumors vs control as visualized by immunofluorescence. Staining as detailed in the figures, which are representative of at least 3 different experiments. (e) Gene expression analysis through q-PCR expressed as fold changes compared to controls, at 5dpf and in the adult tumors. Values represent the means ± SEM of experiments performed in triplicate. p values < 0.05 were considered to be statistically significant (*$p < 0.05$ vs controls). (f) Whole mounts immunofluorescence of Ph3 proliferating cells in controls and in HRAS overexpressing larvae treated or not with 20 um lactate. Green fluorescence

represents tumoral cells expressing eGFP-HRAS$^{G12V.}$ (g) number of proliferating cells in the brains treated as indicated.

Figure 6.

MCT1 expression analysis from the human brain tumor GSE108474 dataset

Analysis of MCT1 gene expression in brain biopsies of patients with astrocytoma, oligodendrocytoma, glioblastoma, and healthy subjects. b) Pearson correlation analysis between MCT1 expression levels and tumor grade of brain biopsies obtained from patients affected by main brain tumors. c) Pearson's correlation between MCT1 and IDH1 expression levels in brain biopsies of patients with glioblastoma. d) Receiver operating characteristic (ROC) analysis between MCT1 brain expression levels in healthy subject's vs glioblastoma patients, between glioblastoma patients vs astrocytoma patients (e), and vs oligodendrocytoma (f). Data are expressed as mean ± SD of at least four independent experiments. (*p<0.05; **p<0.005; ***p<0.001; ****p<0.0001).

Supplementary Figure S 1.

Lactate enhances colony formation capacity in glioblastoma cells.

Effect of Lactate treatment on colony formation capacity in U-87 MG cells (a), A-172 cells (b) and U-251 MG cells (c). Data are expressed as mean ± SEM of at least three independent experiments. (*p<0.05; **p<0.005; ***p<0.001; ****p<0.0001).

REFERENCES

1. Stupp R, Hegi ME, Mason WP, van den Bent MJ, Taphoorn MJ, Janzer RC, et al. Effects of radiotherapy with concomitant and adjuvant temozolomide versus radiotherapy alone on survival in glioblastoma in a randomised phase III study: 5-year analysis of the EORTC-NCIC trial. Lancet Oncol. 2009;

2. Torrisi F, Vicario N, Spitale FM, Cammarata FP, Minafra L, Salvatorelli L, et al. The role of hypoxia and src tyrosine kinase in glioblastoma invasiveness and radioresistance. Cancers (Basel). 2020.

3. Charles N, Holland EC. The perivascular niche microenvironment in brain tumor progression. Cell Cycle. 2010.

4. Liberti M V., Locasale JW. The Warburg Effect: How Does it Benefit Cancer Cells? Trends Biochem. Sci. 2016.

5. Heiden MGV, Cantley LC, Thompson CB. Understanding the warburg effect: The metabolic requirements of cell proliferation. Science (80-.). 2009.

6. Miranda-Gonçalves V, Bezerra F, Costa-Almeida R, Freitas-Cunha M, Soares R, Martinho O, et al. Monocarboxylate transporter 1 is a key player in glioma-endothelial cell crosstalk. Mol Carcinog. 2017;56.

7. Kobayashi M, Narumi K, Furugen A, Iseki K. Transport function, regulation, and biology of human monocarboxylate transporter 1 (hMCT1) and 4 (hMCT4). Pharmacol. Ther. 2021.

8. Park SJ, Smith CP, Wilbur RR, Cain CP, Kallu SR, Valasapalli S, et al. An overview of MCT1 and MCT4 in GBM: small molecule transporters with large implications. Am J Cancer Res. 2018;8.

9. Payen VL, Hsu MY, Rädecke KS, Wyart E, Vazeille T, Bouzin C, et al. Monocarboxylate transporter MCT1 promotes tumor metastasis independently of its activity as a lactate transporter. Cancer Res. 2017;77.

10. Garnier D, Renoult O, Alves-Guerra MC, Paris F, Pecqueur C. Glioblastoma stem-like cells, Metabolic strategy to kill a challenging target. Front. Oncol. 2019.

11. Hoque R, Farooq A, Ghani A, Gorelick F, Mehal WZ. Lactate reduces liver and pancreatic injury in toll-like receptor- and inflammasome-mediated inflammation via gpr81-mediated suppression of innate immunity. Gastroenterology. 2014;146.

12. Brown TP, Ganapathy V. Lactate/GPR81 signaling and proton motive force in cancer: Role in angiogenesis, immune escape, nutrition, and Warburg phenomenon. Pharmacol. Ther. 2020.

13. Ristic B, Bhutia YD, Ganapathy V. Cell-surface G-protein-coupled receptors for tumor-associated metabolites: A direct link to mitochondrial dysfunction in cancer. Biochim. Biophys. Acta - Rev. Cancer. 2017.

14. Ahmed K, Tunaru S, Tang C, Müller M, Gille A, Sassmann A, et al. An Autocrine Lactate Loop Mediates Insulin-Dependent Inhibition of Lipolysis through GPR81. Cell Metab. 2010;11.

15. Roland CL, Arumugam T, Deng D, Liu SH, Philip B, Gomez S, et al. Cell surface lactate receptor GPR81 is crucial for cancer cell survival. Cancer Res. 2014;74.

16. Detrich HW, Westerfield M, Zon LI. Essential zebrafish methods : cell and developmental biology. Reliab. lab Solut. 2009.

17. Mayrhofer M, Gourain V, Reischl M, Affaticati P, Jenett A, Joly JS, et al. A novel brain tumour model in zebrafish reveals the role of YAP activation in MAPK- and PI3K-induced malignant growth. DMM Dis Model Mech. 2017;10.

18. Santoriello C, Gennaro E, Anelli V, Distel M, Kelly A, Köster RW, et al. Kita driven expression of oncogenic HRAS leads to early onset and highly penetrant melanoma in zebrafish. PLoS One. 2010;5.

19. Idilli AI, Pagani F, Kerschbamer E, Berardinelli F, Bernabé M, Cayuela ML, et al. Changes in the expression of pre-replicative complex genes in hTERT and ALT pediatric brain tumors. Cancers (Basel). 2020;12.

20. Clough E, Barrett T. The Gene Expression Omnibus database. Methods Mol Biol. 2016.

21. Gusev Y, Bhuvaneshwar K, Song L, Zenklusen JC, Fine H, Madhavan S. Data descriptor: The REMBRANDT study, a large collection of genomic data from brain cancer patients. Sci Data. 2018;5.

22. Xiao J, Cao H, Chen J. False discovery rate control incorporating phylogenetic tree increases detection power in microbiome-wide multiple testing. Bioinformatics. 2017;33.

23. Smyth GK. Linear models and empirical bayes methods for assessing differential expression in microarray experiments. Stat Appl Genet Mol Biol. 2004;3.

24. Sean D, Meltzer PS. GEOquery: A bridge between the Gene Expression Omnibus (GEO) and BioConductor. Bioinformatics. 2007;23.

25. Box GEP, Tiao GC. Nature of Bayesian Inference. Bayesian Inference Stat Anal. 2011.

26. Cheadle C, Vawter MP, Freed WJ, Becker KG. Analysis of microarray data using Z score transformation. J Mol Diagnostics. 2003;5.

27. Scarpino M, Pinzone MR, Di Rosa M, Madeddu G, Focà E, Martellotta F, et al.

Kidney disease in HIV-infected patients. Eur Rev Med Pharmacol Sci. 2013;17.

28. Feng C, Wu J, Yang F, Qiu M, Hu S, Guo S, et al. Expression of Bcl-2 is a favorable prognostic biomarker in lung squamous cell carcinoma. Oncol Lett. 2018;15.

29. Kang C, Huo Y, Xin L, Tian B, Yu B. Feature selection and tumor classification for microarray data using relaxed Lasso and generalized multi-class support vector machine. J Theor Biol. 2019;463.

30. Care MA, Barrans S, Worrillow L, Jack A, Westhead DR, Tooze RM. A Microarray Platform-Independent Classification Tool for Cell of Origin Class Allows Comparative Analysis of Gene Expression in Diffuse Large B-cell Lymphoma. PLoS One. 2013;8.

31. Wang J, Coombes KR, Highsmith WE, Keating MJ, Abruzzo L V. Differences in gene expression between B-cell chronic lymphocytic leukemia and normal B cells: A meta-analysis of three microarray studies. Bioinformatics. 2004;20.

32. Reddy TBK, Riley R, Wymore F, Montgomery P, Decaprio D, Engels R, et al. TB database: An integrated platform for tuberculosis research. Nucleic Acids Res. 2009;37.

33. Lê Cao KA, Rohart F, McHugh L, Korn O, Wells CA. YuGene: A simple approach to scale gene expression data derived from different platforms for integrated analyses. Genomics. 2014;103.

34. Chen QR, Song YK, Wei JS, Bilke S, Asgharzadeh S, Seeger RC, et al. An integrated cross-platform prognosis study on neuroblastoma patients. Genomics. 2008;92.

35. Mehmood R, El-Ashram S, Bie R, Dawood H, Kos A. Clustering by fast search & merge of local density peaks for gene expression microarray data. Sci Rep. 2017;7.

36. Yasrebi H, Sperisen P, Praz V, Bucher P. Can survival prediction be improved

by merging gene expression data sets? PLoS One. 2009;4.

37. Cheadle C, Cho-Chung YS, Becker KG, Vawter MP. Application of z-score transformation to Affymetrix data. Appl Bioinformatics. 2003;2.

38. Lusted LB. Signal detectability and medical decision-making. Science (80-). 1971;171.

39. Castrogiovanni P, Sanfilippo C, Imbesi R, Maugeri G, Lo Furno D, Tibullo D, et al. Brain CHID1 Expression Correlates with NRGN and CALB1 in Healthy Subjects and AD Patients. Cells. 2021;10.

40. Catrogiovanni P, Musumeci G, Giunta S, Imbesi R, Di Rosa M. The expression levels of CHI3L1 and IL15Rα correlate with TGM2 in duodenum biopsies of patients with celiac disease. Inflamm Res. 2020;69.

41. Zetterberg H, Bozzetta E, Favole A, Corona C, Cavarretta MC, Ingravalle F, et al. Neurofilaments in blood is a new promising preclinical biomarker for the screening of natural scrapie in sheep. PLoS One. 2019;14.

42. Han S, Liu Y, Cai SJ, Qian M, Ding J, Larion M, et al. IDH mutation in glioma: molecular mechanisms and potential therapeutic targets. Br. J. Cancer. 2020.

43. Neagu M, Constantin C, Popescu ID, Zipeto D, Tzanakakis G, Nikitovic D, et al. Inflammation and metabolism in cancer cell—mitochondria key player. Front Oncol. 2019;9.

44. Lee YJ, Shin KJ, Park SA, Park KS, Park S, Heo K, et al. G-protein-coupled receptor 81 promotes a malignant phenotype in breast cancer through angiogenic factor secretion. Oncotarget. 2016;7.

45. Kennedy LH, Emilie R. Glesaaen, Vuk Palibrk, Marco Pannone, Wei Wang, Ali H.J. Al-Jabri, Rajikala Suganthan, Niklas Meyer, Xiaolin Lin, Linda H. Bergersen,

View ORCID ProfileMagnar Bjørås VOPER. Lactate receptor HCAR1 regulates neurogenesis and microglia activation after neonatal hypoxia-ischemia. bioRxiv. 2020;

46. Kennedy KM, Dewhirst MW. Tumor metabolism of lactate: The influence and therapeutic potential for MCT and CD147 regulation. Futur. Oncol. 2010.

47. Sun X, Wang M, Wang M, Yao L, Li X, Dong H, et al. Role of Proton-Coupled Monocarboxylate Transporters in Cancer: From Metabolic Crosstalk to Therapeutic Potential. Front. Cell Dev. Biol. 2020.

48. Merezhinskaya N, Fishbein WN. Monocarboxylate transporters: Past, present, and future. Histol. Histopathol. 2009.

49. Hanahan D, Weinberg RA. Hallmarks of cancer: The next generation. Cell. 2011.

50. Wagner W, Kania KD, Blauz A, Ciszewski WM. The lactate receptor (HCAR1/GPR81) contributes to doxorubicin chemoresistance via abcb1 transporter up-regulation in human cervical cancer hela cells. J Physiol Pharmacol. 2017;68.

51. Zhao Y, Li M, Yao X, Fei Y, Lin Z, Li Z, et al. HCAR1/MCT1 Regulates Tumor Ferroptosis through the Lactate-Mediated AMPK-SCD1 Activity and Its Therapeutic Implications. Cell Rep. 2020;33.

52. Cormio A, Guerra F, Cormio G, Pesce V, Fracasso F, Loizzi V, et al. Mitochondrial DNA content and mass increase in progression from normal to hyperplastic to cancer endometrium. BMC Res Notes. 2012;5.

53. Lebleu VS, O'Connell JT, Gonzalez Herrera KN, Wikman H, Pantel K, Haigis MC, et al. PGC-1α mediates mitochondrial biogenesis and oxidative phosphorylation in cancer cells to promote metastasis. Nat Cell Biol. 2014;16.

54. Li W, Wei Z, Liu Y, Li H, Ren R, Tang Y. Increased 18F-FDG uptake and expression of Glut1 in the EMT transformed breast cancer cells induced by TGF-β. Neoplasma. 2010;57.

55. Li J, Dong L, Wei D, Wang X, Zhang S, Li H. Fatty acid synthase mediates the epithelial-mesenchymal transition of breast cancer cells. Int J Biol Sci. 2014;10.

56. Jiang L, Xiao L, Sugiura H, Huang X, Ali A, Kuro-O M, et al. Metabolic reprogramming during TGFβ1-induced epithelial-to-mesenchymal transition. Oncogene. 2015;34.

57. Rattigan YI, Patel BB, Ackerstaff E, Sukenick G, Koutcher JA, Glod JW, et al. Lactate is a mediator of metabolic cooperation between stromal carcinoma associated fibroblasts and glycolytic tumor cells in the tumor microenvironment. Exp Cell Res. 2012;318.

58. Hanieh H, Ahmed EA, Vishnubalaji R, Alajez NM. SOX4: Epigenetic regulation and role in tumorigenesis. Semin. Cancer Biol. 2020.

59. Bhagat TD, Von Ahgrens D, Dawlaty M, Zou Y, Baddour J, Achreja A, et al. Lactate-mediated epigenetic reprogramming regulates formation of human pancreatic cancer-associated fibroblasts. Elife. 2019;8.

60. Miranda-Gonçalves V, Gonçalves CS, Granja S, de Castro JV, Reis RM, Costa BM, et al. MCT1 is a new prognostic biomarker and its therapeutic inhibition boosts response to temozolomide in human glioblastoma. Cancers (Basel). 2021;13.

61. Viswanath P, Najac C, Izquierdo-Garcia JL, Pankov A, Hong C, Eriksson P, et al. Mutant IDH1 expression is associated with down-regulation of monocarboxylate transporters. Oncotarget. 2016;7.

CHAPTER II

(Submitted) Cancer Immunology & Immunotherapy

Lactate modulates Microglia M2 polarization via IGFBP-6 expression and remodels tumor microenvironment in Glioblastoma

Lucia Longhitano[1], Nunzio Vicario[1], Cesarina Giallongo[2], Giuseppe Broggi[2], Rosario Caltabiano[2], Giuseppe Barbagallo[2], Giuseppina Raciti[3], Michelino Di Rosa[1], Massimo Caruso[1], G. Lazzarino[1], Rosalba Parenti[1], Giuseppe Alberto Palumbo[2], Arcangelo Liso[4], Maria Caterina Mione[5], Giovanni Li Volti[1] and Daniele Tibullo[1]

[1]Department of Biomedical and Biotechnological Sciences, University of Catania, Catania (Italy)

[2]Department of Medical and Surgical Sciences and Advanced Technologies, F. Ingrassia, Anatomic Pathology, University of Catania, Catania (Italy)

[3]Department of Drug Sciences, University of Catania, Catania (Italy)

[4]Department of Medical and Surgical Sciences, University of Foggia, 71100 Foggia, Italy

[5]Department of Cellular, Computational and Integrative Biology (Cibio), University of Trento, 38123 Trento, Italy

*** Correspondence:**
Prof. Giovanni Li Volti, MD, PhD
Department of Biomedical and Biotechnological Sciences
University of Catania
Catania (Italy)
livolti@unict.it

Keywords: Glioblastoma, IGFBP-6, Microglia, Lactate, Microenvironment

Abstract

Lactic acidosis has been reported in various solid tumor microenvironment (TME) including glioblastoma (GBM). In TME a number of signaling molecules, growth factors and metabolites have been identified to induce resistance to chemotherapy and to sustain immune escape. Indeed, in the early phases of the disease, microglia infiltrates TME, contributing to tumorigenesis instead of counteracting its growth.
A critical role in this process is played by insulin-like growth factor (IGF) and IGF-binding proteins (IGFBPs). Among them, IGFBP-6 is expressed during development and it is involved in migration, immune escape and inflammation, thus making it an attractive target for GBM cells modulation and for studying potential interaction with tumor metabolism.
In the present study we aimed at investigating the crosstalk between lactate and IGFBP-6 in microglial cells and how such an interaction modulates TME and GBM progression.
Our results showed that microglia exposed to lactate significantly increased the expression of MCT1, and genes involved in mitochondrial metabolism. Consistently, we also showed an increase in the M2 markers, Arg-1, and a reduction of iNOS suggestive of an M1-proinflammatory state. Furthermore, lactate treatment induced a significant increase in IGFBP-6 expression in microglia and glioblastoma cells. Similarly, IGFBP-6 treatment in GBM cells induced an increase in lactate concentration. Treatment of GBM cells with IGFBP-6 also resulted in a significant increase in cell proliferation, migration and colony formation capacity. Finally, our data showed that IGFBP-6 treatment also resulted in an increase of M2 markers Arg-1, and a reduction of iNOS expression levels. These results were further confirmed in a separate set of experiments by evaluating the expression of mRNA levels of M1 and M2 markers on microglia cells cultured with conditioned media from IGFBP-6 pre-treated GBM cells. Therefore, our results suggested the existence of a crosstalk lactate/IGFBP-6 in microglial cells, so that IGFBP-6 expression is regulated by lactate production in GBM cells and in turn modulates microglia polarization.

INTRODUCTION

Glioblastoma Multiforme (GBM) is the most common primary brain tumor and no effective therapy currently exists [1, 2]. Treatment resistance, tumor recurrence and the poor prognosis is a product of both cancer cell proliferation and the interaction with tumor microenvironment (TME) [3–7] which includes different cell types such as glioma-associated microglia/macrophages (GAMs).

Microglia are sentinels cells of the central nervous system (CNS) [6], and plays key roles under both physiological and pathological conditions [8] contributing to tissue homeostasis in the brain [9]. GAMs are functionally similar to that of tumor-associated macrophages in the peripheral system and closely interact with GBM cells via intracellular communications [10, 11]. Although GAMs have a few innate immune functions intact, their ability to be stimulated via TLRs, secrete cytokines, and upregulate co-stimulatory molecules is not sufficient to initiate antitumor immune responses [11]. However, in malignant gliomas, M2-polarization of microglia leads to an immunosuppressive and tumor-supportive phenotype triggered by a series of tumor cytokines, such as transforming

growth factor-β, interleukin-10, and prostaglandin E2 [12] and other growth factors.

TME is critical to establish malignancy [13–16] and it is characterized by high glycolytic metabolism with increased lactate production. Lactate is largely produced within the TME and is used as an energy-rich substrate, signaling molecule and as an important immune suppressor by tumors [17]. The glycolytic cancer cells and cancer–associated fibroblasts (CAFs) are the main producers of lactate, simply because they are the most abundant populations within the neoplasm [17]. TME enforce to metabolic adaptability, physical pressure, oxidative stress, nutrient deprivation and competition, immune surveillance as well as adaptability to hypoxic and acidic environment having an enormous impact on tumor malignancy [18]. Therefore, a high rate of aerobic glycolysis (glucose metabolism) [19, 20] efflux of resultant lactic acid [21], and concomitant acidification of the TME are hallmarks of several cancers, including GBM [22–24].

Tumor-derived lactate is taken up by GAMs through their MCT active transporters on the cell membrane [25], leading to the transcription of the vascular endothelial growth factor (VEGF) and

the l-arginine- metabolizing enzyme arginase-1 (ARG1) genes [26, 27] inhibiting T-cell activation and proliferation [28]. Furthermore, MCT-mediated H^+ efflux exacerbates extracellular acidification and supports the formation of a hostile environment where cancer cells, that have adapted to these conditions, can outcompete normal cells, which further enhances tumor progression [29]. Over-expression of lactate transporters is a common feature of some cancers with high metabolic rate [30]. For instance, high expression of MCT1, MCT4 and its chaperone CD147 is associated with decreased progression-free survival in clear cell renal cell carcinoma, head and neck cancers and neuroblastoma [31, 32].

The insulin-like growth factor (IGF) system is ubiquitously present and includes the type I and type II IGF receptors (IGF-I and IGF-II) and specific insulin-like growth factor-binding proteins (IGFBPs), which are a family of six proteins functioning as transport proteins for IGF-I and IGF-II in the circulation and regulating their access to the potentially oncogenic IGF-I receptor (IGF1R) [33]. Interestingly, IGFBPs may inhibit and/or enhance IGF-I and IGF-II biological effects. In particular, the insulin-like growth factor binding protein 6 (IGFBP-6) is expressed in a variety of tissues and its

expression is developmentally regulated [34] and is characterized by its high IGF-II binding specificity. Several studies have shown that IGFBP-6 may exert biological effects independently from IGF-II [35], such as regulation of proliferation, apoptosis, angiogenesis and cell migration, suggesting a major role in immunity and in inflammation. Among various growth factors, IGFBP-6 has been reported to play an important role in survival and migration of tumor cells [36], but its effects on tumor and immune system interaction is still poorly understood and the relationships between IGFBP-6 and cancer prognosis remain contradictory in many studies [37].

To this regard, the aim of the present study was to evaluate the crosstalk between lactate and IGFBP-6 in microglial cells and how such interaction modulates TME and GBM progression.

MATHERIALS AND METHODS

Cell Culture and Pharmacological Treatments

Human glioblastoma cell lines (U87-MG, A172 and U251) were purchased from ATCC Company (Milan, Italy). Cells were suspended in DMEM (Gibco, cat. no. 11965092) culture medium containing 10% fetal bovine serum (FBS, Gibco, cat. no. 10082147), 100 U/mL penicillin and 100 U/mL streptomycin (Gibco, cat. no. 15070063). At 80% confluency, cells were passaged using trypsin-EDTA solution (0.05% trypsin and 0.02% EDTA, Gibco, cat. no. 25300054).

Human microglia cell line (HMC3) was purchased from ATCC Company (Milan, Italy). HMC3 cells were cultured according to the recommendations by ATCC, where EMEM (ATCC® 30–2003TM) was used as the base medium and completed by adding 56 mL FBS (ATCC® 30–2020TM) to a 500 mL of base EMEM.

Lactate and IGFBP-6 (Sigma–Aldrich, Milan, Italy) was added to cell culture of all experiments at final concentrations of 20 mM and 400 ng/mL, respectively, for 24, 48 and 72 hours.

Real-Time PCR for Gene Expression Analysis

RNA was extracted by Trizol® reagent (category no. 15596026, Invitrogen, Carlsbad, CA, USA). The first-strand cDNA was then synthesized with High-Capacity cDNA Reverse Transcription kit (category no. 4368814, Applied Biosystems, Foster City, CA, USA). High cDNA quality was checked, taking into consideration the housekeeping gene Ct values. Quantitative real-time PCR was performed in Step-One Fast Real-Time PCR system, Applied Biosystems, using the SYBR Green PCR MasterMix (category no. 4309155, Life Technologies, Monza, Italy). The specific PCR products were detected by the fluorescence of SYBR Green, the double - stranded DNA binding dye. Primers were designed using BLAST® (Basic Local Alignment Search Tool, NBCI, NIH), considering the shortest amplicon proposed: primers' sequences are shown in Table 1, and β-actin was used as the housekeeping gene. Primers were purchased by Metabion International AG (Planneg, Germany). The relative mRNA expression level was calculated by the threshold cycle (Ct) value of each PCR product and normalized with β-actin by using a comparative $2^{-\Delta\Delta Ct}$ method.

Table 2. List of qRT – PCR primers

Gene of Interest	Forward primer (5′ ⟶ 3′)	Reverse primer (5′ ⟶ 3′)
PGC1α	ATGAAGGGTACTTTTCTGCCCC	GGTCTTCACCAACCAGAGCA
TFAM	CCGAGGTGGTTTTCATCTGT	AGTCTTCAGCTTTTCCTGCG
ATP synthase	CCGCCTTCCGCGGTATAATC	ATGTACGCGGGCAATACCAT
COX IV	GCGGCAGAATGTTGGCTAC	AGACAGGTGCTTGACATGGG
COX II	ACGACCTCGATGTTGGATCA	ATCATTTACGGGGGAAGGCG
CyTB	ACGAGCCACCGAAACAGAAT	ACGATTTTCGCCAGTCACCT
ND4	CCAGTGGAATGCCTTGCCTA	TTGATCGCGGTGAGATTCCC
Arg1	TCACCTGAGCTTTGATGTCG	CTGAAAGGAGCCCTGTCTTG
CD206	CAAGGAAGGTTGGCATTTGT	CCTTTCAGTCCTTTGCAAGC
CD163	TCCACACGTCCAGAACAGTC	CCTTGGAAACAGAGACAGGC
TNFα	AGAAGTTCCCAAATGGCCTC	CCACTTGGTGGTTTGCTACG
IL1β	CTGGTGTGTGACGTTCCCATTA	CCGACAGCACGAGGCTTT
β -Actin	CCTTTGCCGATCCGCCG	AACATGATCTGGGTCATCTTCTCGC

Western Blot Analysis

Briefly, for western blot analysis, 30 μg of protein was loaded onto a 12% polyacrylamide gel MiniPROTEAN® TGXTM (BIO-RAD, Milan, Italy) followed by electrotransfer to nitrocellulose membrane TransBlot® TurboTM (BIO-RAD, Milan, Italy) using TransBlot® SE Semi-Dry Transfer Cell (BIO- RAD, Milan, Italy). Subsequently, membrane was blocked in Odyssey Blocking Buffer (Licor, Milan, Italy) for 1 h at room temperature. After blocking, membrane was three times washed in phosphate-buffered saline (PBS) for 5 min and incubated with primary antibodies against MCT1 (1:1000), MCT4

(1:1000), IGFBP (1:500) and β-actin (1:1000) (anti-mouse, Cat. No. 4967S, Cell Signalling Technology, Milan, Italy), overnight at 4 °C. Next day, membranes were three times washed in PBS for 5 min and incubated with infrared anti-mouse IRDye800CW (1:5000) and anti-rabbit IRDye700CW secondary antibodies (1:5000) in PBS/0.5% Tween-20 for 1 h at room temperature. All antibodies were diluted in Odyssey Blocking Buffer. The blots were visualized using Odyssey Infrared Imaging Scanner (Licor, Milan, Italy), and protein levels were quantified by densitometric analysis. Data were normalized to β-actin expression.

Immunocytochemistry Analysis

HMC3 cells were grown directly on coverslips before immunofluorescence and treated with lactate at the final concentration of 20 mM and with IGFBP-6 at the final concentration of 400 ng/mL for 72h. After washing with PBS, cells were fixed in 4% paraformaldehyde (category no. 1004968350 Sigma-Aldrich, Milan, Italy) for 20min at room temperature. Subsequently, cells were incubated with primary antibody against Arg – 1 and iNOS at dilution 1:200, overnight at 4°C. The next day, cells were washed three times

in PBS for 5 min and incubated with secondary antibodies: TRITC (anti-goat, Santa Cruz Biotechnology, Santa Cruz, CA, USA) at dilution 1:200 for 1 h at room temperature. Cells were washed three times in PBS for 5 min and incubated with phalloidin at dilution 1:500 for 30 minutes. The slides were mounted with medium containing DAPI (4′,6- diamidino-2phenylindole, category no. sc-3598, Santa Cruz Biotechnology, Santa Cruz, CA, USA) to visualize nuclei. The fluorescent images were obtained using a Zeiss Axio Imager Z1 microscope with Apotome 2 system (Zeiss, Milan, Italy). As a control, the specificity of immunostaining was verified by omitting incubation with the primary or secondary antibody. Immunoreactivity was evaluated considering the signal-to-noise ratio of immunofluorescence.

Lactate Concentration Assay

The spectrophotometric determination of lactate was carried out using an Agilent 89090A spectrophotometer (Agilent Technologies, Santa Clara Ca, USA) and following the method described by Artiss et al. [38]. Briefly, the reaction mixture contained 100 mM Tris–HCl, 1.5 mM N-ethyl-N-2-hydroxy-3-sulfopropyl-3-methylalanine, 1.7 mM 4-

aminoantipyrine, and 5 IU horseradish peroxidase. Fifty microliters of serum were added to the mixture, let to stand for 5 min and read at 545 nm wavelength. The reaction was started with the addition of 5 IU of lactate oxidase to the cuvette (finale volume = 1 ml) and it was considered ended when no change in absorbance was recorded for at least 3 min. To calculate lactate in samples, the difference in absorbance at 545 nm wavelength (Δabs) of each sample was interpolated with a calibration curve obtained by plotting Δabs measured in standard solutions of lactate with increasing known concentrations.

IGFBP-6 ELISA Test

Cell culture supernatant collected on 24h from cell-laden hydrogel were frozen at −80 °C until use. We determined in culture media the quantitative concentrations of IGFBP-6 with IGFBP-6 Human ELISA Kit (catalog #EHIGFBP-6, Invitrogen) according to the manufacturer's instructions.

Cell Migration

Cell proliferation was studied by employing the "wound healing" assay. Cells were seeded separately in 6-well dishes and cultured until confluence. Cells were scraped with a 200-µl micropipette tip and monitored at 0 h, 24 h and 48 h. The uncovered wound area was measured and quantified at different intervals with ImageJ 1.37v (NIH). The experiments were done in quadruplicates.

Clonogenic Assay

Colony assays performed by seeding cells in 6-well plates at low density (5000 cells/well) and allowing growth for 10 days. Colonies were fixed, stained with crystal violet and colonies were quantified with Operetta high content screening (HCS) System (Perkin Elmer). The experiments were done in quadruplicates.

Zebrafish model

Adult zebrafish (Danio rerio) were housed in the Model Organism Facility – Center for Integrative Biology (CIBIO) University of Trento and maintained under standard conditions [39]. All zebrafish studies were performed according to European and Italian law, D.Lgs.

26/2014, authorization 148/2018-PR to M. C. Mione. Fishes with somatic and germline expression of oncogenic HRAS were generated as described [40, 41].

The following zebrafish transgenic lines were used in the course of this study:

Et(zic4:Gal4TA4, UAS:mCherry)$_{hzm5}$ called zic:Gal4 [40]

Tg(UAS:eGFP-HRAS_G12V)$_{io006}$ called UAS:RAS [41]

The characterization of the GBM model is described in detail in Mayrhofer et al., 2017 [40].

Gene expression analysis

For gene expression analysis of samples, total RNA was extracted from larval heads and brains/tumors with TRIzol reagent (Invitrogen). Total RNA was cleaned up using RNeasy Mini Kit (Qiagen) following the manufacturer's instructions and treated twice with DNase I (1 unit/µg RNA, Qiagen). The RNA concentration was quantified using nanodrop2000 (Thermo Fisher) and VILO superscript KIT (Thermo Fisher) was used for First-strand cDNA synthesis according to the manufacturer's protocol. qRT-PCR analysis was performed using qPCR BIO Sygreen Mix (Resnova - PCR

Biosystem) using a standard amplification protocol. The primers used for zebrafish igfbp6a were: forward 5'-TTCAGGAGGAAGCAGTGTCG-3' and reverse 5'-CATCGCTTCTCCTACGGGAC-3'; for igfbp6b zebrafish were: forward 5'-GGCCACATCCTTCACACAGT-3' and reverse 5'-GAGGACCGACACTGCTTTTTC-3'; for zebrafish rps11 (housekeeping): forward: 5'-ACAGAAATGCCCCTTCACTG-3' and reverse: 5'- GCCTCTTCTCAAAACGGTTG-3'. Real-time PCR was performed with a CFX96 Real-Time PCR Detection System (Bio-Rad) machine. Q-PCR analysis was performed with Microsoft Excel and Graphpad Prism. In all cases, each PCR was performed with triplicate samples and repeated with at least two independent samples.

Immunofluorescence in zebrafish

Adult zebrafish resulting from crosses between zic:Gal4 and UAS:RAS, or from somatic expression of UAS:RAS [42], were screened under a fluorescent stereomicroscope for the presence of GFP-HRAS^{G12V} brain masses. Positive fish (over 90% of screened fish) were sacrificed by MS222 overdose, their brains removed, fixed and sectioned as previously described.

Sections were then washed in PBS (pH 7.4) and incubated primary antibodies diluted in PBS containing 5% normal goat serum and 0.1% triton x-100 at 4°C overnight. The antibody used and their dilutions were as follows: L-plastin (Abcam, 1:100). A secondary antibody conjugated with Alexa 546 (1:250) was used for 2 hours at room temperature, Images were acquired using an inverted Leica TSP8 confocal microscope. For whole-mount immunofluorescence of 5 day postfertilization (dpf) zebrafish, larvae of the zic: Gal4 line (controls) or zic:Gal4 x UAS:RAS line (tumor) were treated with 20 mM lactate Solutions with the drugs were changed every day starting at 1dpf till 5dpf, when the larvae were culled by anesthetic overdose, fixed in 4% PFA for 2 to 12 hrs at 4 C, their brains carefully removed under a stereomicroscope and processed with Ph3 antibody, diluted 1:1000 in 5% NGS, 0.5% Triton X100 in PBS overnight. A secondary antibody conjugated with Alexa 546 was used for 6 hours at room temperature. Images were acquired using an inverted Leica TSP8 confocal microscope, after equilibrating the brains in 100% glycerol.

Glioblastoma biopsies

Formalin-fixed and paraffin-embedded tissue specimens from 10 patients affected by GBM were obtained from the surgical pathology files at the Anatomic Pathology, Department G.F. Ingrassia, University of Catania, Catania, Italy. Multiple sections (at least 5) were obtained from formalin-fixed and paraffin-embedded tissue specimens. Due to the retrospective nature of the study, no written informed consent from patients was obtained. The study included 6 male and 4 female patients (mean age: 61 years; age range: 41-81). According to the World Health Organization criteria, the histologic diagnosis of GBM was rendered in presence of the following morphological criteria: i) high-grade glioma with astrocytic morphology; ii) diffuse growth pattern; iii) foci of necrosis and/or microvascular proliferation.

Immunohistochemistry Analysis

Sections were processed as previously described [43]. Then, the sections were incubated overnight at 4 °C with rabbit polyclonal anti-IGFBP-6 antibody (Sigma, Milan, Italy), ready to use in PBS (Sigma, Milan, Italy) and MIB-1, a monoclonal antibody directed

against the Ki-67 antigen (M7240; Dako Corporation, Glostrup, Denmark), diluted 1:75 in PBS (Sigma, Milan, Italy). The secondary antibody, biotinylated anti-rabbit antibody was applied for 30 min at room temperature, followed by the avidin–biotin–peroxidase complex (Vector Laboratories, Burlingame, CA, USA) for a further 30 min at room temperature. The immunoreaction was visualized by incubating the sections for 4 min in a 0.1% 3,3'-diaminobenzidine (DAB) and 0.02% hydrogen peroxide solution (DAB substrate kit, Vector Laboratories, CA, USA). The sections were lightly counterstained with Mayer's hematoxylin (Histolab Products AB, Göteborg, Sweden) mounted in GVA mountant (Zymed Laboratories, San Francisco, CA, USA) and observed with a Zeiss Axioplan light microscope (Carl Zeiss, Oberkochen, Germany). IGFBP6 staining (both nuclear and cytoplasmic staining) was semi-quantitatively evaluated according to a 0 to 3 scale of Intensity of Staining (IS) and to the percentage of positively stained cells (Extent Score, ES; on a five-tiered system: <5%; 5–30%; 31–50%; 51–75%; >75%. The immunoreactivity score (IRS) has been obtained by multiplying IS and ES: low (L-IRS) and high (H-IRS) expression of IGFBP-6 were respectively defined as IRS < 6 and IRS ≥ 6.

MIB-1 immunohistochemical expression was assessed as low if positive in less than 50% of neoplastic cells, as high if positive in more than 50% of neoplastic cells.

Transcriptome analysis

Dataset selection

The NCBI Gene Expression Omnibus (GEO) database (http://www.ncbi.nlm.nih.gov/geo/) [44] was used to select transcriptomes datasets of interest. Mesh terms "human", "glioblastoma", and "tumor grade", were used to identify the datasets. We sorted the datasets by the number of samples (High to Low), age and sex of the participants and by the clinical data made available by the authors. We selected the GSE108474 dataset [45] over the others available for the number of subjects recruited (541), for the availability of clinical data (tumor staging) and for the variety of tumors analyzed (glioblastoma, oligodendroglioma, astrocytoma and normal subjects).

Data processing, experimental design and statistics

To process and identify Significantly Different Expressed Genes (SDEG) within the datasets, we used the MultiExperiment Viewer (MeV) software (The Institute for Genomic Research (TIGR), J. Craig Venter Institute, La Jolla, USA). In cases where multiple genes probes have insisted on the same GeneID NCBI, we used those with the highest variance.

For GSE108474 we performed a statistical analysis with GEO2R, applying a Benjamini & Hochberg (False discovery rate) [46–48].

Table 2; Samples selected from GSE108474

Disease type	Number	Grade
NT	28	Negative
Astrocytoma	148	G2=65; G3=58; Na=25
Oligodendroglioma	67	G2=30; G3=23; Na =14
Glioblastoma	221	G4=130; Na =91

G= tumor grade; Na= not assigned; NT= non tumor

Significant differences between groups were assessed using the Ordinary one-way ANOVA test, and Tukey's multiple comparisons test correction was performed to compare data between all groups.

Correlations were determined using Pearson correlation. All tests were two-sided and significance was determined at adjusted p value 0.05. The dataset selected was transformed for the analysis in Z-score intensity signal. Z score is constructed by taking the ratio of weighted mean difference and combined standard deviation according to Box and Tiao (1992) [49]. The application of a classical method of data normalization, z-score transformation, provides a way of standardizing data across a wide range of experiments and allows the comparison of microarray data independent of the original hybridization intensities. The z-score it is considered a reliable procedure for this type of analysis and can be considered a state-of-the-art method, as demonstrated by the numerous bibliography [50, 51, 60, 61, 52–59]. The efficiency of each biomarker across the different tumor grade was assessed by the receiver operating characteristic (ROC) curve analyses [62–64]. The ROC curves analyzed brain biopsies of healthy subjects (NT) vs glioblastoma patients, astrocytoma vs glioblastoma, and oligodendroglioma vs glioblastoma. The area under the ROC curve (AUC) and its 95% confidence interval (95% CI) indicates diagnostic

efficiency. The accuracy of the test with the percent error is reported [65].

Statistical Analysis

Statistical analysis was performed using SPSS11.0 software. Statistical significance ($p < 0.05$) of differences between experimental groups was determined by the Fisher method for analysis of multiple comparisons. For comparison between treatment groups, the null hypothesis was tested by either single-factor analysis of variance (ANOVA) for multiple groups or the unpaired t-test for two groups, and the data are presented as mean ± SD.

RESULTS

Lactate induces the expression of MCT1 promoting an oxidative metabolism in microglia cells

We firstly aimed at evaluating the effect of lactate on viability in microglia cells. As shown in **Figure 1A**, Lactate 20mM (48h) did not affect viability, and resulted in a significant increase of cell number (% 135.67 ± 10.03) compared to untreated control cells (% 100 ± 3.7). Therefore, we used this concentration for subsequent experiments. We then evaluated the effect of lactate on MCTs expression and in mitochondrial metabolism concerning mitochondrial biogenesis and oxidative phosphorylation in microglia cells. Our results with microglial cells showed a significant increase in relative mRNA levels of *MCT1* (6.97 ± 0.55) and *MCT4* (2.57 ± 0.3) when exposed to lactate for 24 or 48 hours as compared to untreated control cells (**Figure 1B-C**). These results were further confirmed by western blot analysis, which showed that lactate exposure (24 and 48 hours) induced a significant increase in MCT1 expression levels (24h: 1.25 ± 0.03, 48h:1.43 ± 0.07 lactate *vs* 0.95 ± 0.09 control) (**Figure 1D-E**). Because oxidative cancer cells

expressing MCT1 are capable of taking up lactate secreted by glycolytic cancer cells [66], we analyzed mRNA expression of a panel of genes involved in mitochondrial metabolism. Our results showed that lactate treatment induced a significant change in the expression of genes involved in mitochondrial biogenesis and oxidative phosphorylation. As shown in **Figure 1F-L**, following 24 or 48 hour of Lactate exposition, microglia cells showed a significant increase of the relative mRNA levels of *PGC1α* (48h: 6.97 ± 0.23, **Figure 1F**) and *TFAM* (24h: 1.2 ± 0.05, **Figure 1G**), coupled with an overall increase of *COX IV* (24h: 1.23 ±0.07, **Figure 1I**), *COX II* (24h: 1.40 ± 0.18, **Figure 1J**), *CyTB* (24h: 1.45 ± 0.13, **Figure 1K**) and *ND4* (24h: 1.53 ± 0.11, **Figure 1L**) compared to untreated control cells. We also performed analysis of mitotracker fluorescence intensity on control versus lactate treated cells, showing that lactate was able to significantly increase cytoplasm mitotracker intensity 18 hrs following treatment (**Figure 1M**).

Lactate promotes microglia M2 polarization through the expression of IGFBP-6

To further confirm whether lactate serves as an oncometabolite driving microglia M2-polarization in TME and promoting tumor progression, we assessed the effect of Lactate exposure on the expression of M1 and M2 microglia polarization markers. Firstly, we evaluated the expression of Arg1, CD206, CD163, TGF*ß*, IL6 and TNF$\boldsymbol{\alpha}$ genes. Our data suggested that following 24 and 48 hours, Lactate treatment showed significantly increase in relative mRNA expression levels of M2-markers *Arg1* (24h: 2.70 ± 0.23, 48h: 2.50 ± 0.14, **Figure 2A**), *CD206* (24h: 2.37 ± 0.09, 48h: 4.25 ± 0.12, **Figure 2B**), *CD163* (48h: 4.47 ± 0.34, **Figure 2C**), *TGFß* (24h: 2.67 ± 0.27, 48h: 2.68 ± 0.23, **Figure 2D**) and *IL6* (24h: 1.77 ± 0.18, 48h: 1.55 ± 0.08 **Figure 2E**). Consistently, these results were confirmed by immunocytochemistry analysis, showing that Lactate treated cells (72 hours) showed lower levels of iNOS (M1-marker) and higher levels of Arg1 (M2-marker) compared to their untreated control cells (**Figure 2G-H**).

Given the evidence on cellular modulation exerted by increased extracellular levels of lactate, we sought to link molecular

mechanisms underlying these phenomena with the expression of Insulin Growth Factor Protein Binding 6 (IGFBP-6). To this end, we first analyzed whether lactate was able to increase the expression of IGFBP-6 and, as shown in **Figure 3A-B**, treatment with lactate in microglia cells resulted in a significant increase in both relative of mRNA (24h: 2.02 ± 0.14, **Figure 3A**) and protein (24h: 3.77 ± 0.21, **Figure 3B**) expression levels compared with untreated control cells. These data were confirmed by the ELISA test performed on the cell culture supernatant (1752.6 ug ± 123.5 lactate versus 83.6 ug ± 1.29 control, **Figure 3C**). Then, we treated the microglia cells with the recombinant protein IGFBP-6 (400 ng/mL) for 24 and 48 hours and evaluated whether IGFBP-6 was also able to promote oxidative metabolism and M2 polarization. Consistently, we showed that, similarly to lactate, also IGFBP-6 was able to induce a significant increase in relative mRNA expression levels of genes involved in oxidative phosphorylation pathway, i.e. *ATPsyn* (24h: 2.14 ± 0.21, **Figure 3D**), *COX IV* (24h: 3.69 ± 0.44, **Figure 3E**), *COX II* (24h: 1.32 ± 0.15, **Figure 3F**), *CyTB* (24h: 14.59 ± 0.8, **Figure 3G**) and *ND4* (24h: 14.21 ± 1.2, **Figure 3H**), confirming that IGFBP-6 promotes oxidative metabolism in microglia cells. These data were confirmed by analysis

of mitotracker fluorescence intensity, showing that IGFBP-6 treated cells showed significantly increase in cytoplasm mitotracker intensity 18 hrs post treatment compared to control cells (**Figure 3M**). Then, we evaluated the effect on M1 and M2 markers, as shown in **Figure 3 J-O**. In this regard, our results showed an increase in *Arg1* (24h: 14.21 ± 1.2, 48h: 1.87 ± 0.36, **Figure 3J**), *CD206* (48h: 1.80 ± 0.36, **Figure 3K**), *CD163* (48h: 2.09 ± 0.45, **Figure 3L**) and a decrease in *TNFα* (48h: 0.14 ± 0.03, **Figure 3M**) mRNA expression levels in IGFBP-6 treated microglia cells compared to untreated control cells. Furthermore, we confirmed these results by immunocytochemistry analysis, which showed a reduction in iNOS (**Figure 3N**) expression and an increase in Arg1 (**Figure 3O**) expression following 72 hours of IGFBP-6 treatment compared to untreated cells.

IGFBP-6 enhances migration and colony formation capacity in glioblastoma cells

Microglia plays an important role in the microenvironment that supports Glioblastoma progression. Since lactate promotes tumor proliferation and migration in GBM cells, we evaluated the effect of lactate on IGFBP-6 expression and the effect of IGFBP-6 exposure in

three human GBM lines (i.e. U-87 MG, A172 and U-251). Interestingly, Our results showed that in three GBM cell lines (U-87 MG, A172 and U-251), Lactate induces a significant increase in relative IGFB-6 mRNA expression levels following 24 hours (U-87 MG: 10.48 ± 0.8; A172: 12.79 ± 1.2; U-251: 2.11 ± 0.16, **Figure 4A**) and 48 hours (U-87 MG: 19.16 ± 2.9; A172: 4.96 ± 0.3; U-251: 4.02 ± 0.3, **Figure 4A**) of treatment compared to their untreated control cells. Similarly, we evaluated IGFBP-6 production in cell culture supernatant following 24 hours of lactate treatment, showing that IGFBP-6 production was significantly increased in the supernatant of lactate treated U-87 MG (3.87 ug/mL ± 0.46, **Figure 4B**) cells compared to control cells (0.089 ug/mL ± 0.01, **Figure 4B**). The same results were observed in A172 (4.34 ug/mL ± 0.09 lactate versus 0.23 ug/mL ± 0.04, **Figure 4B**) and U-251 (3.54 ug/mL ± 0.25 lactate versus 0.07 ug/mL ± 0.01 control, **Figure 4B**) cells. Therefore, in order to find a link between lactate and IGFBP-6, we also evaluated lactate production in supernatants of IGFBP-6-treated GBM cells and whether IGFBP-6 exposition affects expression of metabolic enzymes and cell migration on GBM cell lines. Interestingly, our results showed a significant increase in lactate production in

supernatants of IGFBP-6-treated cells, in all three tested cell lines U87 - MG (6.97 mM ± 0.3 lactate versus 6.01 mM ± 0.3 control, **Figure 4C**), A172 (8.5 mM ± 0.7 lactate versus 7.1 mM ± 0.05 control, **Figure 4E**) and U251 (8.65 mM ± 0.6 lactate versus 7.8 ± 0.16 control, **Figure 4G**). Furthermore, exposure to IGFBP-6 for 24 hours in GBM cells resulted in a significant increase in LDHA mRNA levels in U87-MG (1.75 ± 0.15, **Figure 4D**), A172 (36.9 ± 3.9, **Figure 4F**) and U251 (27.2 ± 3.2, **Figure 4H**) compared to their control cells, a significant increase in HK2 mRNA expression levels in all three cell lines (**Figure 4D – H**), and a significant increase in ENO1 mRNA expression levels only in U87 - MG and A172 cells but not in U251 (**Figure 4D – H**). Consistently, we observed a reduced % of wideness of scratch assay test at 48 hours in U-87 MG (9.08 % ± 2.73 IGFBP-6 versus 29.9 % ± 3.9 control, **Figure 4J**), A172 (3.86 % ± 2.3 IGFBP-6 versus 13.84 % ± 4.9 control, **Figure 4K-4I**) and U-251 (7.25 % ± 2.01 IGFBP-6 versus 39.97 % ± 2.5 control, **Figure 4L**) cells. We also confirmed the effects of IGFBP-6 on colony formation capacity, finding a significantly increased in n° of colonies (53.25 ± 3.7 IGFBP-6 versus 32.75 ± 3.31 control, **Figure 4M-N**) but not in the growth area of each colony in U-87 MG cells (**Figure 4M-O**). Whereas, in the A172 cells

we observed a significant increase in both the number of colonies (89.25 ± 2.21 IGFBP-6 versus 48.75 ± 11.6 control, **Figure 4P-Q**) and the area of the colonies (1.83 mm^2 ± 0.16 IGFBP-6 versus 0.93 mm^2 ± 0.01 control, **Figure 4P-R**). Same results were obtained for U-251 cells, showing an increase in number of colonies (436.5 ± 17.8 IGFBP-6 versus 212 ± 44.2 control, **Figure 4S-T**) and in area of colonies (0.4 mm^2 ± 0.06 IGFBP-6 versus 0.13 mm^2 ± 0.01 control, **Figure 4S-U**).

Lactate induces changes in microglia and IGFB-6 and expression in a zebrafish brain tumor model

To investigated whether lactate accumulation affect microglia in vivo, we used a zebrafish model of Glioblastoma [37] (**Figure 5A**), and analyzed the igfbp6 expression of these tumors. Our results showed that lactate exposure in the tumor brain leads to an increase in the number of microglia and a change in the morphology of the microglia. Hence, in order to analyze whether the effect of lactate on igfbp6 expression has similar effects in vivo, we analyzed the expression of the two isoforms of igfbp6 in healthy brain and zebrafish brain tumor after exposure to lactate. Interestingly, our results showed that there are no significant differences in the

expression of the igfbp6a isoform in both healthy and tumor zebrafish brains after lactate exposure compared to untreated brains (**Figure 5B-C**). Moreover we showed no difference in the expression of the igfbp6b isoform in the healthy brain (**Figure 5D**) but a significant up-regulation of the igfbp6b isoform expression in the lactate-exposed zebrafish tumor brain compared to the untreated tumor brain (8.78 ± 3.3 Ras + Lactate *vs* 1.03 ± 0.02 Ras, **Figure 5E**).

IGFBP-6 was modulated in GBM patients

Across the whole cohort of GBM patients, the immunohistochemical expression of IGFBP-6 was high (IRS ≥ 6) in 5 cases (50%) and low (IRS < 6) in the remaining 5 cases (50%). Interestingly, all cases (5 out of 5) that showed high immunohistochemical expression of IGFBP-6, also exhibited MIB-1 levels > 50% (**Figure 6**); conversely, the remaining cases (5 out of 5) with low IGFBP-6 immunoexpression had low MIB-1 proliferative rates (<50%). A positive correlation was found between IGFBP-6 immunohistochemical expression and MIB-1 proliferative rate in all GBM cases examined.

IGFBP6 gene expression analysis in human glioma

The IGFBP6 gene expression analysis obtained from the GSE108474 dataset showed that there were significant differences when the expression levels obtained from brain biopsies of glioblastoma patients were compared to the other brain tumors stages. (**Figure 6**). Specifically, patients with glioblastoma expressed significantly higher levels of the IGFBP6 messenger in the brain than patients with oligodendroglioma ($p<0.0001$), astrocytoma ($p<0.0001$), or healthy subjects ($p<0.0001$) (figure 6a). This finding was confirmed by the significantly positive correlation between IGFBP6 expression levels and tumor grade ($r = 0.3926$; p $p<0.0001$) (**Figure 6B**). According to these results, we investigatated the prognostic potential of IGFBP6 expression in the progression of main brain tumors. Currently the expression analysis of Isocitrate Dehydrogenase (NADP (+)) 1 (IDH1) and the identification of its main mutations (e.g. R132H) are used for glioma diagnosis and prognosis [67]. By carrying out a Pearson correlation analysis between IGFBP6 and IDH1 brain tumor expression levels, we highlighted that in glioblastoma patients the expression levels of the two genes were significantly closely inversely correlated ($r = -0.3743$, $p <0.0001$) (**Figure 6C**).

Furthermore, in order to evaluate the potential diagnostic ability of IGFBP6 gene expression to discriminate against the brain tumors stages, we performed a Receiver operating characteristic (ROC) analysis. We confirmed the diagnostic ability of IGFBP6 to discriminate the glioblastoma patients from healthy subjects (AUC=0.826, p<0.0001) (**Figure 6D**) or from the patients affected to astrocytoma (AUC=0.753, p<0.0001) (**Figure 6E**) or oligodendrocitoma (AUC=0.748, p<0.0001) (**Figure 6F**).

DISCUSSION

The extensive production of acidic metabolites and the enhanced acid export to the extracellular space results in a significant acidification of TME, thus promoting the formation of an acid-resistant tumor cell population with increased invasiveness and metastatic potential [68]. Lactic acidosis has been reported in the TME of several tumors including GBM [69], triggering a series of biochemical mechanisms that modify cell metabolism and signaling; furthermore a variety of oncogenic and environmental factors alter tumor metabolism to meet the distinct cellular biosynthetic and bioenergetic needs present during oncogenesis [70]. Among the most interesting biological processes that are reshaping cell metabolism, those that recap developmental processes, such as the one involving IGFBP-6, hold great potential to understand tumor-related biological processes such as cell proliferation, migration, senescence and changes in metabolism [71]. For this purpose, we aimed at studying a potential crosstalk between lactate and IGFBP-6 in microglial cells and the impact of this interaction on TME and GBM progression. Several studies showed that in the early phases of the

disease, GAMs are abundant in the tumor mass and infiltrate TME contributing to tumorigenesis [14, 72, 73].

We first showed that exposing microglia cells to lactate results in a significant increase in MCT1 gene and protein expression, responsible for the influx of lactate into the cell and involved in a lactate shuttle to provide energetic support. Consistent with our data, Moreira et al. demonstrated for the first time that microglia express the monocarboxylic transporter (MCT) 1 and 2 and take up lactate and ketones [74]. Our data also showed that lactate also induces a significant up-regulation of genes involved in oxidative phosphorylation. Interestingly, MCT1 has a high affinity for lactate and is preferentially expressed in oxidative cells that take up lactate [75–77]. In oxidative cells, lactate reacts intracellularly with NAD+ to yield pyruvate, NADH and H+ (the LDHB reaction), and both pyruvate and NADH can fuel the TCA cycle and OXPHOS in mitochondria, which depends on the malate–aspartate shuttle for the mitochondrial import of NADH [77, 78]. Interestingly, Gasior M. et al. showed that a ketogenic diet correlates with a suppression of microglia activation [79–81]. Therefore, we verified the ability of lactate to promote M2 polarization (immunosuppressive

phenotype) of microglia, showing both by RT-PCR and immunocytochemical analysis an increase in the expression of M2 markers (i.e., Arg-1, CD 206, CD 163) and a decrease in M1 markers (iNOS) in treated cells as compared to untreated cells, suggesting that lactate was able to induce modification of microglia metabolic functions. Recent data have confirmed the link between metabolism and microglia polarization, similar to traditional macrophages. Our data are consistent with a study by Xianmin Mu et al., in which they demonstrate that tumor-derived lactate induced M2 macrophage polarization [82], via ERK / STAT3 signaling, which then facilitates angiogenesis, cancer cell migration, and invasion and that lactate is correlated with cell re-education in the TME [26]. Moreover, increased glycolysis is observed in M1-like microglia, which is dependent on the increase of hexokinase and lactate dehydrogenase activity, and high expression of GLUT1 [83, 84]. Another study by Colegio et al. found that tumor-associated macrophage (TAM) polarization is dependent on tumor-derived lactic acid, and the mechanism is mediated by hypoxia-inducible factor 1α (HIF1α) [26, 85]. The pathways, driven by lactate, that elicit M2-like functional polarization of TAMs are still not fully elucidated. Many signals are

involved in M2-like macrophage polarization, for instance, ERK1/2, STAT3, HIF1α, STAT6 and so forth, can polarizes macrophage via a number of signaling pathways [82, 86, 87]. Furthermore, several studies also showed that lactic acid was sufficient to induce macrophage polarization via pH acidification of TME [82, 88, 89], even if cellular mechanisms and molecular pathways involved in such a modulation are still unknown [85].

Thus, given the evidence on cellular modulation exerted by increased extracellular levels of lactate, we sought to link metabolic reshaping with IGFBP-6 and found that lactate modulates microglia M2 polarization and remodels tumor microenvironment in glioblastoma through IGFBP-6.

Interestingly, we found that microglia exposed to lactate showed a significant increase in both gene and protein expression of IGFBP-6, and this was confirmed by measuring the levels of IGFBP-6 in the supernatant of lactate-treated cells, which showed a significant increase in the production of IGFBP-6 compared to control cells and its release to the extracellular milieu. These data suggest that lactate influences IGFBP-6 signaling. This is in line with the well-known IGF system role and its interaction with cell

metabolism [90]. The regulation of IGF actions is of paramount importance due to their potential contribution to a number of common disease processes, including cancer [90]. Surprisingly, IGFBP-6 treatment was also able to upregulate oxidative phosphorylation and to induced an immunosuppressive phenotype in microglia cells. These data are consistent with the study of Chesik D. et al., in which they examined the expression of IGFBPs (from 1 to -6) in primary rat microglia cultures under basal conditions and after stimulation with LPS, one of the classic activators of microglia, demonstrating that stimulation of microglia by LPS led to a down-regulation of IGFBP-4, -5 and -6 [91].

In recent years, IGFBP-6 has been shown to inhibit IGF-II [92–94] and to modulate nuclear transcription of genes involved in differentiation and survival, leading to increase cell migration [95][96–98]. Indeed, GBM cells exposed to IGFBP-6 significantly increased LDHA mRNA expression, thus confirming the existence of IGFBP-6 to lactate axis that increases cell proliferation and colony-forming capacity. This finding was confirmed on our cohort of GBM specimens; we studied the relationship between the immunohistochemical expression of IGFBP-6 and MIB-1, a widely

used marker of the tumor proliferative activity, and found that a positive correlation between these two markers did exist. In our series, while GBM cases that showed MIB-1 levels >50%, exhibited a strong and diffuse positivity for anti-IGFB6 antibody, those with low MIB-1 proliferative index (<50%) were weakly and patchly stained with IGFB6. Based on these findings, it can be hypothesized that IGFBP-6 may be used in the future as easily detectable prognostic marker of GBM, predictor of increased tumor aggressiveness.

Besides the role of microglia-derived IGFBP-6 on GBM cells, we also observed that conditioned medium from IGFBP-6 treated GBM cells is able to modulate microglia polarization, inducing an M2-like phenotype. Consistent with these data, Li et al. showed that in GBM, microglial cells have been shown to have a pro-tumor phenotype that is associated with the M2-like phenotype of macrophages due to its expression of specific factors, such as ILs, transforming growth factor beta 1 (TGF-β1), monocyte chemoattractant protein (MCP-1), and prostaglandin E2 (PGE-2) [14]. At the same time, the glial cells from TME also release factors that support GBM growth. Furthermore, other studies of Hambardzumyan et al. and Lisi et al. suggested that in the case of

GBM, glioma cells are able to suppress the microglial M1-like phenotype and induce an M2 anti-inflammatory phenotype through the above-mentioned cytokines and chemokines, which in turn induce microglial cells to release different factors that will stimulate tumor growth [99, 100]. Moreover, the presence of microglial M2-like phenotype has been associated with the aggressiveness and poor prognosis in GBM patients [101–103] . These results are consistent with hallmarks of microglial activation seen in cases of disease and histopathological analysis of GBM tumors [104, 105]. Interestingly, several studies have shown that IGFBP-3, known to regulate cell proliferation, was also increased in GBM-microglia crosstalk, though its role in cancer progression remains to be fully understood [106–108].

Further confirmation of our study was obtained by analyzing the human GSE108474 dataset. The analysis allowed us to highlight that IGFBP6 is significantly modulated during the progression of the disease. In particular, significant expression changes were highlighted with the increase in the degree of malignancy. Furthermore, our results showed that IGFBP6 can potentially be used in order to discriminate patients with glioblastoma versus

those with astrocytoma and oligodendroglioma. These data are in agreement with the current bibliography which considers IGFBP6 a prognostic biomarker in human glioblastoma [109]. Interestingly, the correlation analysis between IGFBP6 and IDH1 brain expression levels in glioblastoma patients was inversely proportional. Currently, no data is available in the literature that confirms or refutes the correlation that has been highlighted between IGFBP6 and IDH1 during our analysis. This result could be considered a good starting point for future investigation.

In conclusion, our results demonstrate that IGFBP-6 modulates polarization of microglia and that its expression is regulated by lactate production in GBM cells suggesting the existence of a lactate to IGFBP-6 crosstalk between microglial cells and GBM and this relationship modulates TME, which could affect tumor progression and resistance to therapy and that the complex network of interaction between microglial cells and GBM could be a potential therapeutic target to overcome tumor malignancy.

Figure Legends

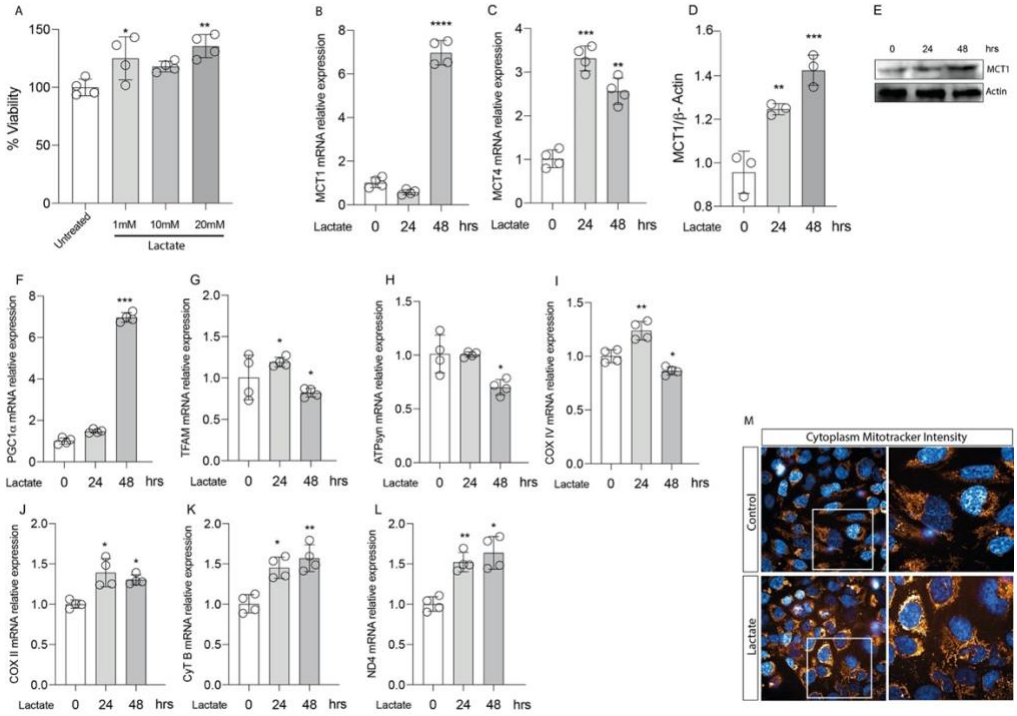

Figure 1.

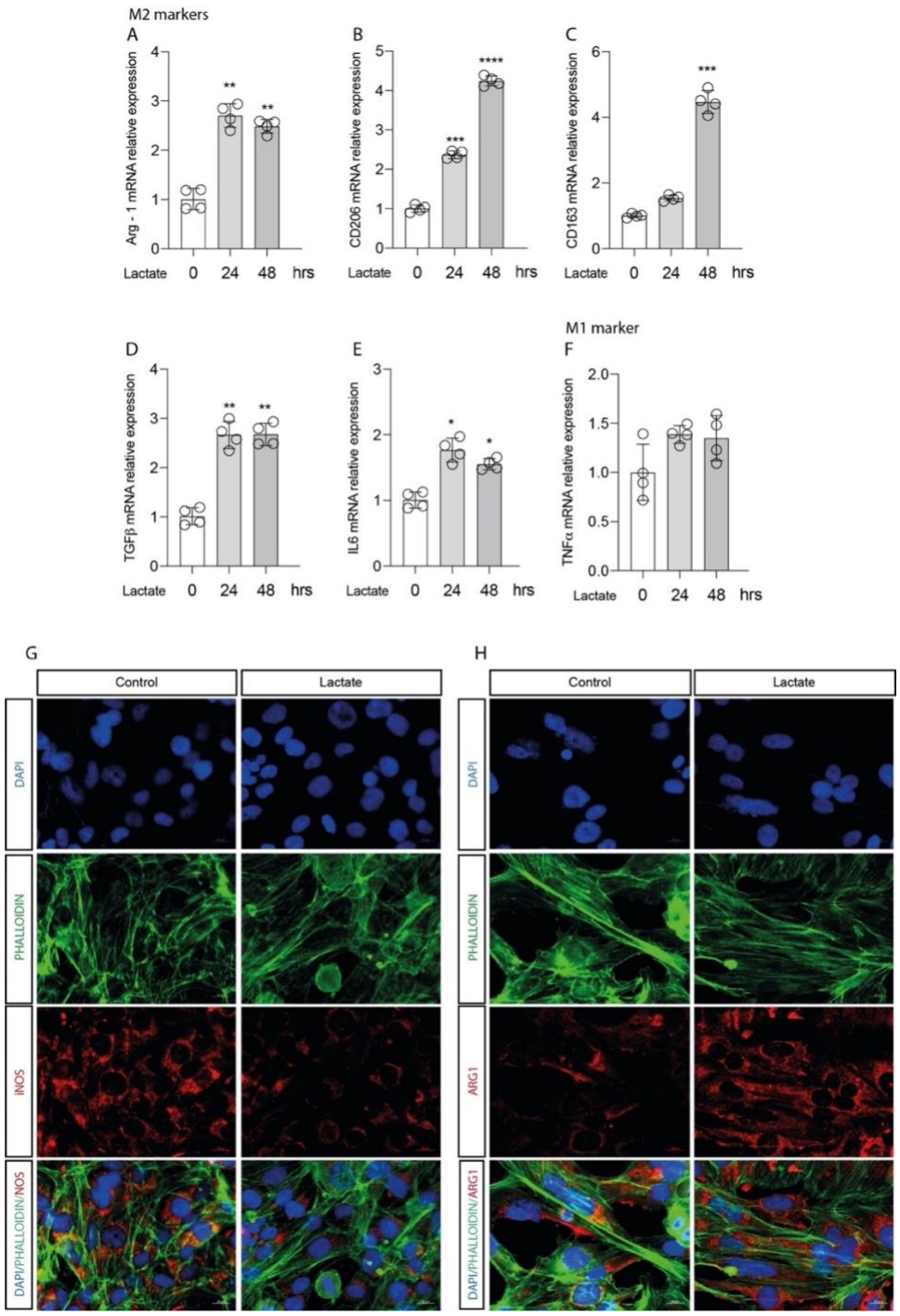
M2 markers
A
Arg - 1 mRNA relative expression
B
CD206 mRNA relative expression
C
CD163 mRNA relative expression
Lactate 0 24 48 hrs
M1 marker
D
TGFβ mRNA relative expression
E
IL6 mRNA relative expression
F
TNFα mRNA relative expression
G
H
Control
Lactate
DAPI
PHALLOIDIN
iNOS
ARG1
DAPI/PHALLOIDIN/NOS
DAPI/PHALLOIDIN/ARG1

Figure 2.

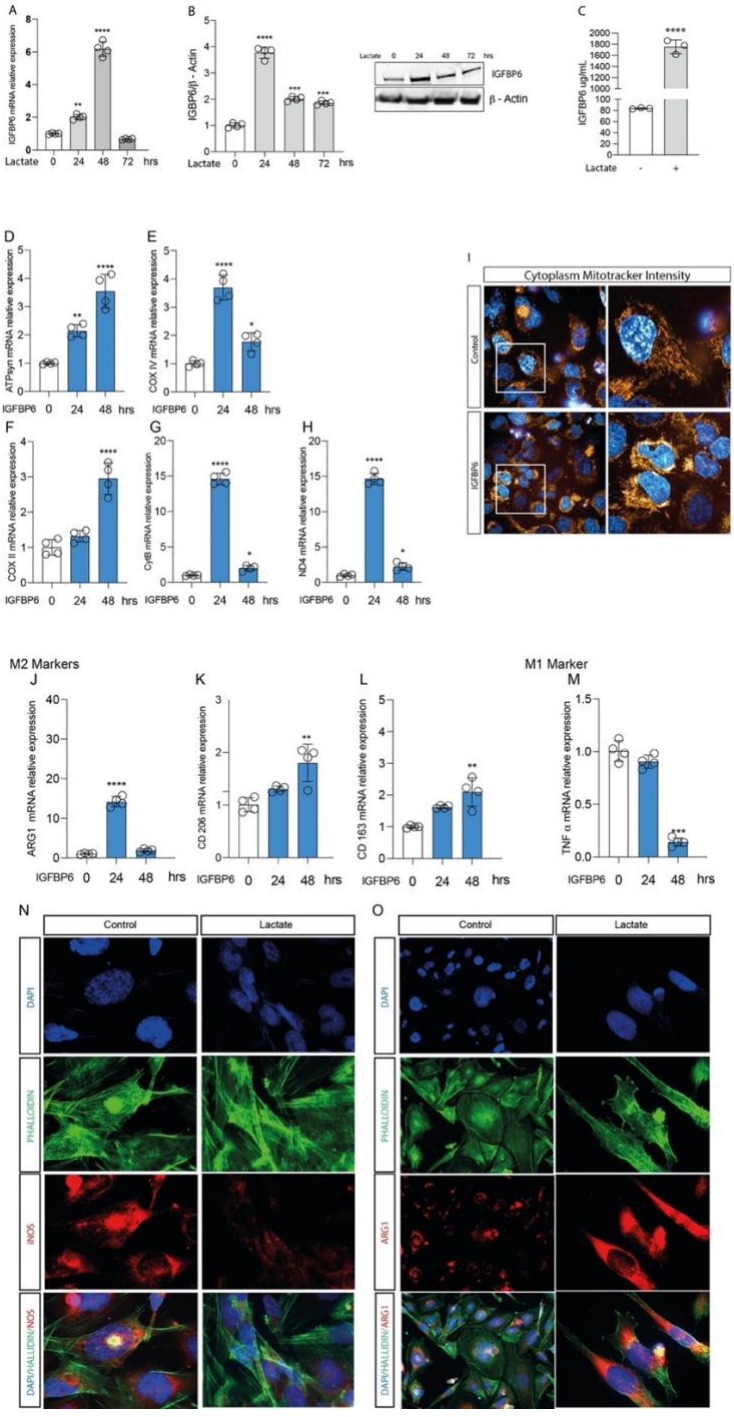
A
IGFBP6 mRNA relative expression
Lactate 0 24 48 72 hrs
B
IGBP6/β - Actin
Lactate 0 24 48 72 hrs
Lactate 0 24 48 72 hrs
IGFBP6
β - Actin
C
IGFBP6 ug/mL
Lactate - +
D
ATPsyn mRNA relative expression
IGFBP6 0 24 48 hrs
E
COX IV mRNA relative expression
IGFBP6 0 24 48 hrs
I
Cytoplasm Mitotracker Intensity
Control
IGFBP6
F
COX II mRNA relative expression
IGFBP6 0 24 48 hrs
G
CytB mRNA relative expression
IGFBP6 0 24 48 hrs
H
ND4 mRNA relative expression
IGFBP6 0 24 48 hrs
M2 Markers
M1 Marker
J
ARG1 mRNA relative expression
IGFBP6 0 24 48 hrs
K
CD 206 mRNA relative expression
IGFBP6 0 24 48 hrs
L
CD 163 mRNA relative expression
IGFBP6 0 24 48 hrs
M
TNF α mRNA relative expression
IGFBP6 0 24 48 hrs
N
Control
Lactate
DAPI
PHALLOIDIN
iNOS
DAPI/HALLOIDIN/NOS
O
Control
Lactate
DAPI
PHALLOIDIN
ARG1
DAPI/HALLOIDIN/ARG1

Figure 3.

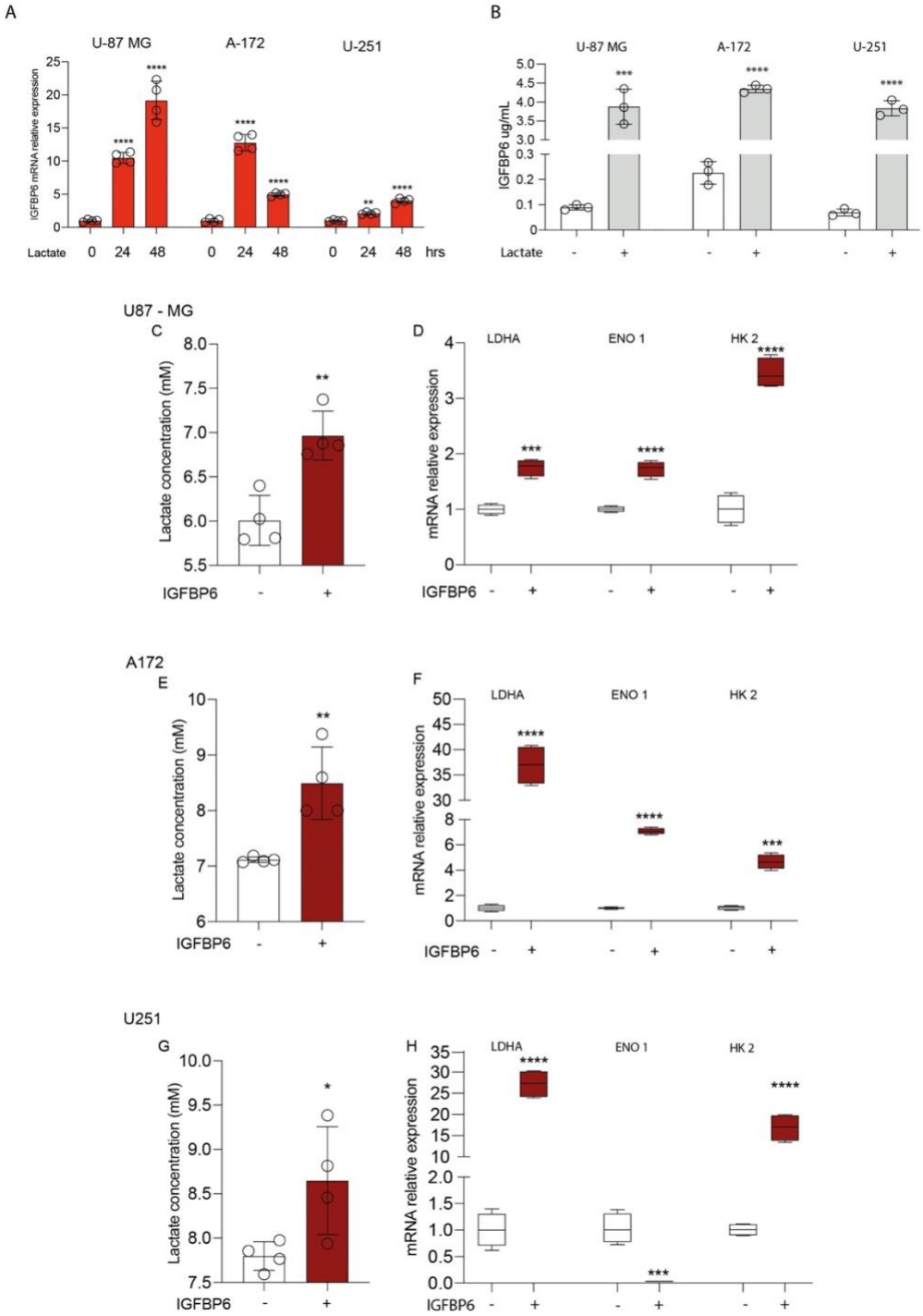
A
U-87 MG
A-172
U-251
IGFBP6 mRNA relative expression
Lactate 0 24 48 0 24 48 0 24 48 hrs
B
U-87 MG
A-172
U-251
IGFBP6 ug/mL
Lactate - + - + - +
U87 - MG
C
Lactate concentration (mM)
IGFBP6 - +
D
LDHA
ENO 1
HK 2
mRNA relative expression
IGFBP6 - + - + - +
A172
E
Lactate concentration (mM)
IGFBP6 - +
F
LDHA
ENO 1
HK 2
mRNA relative expression
IGFBP6 - + - + - +
U251
G
Lactate concentration (mM)
IGFBP6 - +
H
LDHA
ENO 1
HK 2
mRNA relative expression
IGFBP6 - + - + - +

Figure 4.

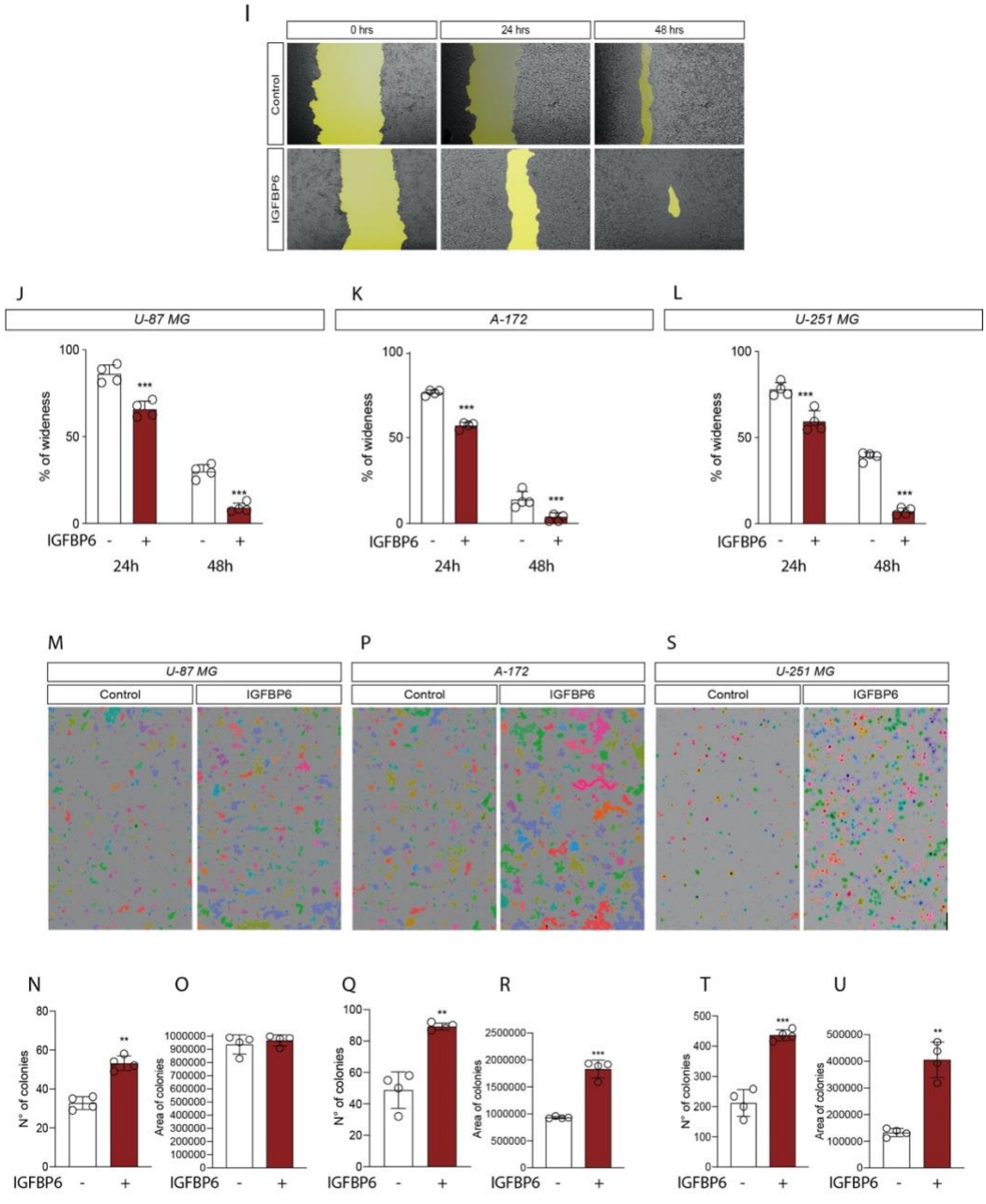
I
0 hrs
24 hrs
48 hrs
Control
IGFBP6
J
U-87 MG
K
A-172
L
U-251 MG
% of wideness
IGFBP6
24h
48h
M
P
S
Control
IGFBP6
N
O
Q
R
T
U
N° of colonies
Area of colonies

Figure 4.

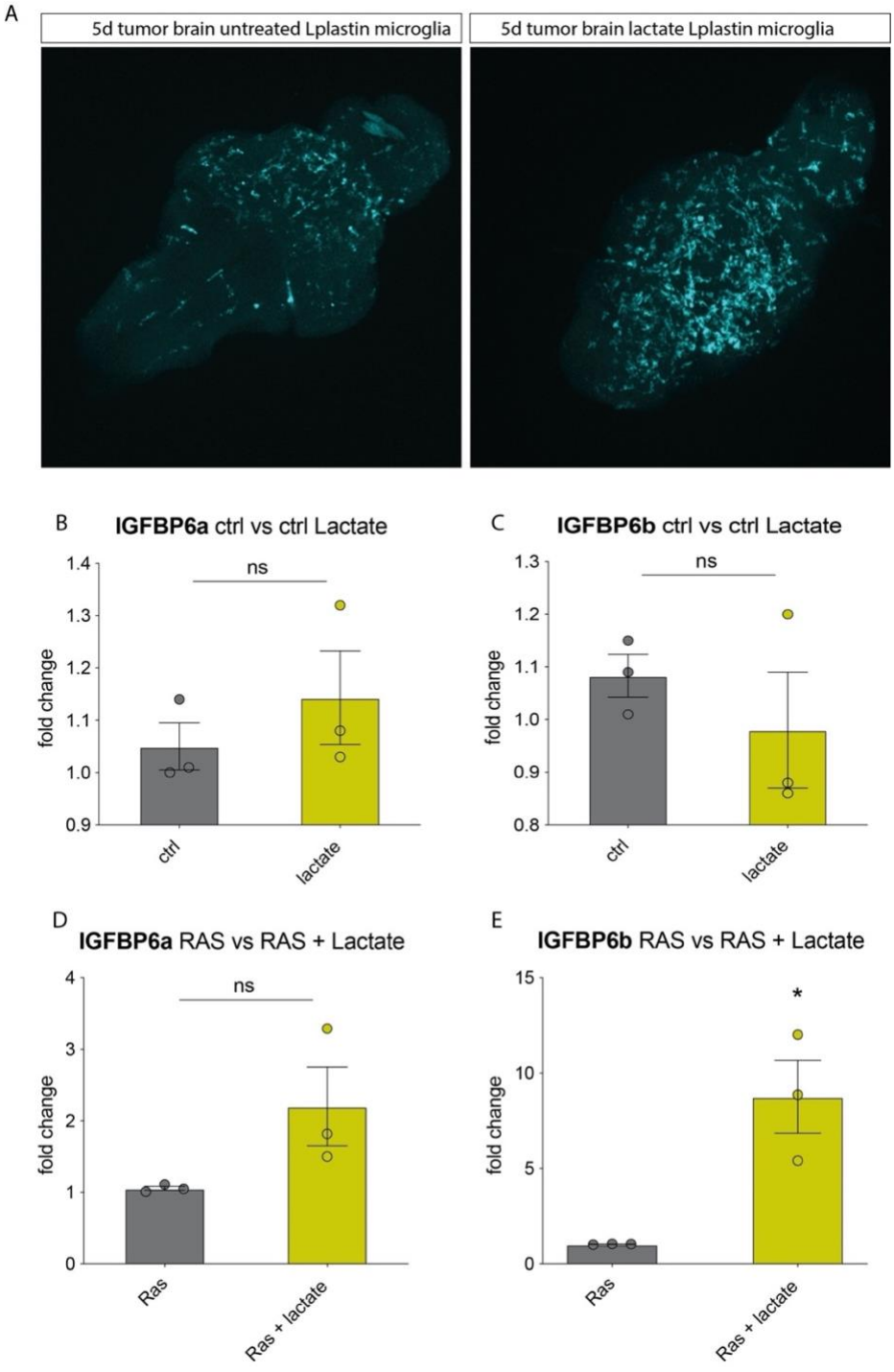
A
5d tumor brain untreated Lplastin microglia
5d tumor brain lactate Lplastin microglia
B
IGFBP6a ctrl vs ctrl Lactate
ns
fold change
1.4
1.3
1.2
1.1
1.0
0.9
ctrl
lactate
C
IGFBP6b ctrl vs ctrl Lactate
ns
fold change
1.3
1.2
1.1
1.0
0.9
0.8
ctrl
lactate
D
IGFBP6a RAS vs RAS + Lactate
ns
fold change
4
3
2
1
0
Ras
Ras + lactate
E
IGFBP6b RAS vs RAS + Lactate
*
fold change
15
10
5
0
Ras
Ras + lactate

Figure 5.

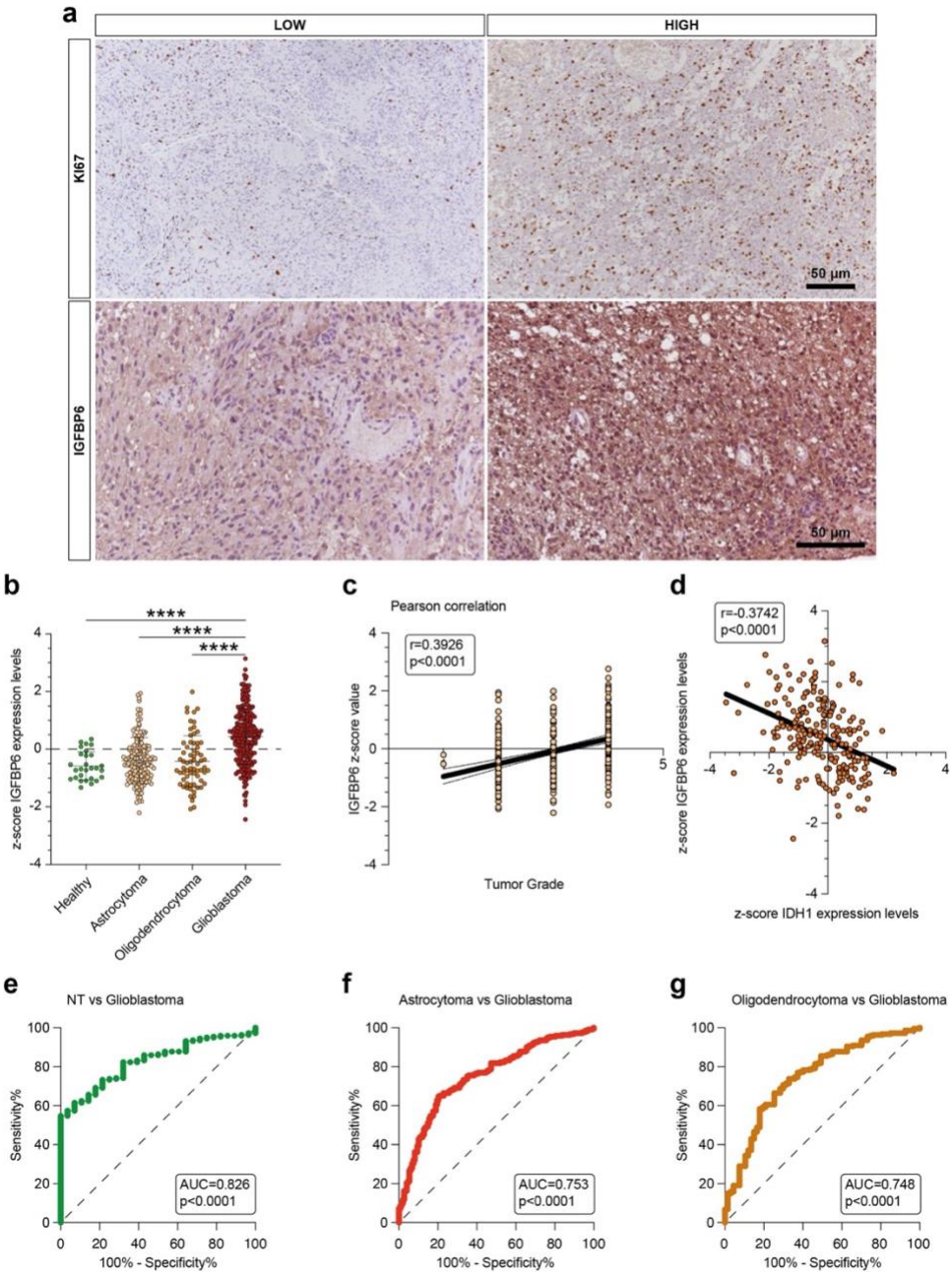
a
LOW
HIGH
KI67
IGFBP6
50 µm
50 µm
b
****
****
****
z-score IGFBP6 expression levels
Healthy
Astrocytoma
Oligodendrocytoma
Glioblastoma
c
Pearson correlation
r=0.3926
p<0.0001
IGFBP6 z-score value
Tumor Grade
d
r=-0.3742
p<0.0001
z-score IGFBP6 expression levels
z-score IDH1 expression levels
e
NT vs Glioblastoma
Sensitivity%
100% - Specificity%
AUC=0.826
p<0.0001
f
Astrocytoma vs Glioblastoma
Sensitivity%
100% - Specificity%
AUC=0.753
p<0.0001
g
Oligodendrocytoma vs Glioblastoma
Sensitivity%
100% - Specificity%
AUC=0.748
p<0.0001

Figure 6.

Figures Legends

Figure 1. Lactate induces the expression of MCT1, promoting an oxidative metabolism in microglia cells. Effect of Lactate on (**A**) cell viability, (**B**) *MCT1* and (**C**) *MCT4* mRNA expression levels, and (**D - E**) MCT1 protein expression levels, in microglia cells. Evaluation of relative mRNA expression levels of (**F**) *PGC1a*, (**G**) *TFAM*, (**H**) *ATPsyn*, (**I**) *COX IV*, (**J**) *COX II*, (**K**) *CyTB*, (**L**) *ND4*, following 24 and 48 hours of lactate exposition, analyzed by Real time PCR. The calculated value of $2^{-\Delta\Delta Ct}$ in untreated controls is 1. (**M**) Cytoplasm Mitotracker Intensity. Data are expressed as mean ± SD of at least four independent experiments. (*p<0.05; **p<0.005; ***p<0.001; ****p<0.0001).

Figure 2. Lactate promotes M2 polarization of microglia. Evaluation of relative mRNA expression levels of (**A**) Arg1, (**B**) CD 206, (**C**) CD 163, (**D**) TGF b, (**E**) IL6, (**F**) TNF a, following 24 and 48 hours of lactate exposition, analyzed by Real time PCR. The calculated value of $2^{-\Delta\Delta Ct}$ in untreated controls is 1. Immunocytochemistry analysis of (**G**) iNOS and (**H**) Arg1, following 72 hours of lactate treatment. Data are expressed as mean ± SD of at least four independent experiments. (*p<0.05; **p<0.005; ***p<0.001; ****p<0.0001).

Figure 3. Lactate induces IGFBP-6 expression which promotes M2 polarization of microglia. Effect of Lactate on IGFBP-6 (**A**) mRNA expression levels, (**B**) protein expression and (**C**) production in microglia cells. Evaluation of relative mRNA expression levels of (**D**) *ATPsyn*, (**E**) *COX IV*, (**F**) *COX II*, (**G**) *CyTB*, (**H**) *ND4*. (I) Citoplasm Mitoracker Intensity. Evaluation of Evaluation of relative mRNA

expression levels of (**J**) *Arg1,* (**K**) *CD 206*, (**L**) *CD 163* and (**M**) *TNF a*, analyzed by Real time PCR. The calculated value of $2^{-\Delta\Delta Ct}$ in untreated controls is 1. Immunocytochemistry analysis of (**N**) iNOS and (**O**) Arg1, following 72 hours of IGFBP-6 treatment. Data are expressed as mean ± SD of at least four independent experiments. (*p<0.05; **p<0.005; ***p<0.001; ****p<0.0001).

Figure 4. IGFBP-6 enhances migratory and colony formation capacity in glioblastoma cells. Effect of Lactate on IGFBP-6 (**A**) mRNA expression levels and (**B**) production in Glioblastoma cells. Effect of IGFBP-6 treatment on Lactate production in (**C**) U87 – MG, (**E**) A172 and (**G**) U251 cells. Evaluation of mRNA expression levels of LDHA, ENO1 and HK2 in (**D**) U87 – MG, (**F**) A172 and (**H**) U251 cells. Effect of IGFBP-6 treatment on migratory capacity (**I-L**) and colony formation capacity (**M-U**) in Glioblastoma cells. Data are expressed as mean ± SD of at least four independent experiments. (*p<0.05; **p<0.005; ***p<0.001; ****p<0.0001).

Figure 5. IGFBP-6 produced by glioblastoma cells promote microglia M2 polarization.

Whole mounts immunofluorescence of L-plastin microglia cells in controls and in HRAS overexpressing 5dpi zebrafish treated or not with 20 um lactate. Gene expression analysis through q-PCR expressed as fold changes compared to controls, at 5dpf and in the adult tumors. Values represent the means ± SEM of experiments performed in triplicate. p values < 0.05 were considered to be statistically significant (*p < 0.05 vs controls).

Figure 6. IGFBP-6 was modulated in GBM patients.

Analysis of IGFBP6 gene expression in brain biopsies of patients with astrocytoma, oligodendrocytoma, glioblastoma, and healthy subjects. b) Pearson correlation analysis between IGFBP6 expression levels and tumor grade of brain biopsies obtained from patients affected by main brain tumors. c) Pearson's correlation between IGFBP6 and IDH1 expression levels in brain biopsies of patients with glioblastoma. d) Receiver operating characteristic (ROC) analysis between IGFBP6 brain expression levels in healthy subjects vs glioblastoma patients, between glioblastoma patients vs astrocytoma patients (e), and vs oligodendrocytoma (f). Data are expressed as mean ± SD of at least four independent experiments. (*p<0.05; **p<0.005; ***p<0.001; ****p<0.0001).

Referecens

1. Barbagallo D, Caponnetto A, Barbagallo C, et al (2021) The gaugaa motif is responsible for the binding between circsmarca5 and srsf1 and related downstream effects on glioblastoma multiforme cell migration and angiogenic potential. Int J Mol Sci 22:. https://doi.org/10.3390/ijms22041678
2. Certo F, Altieri R, Maione M, et al (2021) FLAIRectomy in Supramarginal Resection of Glioblastoma Correlates with Clinical Outcome and Survival Analysis: A Prospective, Single Institution, Case Series. Oper Neurosurg 20:. https://doi.org/10.1093/ons/opaa293
3. Poon CC, Sarkar S, Yong VW, Kelly JJP (2017) Glioblastoma-associated microglia and macrophages: Targets for therapies to improve prognosis. Brain 140
4. Lorger M (2012) Tumor microenvironment in the brain. Cancers (Basel). 4
5. Zhou W, Bao S (2014) Reciprocal supportive interplay between glioblastoma and tumor-associated macrophages. Cancers (Basel). 6
6. Hambardzumyan D, Bergers G (2015) Glioblastoma: Defining Tumor Niches. Trends in Cancer 1
7. Quail DF, Bowman RL, Akkari L, et al (2016) The tumor microenvironment underlies acquired resistance to CSF-1R inhibition in gliomas. Science (80-) 352:. https://doi.org/10.1126/science.aad3018
8. Prionisti I, Bühler LH, Walker PR, Jolivet RB (2019) Harnessing microglia and macrophages for the treatment of glioblastoma. Front. Pharmacol. 10
9. Wolf SA, Boddeke HWGM, Kettenmann H (2017) Microglia in Physiology and Disease. Annu. Rev. Physiol. 79
10. Hussain SF, Yang D, Suki D, et al (2006) The role of human glioma-infiltrating microglia/macrophages in mediating antitumor immune responses. Neuro Oncol. https://doi.org/10.1215/15228517-2006-008
11. Gieryng A, Pszczolkowska D, Walentynowicz KA, et al (2017) Immune microenvironment of gliomas. Lab. Investig. 97
12. Borisov KE, Sakaeva DD (2015) The immunosuppressive microenvironment of malignant gliomas. Arkh Patol 77:. https://doi.org/10.17116/patol201577654-63
13. Charles NA, Holland EC, Gilbertson R, et al (2012) The brain

tumor microenvironment. Glia. https://doi.org/10.1002/glia.21264
14. Li W, Graeber MB (2012) The molecular profile of microglia under the influence of glioma. Neuro. Oncol.
15. Watters JJ, Schartner JM, Badie B (2005) Microglia function in brain tumors. J. Neurosci. Res.
16. Zhai H, Heppner FL, Tsirka SE (2011) Microglia/macrophages promote glioma progression. Glia. https://doi.org/10.1002/glia.21117
17. Ippolito L, Morandi A, Giannoni E, Chiarugi P (2019) Lactate: A Metabolic Driver in the Tumour Landscape. Trends Biochem. Sci. 44
18. Morandi A, Giannoni E, Chiarugi P (2016) Nutrient Exploitation within the Tumor–Stroma Metabolic Crosstalk. Trends in Cancer 2
19. Baggetto LG (1992) Deviant energetic metabolism of glycolytic cancer cells. Biochimie 74:. https://doi.org/10.1016/0300-9084(92)90016-8
20. Howe FA, Barton SJ, Cudlip SA, et al (2003) Metabolic profiles of human brain tumors using quantitative in vivo 1H magnetic resonance spectroscopy. Magn Reson Med 49:. https://doi.org/10.1002/mrm.10367
21. Hirschhaeuser F, Sattler UGA, Mueller-Klieser W (2011) Lactate: A metabolic key player in cancer. Cancer Res. 71
22. Gatenby RA, Gillies RJ (2004) Why do cancers have high aerobic glycolysis? Nat. Rev. Cancer 4
23. Gillies RJ, Robey I, Gatenby RA (2008) Causes and consequences of increased glucose metabolism of cancers. J. Nucl. Med. 49
24. Colen CB, Shen Y, Ghoddoussi F, et al (2011) Metabolic targeting of lactate efflux by malignant glioma inhibits invasiveness and induces necrosis: An in vivo study1. Neoplasia 13:. https://doi.org/10.1593/neo.11134
25. Romero-Garcia S, Moreno-Altamirano MMB, Prado-Garcia H, Sánchez-García FJ (2016) Lactate contribution to the tumor microenvironment: Mechanisms, effects on immune cells and therapeutic relevance. Front. Immunol. 7
26. Colegio OR, Chu NQ, Szabo AL, et al (2014) Functional polarization of tumour-associated macrophages by tumour-derived lactic acid. Nature 513:.

https://doi.org/10.1038/nature13490
27. Bronte V (2014) Tumor cells hijack macrophages via lactic acid. Immunol. Cell Biol. 92
28. Ohashi T, Akazawa T, Aoki M, et al (2013) Dichloroacetate improves immune dysfunction caused by tumor-secreted lactic acid and increases antitumor immunoreactivity. Int J Cancer 133:. https://doi.org/10.1002/ijc.28114
29. de la Cruz-López KG, Castro-Muñoz LJ, Reyes-Hernández DO, et al (2019) Lactate in the Regulation of Tumor Microenvironment and Therapeutic Approaches. Front. Oncol. 9
30. Pinheiro C, Garcia EA, Morais-Santos F, et al (2014) Lactate transporters and vascular factors in HPV-induced squamous cell carcinoma of the uterine cervix. BMC Cancer 14:. https://doi.org/10.1186/1471-2407-14-751
31. Fang J, Quinones QJ, Holman TL, et al (2006) The H+-linked monocarboxylate transporter (MCT1/SLC16A1): A potential therapeutic target for high-risk neuroblastoma. Mol Pharmacol 70:. https://doi.org/10.1124/mol.106.026245
32. Curry JM, Tuluc M, Whitaker-Menezes D, et al (2013) Cancer metabolism, stemness and tumor recurrence : MCT1 and MCT4 are functional biomarkers of metabolic symbiosis in head and neck cancer. Cell Cycle 12:. https://doi.org/10.4161/cc.24092
33. Baxter RC (2014) IGF binding proteins in cancer: Mechanistic and clinical insights. Nat. Rev. Cancer 14
34. Jeon HJ, Park J, Shin JH, Chang MS (2017) Insulin-like growth factor binding protein-6 released from human mesenchymal stem cells confers neuronal protection through IGF-1R-mediated signaling. Int J Mol Med 40:. https://doi.org/10.3892/ijmm.2017.3173
35. Liso A, Capitanio N, Gerli R, Conese M (2018) From fever to immunity: A new role for IGFBP-6? J. Cell. Mol. Med. 22
36. Aboalola D, Han VKM (2019) Insulin-Like Growth Factor Binding Protein-6 Promotes the Differentiation of Placental Mesenchymal Stem Cells into Skeletal Muscle Independent of Insulin-Like Growth Factor Receptor-1 and Insulin Receptor. Stem Cells Int 2019:. https://doi.org/10.1155/2019/9245938
37. Zheng R, Chen W, Xia W, et al (2020) The Prognostic Values of the Insulin-Like Growth Factor Binding Protein Family in Ovarian Cancer. Biomed Res Int 2020:. https://doi.org/10.1155/2020/7658782

38. Artiss JD, Karcher RE, Cavanagh KT, et al (2000) A liquid-stable reagent for lactic acid levels: Application to the Hitachi 911 and Beckman CX7. Am J Clin Pathol 114:. https://doi.org/10.1309/65UJ-FQ75-DVGC-XX1N
39. Detrich HW, Westerfield M, Zon LI (2009) Essential zebrafish methods : cell and developmental biology
40. Mayrhofer M, Gourain V, Reischl M, et al (2017) A novel brain tumour model in zebrafish reveals the role of YAP activation in MAPK- and PI3K-induced malignant growth. DMM Dis Model Mech 10:. https://doi.org/10.1242/dmm.026500
41. Santoriello C, Gennaro E, Anelli V, et al (2010) Kita driven expression of oncogenic HRAS leads to early onset and highly penetrant melanoma in zebrafish. PLoS One 5:. https://doi.org/10.1371/journal.pone.0015170
42. Idilli AI, Pagani F, Kerschbamer E, et al (2020) Changes in the expression of pre-replicative complex genes in hTERT and ALT pediatric brain tumors. Cancers (Basel) 12:. https://doi.org/10.3390/cancers12041028
43. Broggi G, Salvatorelli L, Barbagallo D, et al (2021) Diagnostic Utility of the Immunohistochemical Expression of Serine and Arginine Rich Splicing Factor 1 (SRSF1) in the Differential Diagnosis of Adult Gliomas. Cancers (Basel) 13:. https://doi.org/10.3390/cancers13092086
44. Clough E, Barrett T (2016) The Gene Expression Omnibus database. In: Methods in Molecular Biology
45. Gusev Y, Bhuvaneshwar K, Song L, et al (2018) Data descriptor: The REMBRANDT study, a large collection of genomic data from brain cancer patients. Sci Data 5:. https://doi.org/10.1038/sdata.2018.158
46. Xiao J, Cao H, Chen J (2017) False discovery rate control incorporating phylogenetic tree increases detection power in microbiome-wide multiple testing. Bioinformatics 33:. https://doi.org/10.1093/bioinformatics/btx311
47. Smyth GK (2004) Linear models and empirical bayes methods for assessing differential expression in microarray experiments. Stat Appl Genet Mol Biol 3:. https://doi.org/10.2202/1544-6115.1027
48. Sean D, Meltzer PS (2007) GEOquery: A bridge between the Gene Expression Omnibus (GEO) and BioConductor. Bioinformatics 23:.

https://doi.org/10.1093/bioinformatics/btm254
49. Box GEP, Tiao GC (2011) Nature of Bayesian Inference. In: Bayesian Inference in Statistical Analysis
50. Cheadle C, Vawter MP, Freed WJ, Becker KG (2003) Analysis of microarray data using Z score transformation. J Mol Diagnostics 5:. https://doi.org/10.1016/S1525-1578(10)60455-2
51. Scarpino M, Pinzone MR, Di Rosa M, et al (2013) Kidney disease in HIV-infected patients. Eur Rev Med Pharmacol Sci 17:
52. Care MA, Barrans S, Worrillow L, et al (2013) A Microarray Platform-Independent Classification Tool for Cell of Origin Class Allows Comparative Analysis of Gene Expression in Diffuse Large B-cell Lymphoma. PLoS One 8:. https://doi.org/10.1371/journal.pone.0055895
53. Wang J, Coombes KR, Highsmith WE, et al (2004) Differences in gene expression between B-cell chronic lymphocytic leukemia and normal B cells: A meta-analysis of three microarray studies. Bioinformatics 20:. https://doi.org/10.1093/bioinformatics/bth381
54. Reddy TBK, Riley R, Wymore F, et al (2009) TB database: An integrated platform for tuberculosis research. Nucleic Acids Res 37:. https://doi.org/10.1093/nar/gkn652
55. Lê Cao KA, Rohart F, McHugh L, et al (2014) YuGene: A simple approach to scale gene expression data derived from different platforms for integrated analyses. Genomics 103:. https://doi.org/10.1016/j.ygeno.2014.03.001
56. Chen QR, Song YK, Wei JS, et al (2008) An integrated cross-platform prognosis study on neuroblastoma patients. Genomics 92:. https://doi.org/10.1016/j.ygeno.2008.05.014
57. Mehmood R, El-Ashram S, Bie R, et al (2017) Clustering by fast search & merge of local density peaks for gene expression microarray data. Sci Rep 7:. https://doi.org/10.1038/srep45602
58. Yasrebi H, Sperisen P, Praz V, Bucher P (2009) Can survival prediction be improved by merging gene expression data sets? PLoS One 4:. https://doi.org/10.1371/journal.pone.0007431
59. Cheadle C, Cho-Chung YS, Becker KG, Vawter MP (2003) Application of z-score transformation to Affymetrix data. Appl Bioinformatics 2:
60. Feng C, Wu J, Yang F, et al (2018) Expression of Bcl-2 is a favorable prognostic biomarker in lung squamous cell carcinoma. Oncol Lett 15:. https://doi.org/10.3892/ol.2018.8198

61. Kang C, Huo Y, Xin L, et al (2019) Feature selection and tumor classification for microarray data using relaxed Lasso and generalized multi-class support vector machine. J Theor Biol 463:. https://doi.org/10.1016/j.jtbi.2018.12.010
62. Lusted LB (1971) Signal detectability and medical decision-making. Science (80-) 171:. https://doi.org/10.1126/science.171.3977.1217
63. Castrogiovanni P, Sanfilippo C, Imbesi R, et al (2021) Brain CHID1 Expression Correlates with NRGN and CALB1 in Healthy Subjects and AD Patients. Cells 10:. https://doi.org/10.3390/cells10040882
64. Catrogiovanni P, Musumeci G, Giunta S, et al (2020) The expression levels of CHI3L1 and IL15Rα correlate with TGM2 in duodenum biopsies of patients with celiac disease. Inflamm Res 69:. https://doi.org/10.1007/s00011-020-01371-9
65. Zetterberg H, Bozzetta E, Favole A, et al (2019) Neurofilaments in blood is a new promising preclinical biomarker for the screening of natural scrapie in sheep. PLoS One 14:. https://doi.org/10.1371/journal.pone.0226697
66. Payen VL, Hsu MY, Rädecke KS, et al (2017) Monocarboxylate transporter MCT1 promotes tumor metastasis independently of its activity as a lactate transporter. Cancer Res 77:. https://doi.org/10.1158/0008-5472.CAN-17-0764
67. Han S, Liu Y, Cai SJ, et al (2020) IDH mutation in glioma: molecular mechanisms and potential therapeutic targets. Br. J. Cancer 122
68. Böhme I, Bosserhoff AK (2016) Acidic tumor microenvironment in human melanoma. Pigment Cell Melanoma Res. 29
69. Andreucci E, Peppicelli S, Ruzzolini J, et al (2020) The acidic tumor microenvironment drives a stem-like phenotype in melanoma cells. J Mol Med 98:. https://doi.org/10.1007/s00109-020-01959-y
70. LaMonte G, Tang X, Chen JL-Y, et al (2013) Acidosis induces reprogramming of cellular metabolism to mitigate oxidative stress. Cancer Metab 1:. https://doi.org/10.1186/2049-3002-1-23
71. Kasprzak A (2021) Insulin-like growth factor 1 (Igf-1) signaling in glucose metabolism in colorectal cancer. Int. J. Mol. Sci. 22
72. Brandenburg S, Müller A, Turkowski K, et al (2016) Resident microglia rather than peripheral macrophages promote vascularization in brain tumors and are source of alternative pro-

angiogenic factors. Acta Neuropathol 131:. https://doi.org/10.1007/s00401-015-1529-6
73. Gabrusiewicz K, Ellert-Miklaszewska A, Lipko M, et al (2011) Characteristics of the alternative phenotype of microglia/macrophages and its modulation in experimental gliomas. PLoS One 6:. https://doi.org/10.1371/journal.pone.0023902
74. Moreira TJTP, Pierre K, Maekawa F, et al (2009) Enhanced cerebral expression of MCT1 and MCT2 in a rat ischemia model occurs in activated microglial cells. J Cereb Blood Flow Metab 29:. https://doi.org/10.1038/jcbfm.2009.50
75. Sonveaux P, Végran F, Schroeder T, et al (2008) Targeting lactate-fueled respiration selectively kills hypoxic tumor cells in mice. J Clin Invest 118:. https://doi.org/10.1172/JCI36843
76. de Saedeleer CJ, Copetti T, Porporato PE, et al (2012) Lactate Activates HIF-1 in Oxidative but Not in Warburg-Phenotype Human Tumor Cells. PLoS One 7:. https://doi.org/10.1371/journal.pone.0046571
77. Pérez-Escuredo J, Van Hée VF, Sboarina M, et al (2016) Monocarboxylate transporters in the brain and in cancer. Biochim Biophys Acta - Mol Cell Res 1863:. https://doi.org/10.1016/j.bbamcr.2016.03.013
78. Van Hée VF, Pérez-Escuredo J, Cacace A, et al (2015) Lactate does not activate NF-κB in oxidative tumor cells. Front Pharmacol 6:. https://doi.org/10.3389/fphar.2015.00228
79. Gasior M, Rogawski MA, Hartman AL (2006) Neuroprotective and disease-modifying effects of the ketogenic diet. Behav. Pharmacol. 17
80. Fann DYW, Santro T, Manzanero S, et al (2014) Intermittent fasting attenuates inflammasome activity in ischemic stroke. Exp Neurol 257:. https://doi.org/10.1016/j.expneurol.2014.04.017
81. Longo VD, Mattson MP (2014) Fasting: Molecular mechanisms and clinical applications. Cell Metab. 19
82. Mu X, Shi W, Xu Y, et al (2018) Tumor-derived lactate induces M2 macrophage polarization via the activation of the ERK/STAT3 signaling pathway in breast cancer. Cell Cycle 17:. https://doi.org/10.1080/15384101.2018.1444305
83. Gimeno-Bayón J, López-López A, Rodríguez MJ, Mahy N (2014) Glucose pathways adaptation supports acquisition of activated microglia phenotype. J Neurosci Res 92:.

https://doi.org/10.1002/jnr.23356
84. Holland R, McIntosh AL, Finucane OM, et al (2018) Inflammatory microglia are glycolytic and iron retentive and typify the microglia in APP/PS1 mice. Brain Behav Immun 68:. https://doi.org/10.1016/j.bbi.2017.10.017
85. Zhang J, Huang F, Chen L, et al (2021) Sodium Lactate Accelerates M2 Macrophage Polarization and Improves Cardiac Function after Myocardial Infarction in Mice. Cardiovasc Ther 2021:. https://doi.org/10.1155/2021/5530541
86. Zhang W, Xu W, Xiong S (2011) Macrophage Differentiation and Polarization via Phosphatidylinositol 3-Kinase/Akt–ERK Signaling Pathway Conferred by Serum Amyloid P Component. J Immunol 187:. https://doi.org/10.4049/jimmunol.1002315
87. Peda JD, Salah SM, Wallace DP, et al (2016) Autocrine IL-10 activation of the STAT3 pathway is required for pathological macrophage differentiation in Polycystic kidney disease. DMM Dis Model Mech 9:. https://doi.org/10.1242/dmm.024745
88. Ohashi T, Aoki M, Tomita H, et al (2017) M2-like macrophage polarization in high lactic acid-producing head and neck cancer. Cancer Sci 108:. https://doi.org/10.1111/cas.13244
89. Chen P, Zuo H, Xiong H, et al (2017) Gpr132 sensing of lactate mediates tumor-macrophage interplay to promote breast cancer metastasis. Proc Natl Acad Sci U S A 114:. https://doi.org/10.1073/pnas.1614035114
90. Clemmons DR (2007) Modifying IGF1 activity: An approach to treat endocrine disorders, atherosclerosis and cancer. Nat. Rev. Drug Discov. 6
91. Chesik D, Glazenburg K, Wilczak N, et al (2004) Insulin-like growth factor binding protein-1-6 expression in activated microglia. Neuroreport 15:. https://doi.org/10.1097/00001756-200404290-00020
92. Bach LA, Fu P, Yang Z (2013) Insulin-like growth factor-binding protein-6 and cancer. Clin. Sci. 124
93. Alunno A, Bistoni O, Manetti M, et al (2017) Insulin-like growth factor binding protein 6 in rheumatoid arthritis: A possible novel chemotactic factor? Front Immunol 8:. https://doi.org/10.3389/fimmu.2017.00554
94. Gonzalez MM (2019) The insulin-like growth factor-binding protein (IGFBP) family and its role in obesity and cancer. Biomed J Sci Tech Res 13:.

https://doi.org/10.26717/bjstr.2019.13.002436
95. Bach LA (2015) Recent insights into the actions of IGFBP-6. J Cell Commun Signal 9:. https://doi.org/10.1007/s12079-015-0288-4
96. Fu P, Thompson JA, Bach LA (2007) Promotion of cancer cell migration: An insulin-like growth factor (IGF)-independent action of IGF-binding protein-6. J Biol Chem 282:. https://doi.org/10.1074/jbc.M703066200
97. Fu P, Liang GJ, Khot SS, et al (2010) Cross-talk between MAP kinase pathways is involved in IGF-independent, IGFBP-6-induced Rh30 rhabdomyosarcoma cell migration. J Cell Physiol 224:. https://doi.org/10.1002/jcp.22156
98. Yang Z, Bach LA (2014) Differential effects of insulin-like growth factor binding protein-6 (IGFBP-6) on migration of two ovarian cancer cell lines. Front Endocrinol (Lausanne) 5:. https://doi.org/10.3389/fendo.2014.00231
99. Hambardzumyan D, Gutmann DH, Kettenmann H (2015) The role of microglia and macrophages in glioma maintenance and progression. Nat. Neurosci. 19
100. Lisi L, Ciotti GMP, Braun D, et al (2017) Expression of iNOS, CD163 and ARG-1 taken as M1 and M2 markers of microglial polarization in human glioblastoma and the surrounding normal parenchyma. Neurosci Lett 645:. https://doi.org/10.1016/j.neulet.2017.02.076
101. Mieczkowski J, Kocyk M, Nauman P, et al (2015) Down-regulation of IKKβ expression in glioma-infiltrating microglia/macrophages is associated with defective inflammatory/immune gene responses in glioblastoma. Oncotarget 6:. https://doi.org/10.18632/oncotarget.5310
102. Iglesia MD, Parker JS, Hoadley KA, et al (2016) Genomic analysis of immune cell infiltrates across 11 tumor types. J Natl Cancer Inst 108:. https://doi.org/10.1093/jnci/djw144
103. Gieryng A, Pszczolkowska D, Bocian K, et al (2017) Immune microenvironment of experimental rat C6 gliomas resembles human glioblastomas. Sci Rep 7:. https://doi.org/10.1038/s41598-017-17752-w
104. Mignogna C, Signorelli F, Vismara MFM, et al (2016) A reappraisal of macrophage polarization in glioblastoma: Histopathological and immunohistochemical findings and review of the literature. Pathol Res Pract 212:.

https://doi.org/10.1016/j.prp.2016.02.020
105. Lemstra AW, Groen in't Woud JCM, Hoozemans JJM, et al (2007) Microglia activation in sepsis: A case-control study. J Neuroinflammation 4:. https://doi.org/10.1186/1742-2094-4-4
106. Gill ZP, Perks CM, Newcomb P V., Holly JMP (1997) Insulin-like growth factor-binding protein (IGFBP-3) predisposes breast cancer cells to programmed cell death in a non-IGF-dependent manner. J Biol Chem 272:. https://doi.org/10.1074/jbc.272.41.25602
107. Watanabe K, Uemura K, Asada M, et al (2015) The participation of insulin-like growth factor-binding protein 3 released by astrocytes in the pathology of Alzheimer's disease. Mol Brain 8:. https://doi.org/10.1186/s13041-015-0174-2
108. Kielczewski JL, Hu P, Shaw LC, et al (2011) Novel protective properties of IGFBP-3 result in enhanced pericyte ensheathment, reduced microglial activation, increased microglial apoptosis, and neuronal protection after ischemic retinal injury. Am J Pathol 178:. https://doi.org/10.1016/j.ajpath.2010.12.031
109. Zong Z, Xin L, Tang X, Guo H (2021) The clinical characteristics and prognostic value of IGFBP6 in glioma. Neurol Res. https://doi.org/10.1080/01616412.2021.1963620

GENERAL DISCUSSION AND CONCLUSIONS

The first part of the present project aimed to investigate the role of lactate and GPR81 agonist (3,5 – DHBA) in Glioblastoma progression and metabolism both in an *in vitro* and *in vivo* model.

Firstly, we evaluated the effect of lactate and its receptor stimulation in cell proliferation, cell migration and colony formation capacity. In this regard, we used three human Glioblastoma cell lines (i.e., U-87 MG, A-172 and U-251 MG). Our results showed that both Lactate (20 mM) and 3,5 – DHBA (150 uM) result in a significant increase in cell proliferation, cell migration and colony formation capacity in all three tested cell lines, compared to their untreated cells. Several authors showed that stimulation of GPR81 leads to the activation of cell survival signaling promoting cell proliferation via the inhibition of apoptosis and stimulates the secretion of several angiogenic

factors in a PI3K/Akt-CREB signaling pathway-dependent manner [322]. Consistently, another study of Brown, T.P. et al. showed that lactate receptor GPR81 is important as drivers of tumor growth [323].

Gliomas exhibit high glycolytic rates, and MCTs play a major role in the maintenance of the glycolytic metabolism through the proton-linked transmembrane transport of lactate [324]. Over the years, in fact, the study of the metabolic reprogramming of cancer cells has assumed considerable importance; these, at least in the early stages of the disease, are reprogrammed to preferentially use glycolysis rather than OXPHOS for energy production. This phenomenon, called Warburg effect, involves the excessive conversion of glucose into lactate, with a consequent increase in the concentration of lactate which in tumors can reach 40 mM, while in physiological conditions the concentration is about 1.8-2. mM. Therefore, lactate trafficking in cancer cells is regulated by lactate MCTs which also regulate cell metabolism. MCT1 (responsible for the influx of lactate inside the cell) is preferentially

expressed in oxidative cells, while MCT4 (responsible for the efflux of lactate towards the outside of the cell) in glycolytic cells. Therefore, to link lactate as a positive modulator of cell proliferation and migration and to determine the metabolic phenotype of the cells under examination, we analyzed the expression of MCT1 and MCT4 proteins. Our results showed that all three cell lines exhibited significant MCT1 up-regulation, and only two of the cell lines (A-172 and U-251 MG) exhibited significant increases in MCT4 expression, while in U-87 MG we showed a significant decrease in MCT4 expression. These results are in accordance with the study of Froberg et al. [325], who showed that MCT1 was upregulated in glioblastoma tissues (n=17), compared with normal brain and low-grade astrocytomas (n=14). Our results are, also, consistent with previous study, in which it was shown that There was a significant increase in MCT1, MCT4, and CD147 expressions in human glioblastomas samples, compared to nontumoral tissues [324]. The same study also demonstrated that

inhibition of expression of one of the lactate transposers, MCT1, resulted in a reduction in cell migration and lactate production. Moreover, our data suggest that U-87 MG have a different response as compared to the other cell lines in terms of timing to repurpose their transporters and metabolism. Indeed, upon 3,5-DHBA stimulation of HCAR1 we observed a significant increase of MCT4 in U-87 MG, where we obtained contrasting results for A-172 and U-251 MG.

This set of experiments suggest that HCAR1 activation induces MCT1 increase, thus mediating lactate intake in stimulated cells. It is therefore conceivable that intercellular metabolism and mitochondrial content are closely related to HCAR1 activation by several pathways including lactate as a metabolite and other receptor-mediated mechanisms. To this regard, Zaho Y., et al., showed that increasing lactate concentration in liver tumor microenvironment could activate HCAR1 receptor and facilitate

MCT1-mediated uptake of lactate, leading to increased ATP production and decrease of the AMP:ATP ratio in the intracellular compartment [326].

Thus, upregulation of MCTs likely plays an important role in glioma intracellular homeostasis and, thus, contributes to its high aggressiveness [324].

Several studies showed that MCTs are involved in metabolic reprogramming in cancer cells. To this regard we examined the effect of Lactate and its receptor stimulation in the expression of genes involved in mitochondrial metabolism, showing that both lactate and GPR81 agonist induce a significant increase in PGC1a, TFAM and SIRT1 gene expression, suggesting that lactate (both as a metabolite and as a signal molecule) promotes mitochondrial biogenesis, and also induce a significant increase in genes involved in OXPHOS, in all three tested cell lines. Tumor cells stimulate mitochondrial biogenesis not only for proliferation but also for promoting malignant

transformation, in migration and invasiveness and during tumor adaptation to hypoxia [327,328]. As previously mentioned, we observed an increase of mitochondrial biogenesis in GBM cell treated with lactate or HCAR1 inducer, this phenomenon could be due to the increase of lactate uptake after MCT1 overproduction. Moreover, we also showed that the increase of mitochondrial mass also induces an increase of OXPHOS gene expression. Exogenous treatment of lactate in various tumor cell lines induced an increase in ROS levels. We hypothesize that this latter increase in oxidative state determines an enhances of mitochondrial biogenesis such as showed by increase of PGC1a, SIRT1 expression and oxidative genes [329–331].

Interestingly, our results indicate also that HCAR1 activation promotes the modulation of b-catenin and e-cadherin expression suggesting that lactate participates to the epithelial-mesenchymal transition (EMT) in GBM. several studies have been conducted investigating the metabolic changes during EMT in breast, lung, and ovarian cancers, following an

increased recognition of metabolic reprogramming as a hallmark of tumor development [332–334].

Given the insights coming from in vitro experiment on relevant human GBM cell lines, we enrolled a HRAS overexpressing zebrafish model of GBM. Our data confirmed that tumor microenvironment induced HCAR1 upregulation and this was coupled with a significantly increased proton leak and less efficient ATP production.

Lactate exposition determined a significant increase in proliferating PH3 positive cells in RAS-overexpressing zebrafish brain, and this was reverted by selective inhibition of MCT1. This evidence suggest that lactate intake support cell proliferation and that metabolic reshaping is a critical stimulus in GBM microenvironment. Our data from human GBM biopsies were also consistent with preclinical evidence we are providing herein. We observed that in high proliferative GBM biopsies, Ki67 negative cells were expressing significantly higher levels of MCT1 as compared to proliferative cells and low proliferative GBM cells. This

indicates that GBM cells response to lactate, besides sustaining metabolic reshaping and response, it favours proliferation of neighborhood cells by cooperating with their glycolytic metabolism, sensing and removing extracellular lactate. Our data is consistent with other studies in patients with advanced cancer showing that MCT-1 inhibition may provide a significant role in cancer growth and progression and may represent a druggable target for development of new therapeutic strategies (ClinicalTrials.gov identifier (NCT number): NCT01791595).

In the second part of the present project, we studied the crosstalk between lactate and IGFBP6 in microglial cells and how such interaction modulates TME and the GBM progression.

The extensive production of acidic metabolites and the enhanced acid export to the extracellular space results in a significant acidification of TME, thus promoting the formation of an acid-resistant tumor cell population with increased invasive and metastatic potential [335]. Furthermore, several studies showed that

in early phases of the disease, Glioma-associated microglia/macrophages (GAMs) are abundant in the tumor mass and infiltrate TME thus contributing to tumorigenesis [166,167,336] and it has recently been suggested that IGFBP6 is involved in such mechanisms by also modulating important biological processes, including cell proliferation, survival, migration [319], senescence, autophagy and angiogenesis [337], metabolism, maintenance and stem cell differentiation and immune regulation [301,338,339], and although it appears to exert an inhibitory effect on the tumorigenic properties of IGF-II [309,312], this protein has been raising a growing interest for its properties in promoting cancer cell migration [340–342]. We firstly studied the effect of lactate on microglia metabolism, showing that the direct exposure of microglia cells to lactate (20 mM) results in an increase in mitochondrial metabolism. Consistently with our data, Lauro C et al., and Cherry JD et al., in their studies showed that a metabolic switch toward

oxidative metabolism might contribute to promote protective microglia in some pathophysiological conditions, resulting in the production of metabolites beneficial for neurons [343,344]. Furthermore, in our study, Lactate was able to induce microglia M2 polarization. This is in agreement with the results of a study by Xianmin Mu et al. [345]where it appears that lactate is a key oncometabolite in TME that drives M2 polarization of macrophages to promote breast cancer proliferation, migration and angiogenesis through activation of the ERK/STAT3 pathway. Furthermore, the metabolism of lactate is particularly relevant not only for the metabolic balance between hypoxic (lactate-generating) and normoxic (important lactate) tumor cells [346] but also for the polarization of TAMs by hypoxic tumor cells towards a similar profile. a low glycolytic M2 [220,347]. Lactate specifically directs TAMs to a "tumor-friendly" M2-like phenotype, which helps tumor cells evade immunosurveillance [348]. In the study of Anke Zhang et

al. [349] they found that invasive PAs produce excess lactate to promote polarization of TAM towards an M2-like phenotype. These data indicated that lactate plays a key role in TME remodeling and the regulation of intracellular crosstalk between PA and TAM cells.

Given the evidence on cellular modulation exerted by increased extracellular levels of lactate, we sought to link molecular mechanisms underlying these phenomena with the expression of IGFBP6. It is well known that the IGF system plays general roles in metabolism that are evolutionarily conserved [350]. our results showed that microglia exposed to lactate showed a significant increase in both gene and protein expression of IGFBP6, and this was confirmed by measuring the levels of IGFBP6 in the supernatant of the lactate-treated cells, which showed a significant increase in the production of IGFBP6 compared to control cells. These data suggest the existence of a crosstalk between lactate and IGFBP6. Therefore, we analyzed the effect of IGFBP6 treatment on the metabolism and

polarization of microglia cells. Surprisingly, IGFBP6 treatment was also able to upregulate the genes involved in the oxidative phosphorylation pathway and induced the M2 polarization of microglia, as shown by the increase in M2 markers (i.e. Arg - 1, CD206, CD163) and by the reduction of M1 markers (i.e. TNF-α, iNOS). These data are consistent with the study of Chesik D. et al., in which they examined the expression of IGFBPs (from 1 to -6) in primary rat microglia cultures under basal conditions and after stimulation with LPS, one of the classic activators of microglia, demonstrating that stimulation of microglia by LPS led to a down-regulation of IGFBP-4, -5 and -6 [351]. In this regard, we studied the effect of IGFBP6 exposure in GBM cells. Our results showed a significant increase in IGFBP6 production in lactate-treated GBM cells compared to their control cells. Furthermore, direct exposure to IGFBP6 in GBM cells induced a significant increase in the expression of LDHA enzyme mRNA, further confirming the existence

of lactate/IGFBP6 crosstalk. Interestingly, in our experiments, the IGFBP6 protein also induced a significant increase in cell proliferation and colony-forming capacity in GBM cells. [299,352,353]. In addition, IGFBP6 seems able to enter the nucleus where it modulates cell differentiation and survival [312], to interfere with angiogenic processes and to favor cell migration. In particular, recent data suggest that it can induce the migration of tumor cells thus worsening the prognosis of the disease [340–342].

These results were confirmed by transcriptome analysis showing that glioblastoma patients showed a significant increase in IGFBP6 expression compared both to healthy control and Astrocitoma and Oligodendrocitoma patients.

In conclusion, our study showed that lactate is involved in various mechanisms favoring tumor development and progression.

In particular, lactate possesses a dual role being involved in the metabolic changes of tumor cells and acting as a molecule promoting cellular signaling through its membrane receptors. The ability to metabolically shift from glycolytic to oxidative metabolism and vice versa, is likely to confer an advantage in survival, progression and drug resistance. A glycolytic metabolism (Warburg effect), at least in the first phase of disease expansion, determines an advantage in tumor proliferation. Therefore, lactate metabolism may be considered as a therapeutic target to develop novel pharmacological strategies to GBM therapy and improve the outcome and quality of life of such patients. Moreover, our results demonstrate that IGFBP6 modulates polarization of microglia and that its expression is regulated by lactate production in GBM cells suggesting the existence of a lactate/IGFBP6 crosstalk between microglial cells and GBM and this relationship modulates TME which could affect tumor progression and resistance to therapy and that the complex network

of interaction between microglial cells and GBM could be a potential therapeutic target to overcome tumor malignancy.

REFERENCES

1. Lombardi G, Della Puppa A, Di Stefano AL, Pace A, Rudà R, Tabouret E, Zagonel V. Gliomas. Biomed Res Int [Internet]. 2014; 2014: 470523. Available from: http://dx.doi.org/10.1155/2014/470523
2. Hanif F, Muzaffar K, Perveen K, Malhi SM, Simjee SU. Glioblastoma multiforme: A review of its epidemiology and pathogenesis through clinical presentation and treatment. Asian Pacific Journal of Cancer Prevention. 2017.
3. Holland EC. Glioblastoma multiforme: The terminator. Proceedings of the National Academy of Sciences of the United States of America. 2000.
4. Maher EA, Furnari FB, Bachoo RM, Rowitch DH, Louis DN, Cavenee WK, DePinho RA. Malignant glioma: Genetics and biology of a grave matter. Genes and Development. 2001.
5. Schwartzbaum JA, Fisher JL, Aldape KD, Wrensch M. Epidemiology and molecular pathology of glioma. Nature Clinical Practice Neurology. 2006.
6. Agnihotri S, Burrell KE, Wolf A, Jalali S, Hawkins C, Rutka JT, Zadeh G. Glioblastoma, a brief review of history, molecular genetics, animal models and novel therapeutic strategies. Archivum Immunologiae et Therapiae Experimentalis. 2013.
7. Messali A, Villacorta R, Hay JW. A Review of the Economic Burden of Glioblastoma and the Cost Effectiveness of Pharmacologic Treatments. PharmacoEconomics. 2014.
8. Zhang X, Zhang W, Cao WD, Cheng G, Zhang YQ. Glioblastoma multiforme: Molecular characterization and current treatment strategy (Review). Experimental and Therapeutic Medicine. 2012.
9. Delgado-Martín B, Medina MÁ. Advances in the Knowledge of the Molecular Biology of Glioblastoma and Its Impact in Patient Diagnosis, Stratification, and Treatment. Advanced Science. 2020.
10. Ohka F, Natsume A, Wakabayashi T. Current trends in targeted therapies for glioblastoma multiforme. Neurology Research International. 2012.
11. Thakkar JP, Dolecek TA, Horbinski C, Ostrom QT, Lightner DD, Barnholtz-Sloan JS, Villano JL. Epidemiologic and molecular

prognostic review of glioblastoma. Cancer Epidemiology Biomarkers and Prevention. 2014.
12. Iacob G, Dinca EB. Current data and strategy in glioblastoma multiforme. Journal of medicine and life. 2009.
13. Rock K, McArdle O, Forde P, Dunne M, Fitzpatrick D, O'Neill B, Faul C. A clinical review of treatment outcomes in glioblastoma multiforme - The validation in a non-trial population of the results of a randomised Phase III clinical trial: Has a more radical approach improved survival? Br J Radiol. 2012; .
14. Ohgaki H, Kleihues P. Epidemiology and etiology of gliomas. Acta Neuropathologica. 2005.
15. Silantyev AS, Falzone L, Libra M, Gurina OI, Kardashova KS, Nikolouzakis TK, Nosyrev AE, Sutton CW, Mitsias PD, Tsatsakis A. Current and Future Trends on Diagnosis and Prognosis of Glioblastoma: From Molecular Biology to Proteomics. Cells. 2019.
16. Omuro A. Glioblastoma and Other Malignant Gliomas. JAMA. 2013; .
17. Houben MPWA, van Duijn CM, Coebergh JWW, Tijssen CC. [Gliomas: the role of environmental risk factors and genetic predisposition]. Ned Tijdschr Geneeskd. 2005; 149.
18. Bondy ML, Scheurer ME, Malmer B, Barnholtz-Sloan JS, Davis FG, Il'yasova D, Kruchko C, McCarthy BJ, Rajaraman P, Schwartzbaum JA, Sadetzki S, Schlehofer B, Tihan T, et al. Brain tumor epidemiology: Consensus from the Brain Tumor Epidemiology Consortium. Cancer. 2008.
19. Salvati M, Frati A, Russo N, Caroli E, Polli FM, Minniti G, Delfini R. Radiation-induced gliomas: Report of 10 cases and review of the literature. Surg Neurol. 2003; 60.
20. Grips E, Wentzensen N, Sutter C, Sedlaczek O, Gebert J, Weigel R, Schwartz A, von Knebel-Doeberitz M, Hennerici M. [Glioblastoma multiforme as a manifestation of Turcot syndrome]. Nervenarzt. 2002; 73.
21. Ruth Sánchez-Ortiga, Evangelina Boix Carreño, Oscar Moreno-Pérez APA. [Glioblastoma multiforme and multiple endocrine neoplasic type 2 A]. Med Clin. 2009; .
22. Broekman MLD, Risselada R, Engelen-Lee J, Spliet WGM, Verweij BH. Glioblastoma Multiforme in the Posterior Cranial Fossa in a Patient with Neurofibromatosis Type I. Case Rep

Med. 2009; 2009.
23. Adamson C, Kanu OO, Mehta AI, Di C, Lin N, Mattox AK, Bigner DD. Glioblastoma multiforme: A review of where we have been and where we are going. Expert Opinion on Investigational Drugs. 2009.
24. Karl Herholz 1 , Karl-Josef Langen, Christiaan Schiepers JMM. Brain tumors. Semin Nucl Med. 2012; .
25. Louis DN, Perry A, Reifenberger G, von Deimling A, Figarella-Branger D, Cavenee WK, Ohgaki H, Wiestler OD, Kleihues P, Ellison DW. The 2016 World Health Organization Classification of Tumors of the Central Nervous System: a summary. Acta Neuropathologica. 2016.
26. Collins VP. Brain tumours: Classification and genes. Neurology in Practice. 2004.
27. Liang J, Lv X, Lu C, Ye X, Chen X, Fu J, Luo C, Zhao Y. Prognostic factors of patients with Gliomas- A n analysis on 335 patients with Glioblastoma and other forms of Gliomas. BMC Cancer. 2020; 20.
28. Chen R, Smith-Cohn M, Cohen AL, Colman H. Glioma Subclassifications and Their Clinical Significance. Neurotherapeutics. 2017.
29. Collins JM, Christoforidis GA. Low-Grade Astrocytomas. Handbook of Neuro-Oncology Neuroimaging: Second Edition. 2016.
30. Newton HB. Primary brain tumors: Review of etiology, diagnosis and treatment. American Family Physician. 1994.
31. Balañá C, Alonso M, Hernandez A, Perez-Segura P, Pineda E, Ramos A, Sanchez AR, Teixidor P, Verger E, Benavides M. SEOM clinical guidelines for anaplastic gliomas (2017). Clin Transl Oncol. 2018; 20.
32. Faulkner K, Bowman B, Sosnowski J. Glioblastoma Multiforme (Gliosarcoma) WHO Grade IV With Osteosarcomatous Differentiation: A Case Study. Am J Clin Pathol. 2012; 138.
33. Olar A, Raghunathan A, Albarracin CT, Aldape KD, Cahill DP, Powell SZ, Goodman JC, Fuller GN. Absence of IDH1-R132H mutation predicts rapid progression of nonenhancing diffuse glioma in older adults. Ann Diagn Pathol. 2012; 16.
34. Ohgaki H, Kleihues P. Genetic profile of astrocytic and oligodendroglial gliomas. Brain Tumor Pathology. 2011.
35. Parsons DW, Jones S, Zhang X, Lin JCH, Leary RJ, Angenendt P,

Mankoo P, Carter H, Siu IM, Gallia GL, Olivi A, McLendon R, Rasheed BA, et al. An integrated genomic analysis of human glioblastoma multiforme. Science (80-). 2008; 321.
36. Verhaak RGW, Hoadley KA, Purdom E, Wang V, Qi Y, Wilkerson MD, Miller CR, Ding L, Golub T, Mesirov JP, Alexe G, Lawrence M, O'Kelly M, et al. Integrated Genomic Analysis Identifies Clinically Relevant Subtypes of Glioblastoma Characterized by Abnormalities in PDGFRA, IDH1, EGFR, and NF1. Cancer Cell. 2010; 17.
37. Brennan CW, Verhaak RGW, McKenna A, Campos B, Noushmehr H, Salama SR, Zheng S, Chakravarty D, Sanborn JZ, Berman SH, Beroukhim R, Bernard B, Wu CJ, et al. The somatic genomic landscape of glioblastoma. Cell. 2013; 155.
38. Pearson JRD, Regad T. Targeting cellular pathways in glioblastoma multiforme. Signal Transduction and Targeted Therapy. 2017.
39. McLendon R, Friedman A, Bigner D, Van Meir EG, Brat DJ, Mastrogianakis GM, Olson JJ, Mikkelsen T, Lehman N, Aldape K, Yung WKA, Bogler O, Weinstein JN, et al. Comprehensive genomic characterization defines human glioblastoma genes and core pathways. Nature. 2008; 455.
40. Olar A, Aldape KD. Using the molecular classification of glioblastoma to inform personalized treatment. Journal of Pathology. 2014.
41. Gondim DD, Gener MA, Curless KL, Cohen-Gadol AA, Hattab EM, Cheng L. Determining IDH-Mutational Status in Gliomas Using IDH1-R132H Antibody and Polymerase Chain Reaction. Applied Immunohistochemistry and Molecular Morphology. 2019.
42. Dang L, White DW, Gross S, Bennett BD, Bittinger MA, Driggers EM, Fantin VR, Jang HG, Jin S, Keenan MC, Marks KM, Prins RM, Ward PS, et al. Cancer-associated IDH1 mutations produce 2-hydroxyglutarate. Nature. 2009; 462.
43. Xu W, Yang H, Liu Y, Yang Y, Wang P, Kim SH, Ito S, Yang C, Wang P, Xiao MT, Liu LX, Jiang WQ, Liu J, et al. Oncometabolite 2-hydroxyglutarate is a competitive inhibitor of α-ketoglutarate-dependent dioxygenases. Cancer Cell. 2011; 19.
44. Noushmehr H, Weisenberger DJ, Diefes K, Phillips HS, Pujara K, Berman BP, Pan F, Pelloski CE, Sulman EP, Bhat KP,

Verhaak RGW, Hoadley KA, Hayes DN, et al. Identification of a CpG Island Methylator Phenotype that Defines a Distinct Subgroup of Glioma. Cancer Cell. 2010; 17.
45. Malta TM, De Souza CF, Sabedot TS, Silva TC, Mosella MS, Kalkanis SN, Snyder J, Castro AVB, Noushmehr H. Glioma CpG island methylator phenotype (G-CIMP): Biological and clinical implications. Neuro Oncol. 2018; 20.
46. Liu XY, Gerges N, Korshunov A, Sabha N, Khuong-Quang DA, Fontebasso AM, Fleming A, Hadjadj D, Schwartzentruber J, Majewski J, Dong Z, Siegel P, Albrecht S, et al. Frequent ATRX mutations and loss of expression in adult diffuse astrocytic tumors carrying IDH1/IDH2 and TP53 mutations. Acta Neuropathol. 2012; 124.
47. Cairncross G, Wang M, Shaw E, Jenkins R, Brachman D, Buckner J, Fink K, Souhami L, Laperriere N, Curran W, Mehta M. Phase III trial of chemoradiotherapy for anaplastic oligodendroglioma: Long-term results of RTOG 9402. J Clin Oncol. 2013; 31.
48. Zheng S, Chheda MG, Verhaak RGW. Studying a complex tumor: Potential and pitfalls. Cancer Journal. 2012.
49. Ramirez C, Bowman C, Maurage CA, Dubois F, Blond S, Porchet N, Escande F. Loss of 1p, 19q, and 10q heterozygosity prospectively predicts prognosis of oligodendroglial tumors-towards individualized tumor treatment? Neuro Oncol. 2010; 12.
50. Zhao J, Ma W, Zhao H. Loss of heterozygosity 1p/19q and survival in glioma: A meta-analysis. Neuro Oncol. 2014; 16.
51. Li J, Miao N, Liu M, Cui W, Liu X, Li X, Shi X, Qing S, Ma Y, Zhang W, Biekemituofu H. Clinical significance of chromosome 1p/19q loss of heterozygosity and Sox17 expression in oligodendrogliomas. Int J Clin Exp Pathol. 2014; 7.
52. Labussière M, Idbaih A, Wang XW, Marie Y, Boisselier B, Falet C, Paris S, Laffaire J, Carpentier C, Crinière E, Ducray F, El Hallani S, Mokhtari K, et al. All the 1p19q codeleted gliomas are mutated on IDH1 or IDH2. Neurology. 2010; 74.
53. Yip S, Butterfield YS, Morozova O, Chittaranjan S, Blough MD, An J, Birol I, Chesnelong C, Chiu R, Chuah E, Corbett R, Docking R, Firme M, et al. Concurrent CIC mutations, IDH mutations, and 1p/19q loss distinguish oligodendrogliomas

from other cancers. J Pathol. 2012; 226.
54. Wiestler B, Capper D, Hovestadt V, Sill M, Jones DTW, Hartmann C, Felsberg J, Platten M, Feiden W, Keyvani K, Pfister SM, Wiestler OD, Meyermann R, et al. Assessing CpG island methylator phenotype, 1p/19q codeletion, and MGMT promoter methylation from epigenome-wide data in the biomarker cohort of the NOA-04 trial. Neuro Oncol. 2014; 16.
55. de Souza CF, Sabedot TS, Malta TM, Stetson L, Morozova O, Sokolov A, Laird PW, Wiznerowicz M, Iavarone A, Snyder J, deCarvalho A, Sanborn Z, McDonald KL, et al. A Distinct DNA Methylation Shift in a Subset of Glioma CpG Island Methylator Phenotypes during Tumor Recurrence. Cell Rep. 2018; 23.
56. Lei L, Jiang Z, Zhang G, Cheng Q, Lu H. MGMT promoter methylation and 1p/19q co-deletion of surgically resected pulmonary carcinoid and large-cell neuroendocrine carcinoma. World J Surg Oncol. 2018; 16.
57. Xiong J, Liu Y, Wang Y, Ke RH, Mao Y, Ye ZR. Chromosome 1p/19q status combined with expression of p53 protein improves the diagnostic and prognostic evaluation of oligodendrogliomas. Chin Med J (Engl). 2010; 123.
58. Eoli M, Menghi F, Bruzzone MG, De Simone T, Valletta L, Pollo B, Bissola L, Silvani A, Bianchessi D, D'Incerti L, Filippini G, Broggi G, Boiardi A, et al. Methylation of O6-methylguanine DNA methytransferase and loss of heterozygosity on 19q and/or 17p are overlapping features of secondary glioblastomas with prolonged survival. Clin Cancer Res. 2007; 13.
59. Cairncross G, Jenkins R. Gliomas With 1p/19q codeletion: A.k.a. oligodendroglioma. Cancer Journal. 2008.
60. Phillips HS, Kharbanda S, Chen R, Forrest WF, Soriano RH, Wu TD, Misra A, Nigro JM, Colman H, Soroceanu L, Williams PM, Modrusan Z, Feuerstein BG, et al. Molecular subclasses of high-grade glioma predict prognosis, delineate a pattern of disease progression, and resemble stages in neurogenesis. Cancer Cell. 2006; 9.
61. Yu W, Zhang L, Wei Q, Shao A. O6-Methylguanine-DNA Methyltransferase (MGMT): Challenges and New Opportunities in Glioma Chemotherapy. Frontiers in Oncology. 2020.
62. Fan CH, Liu WL, Cao H, Wen C, Chen L, Jiang G. O6-

methylguanine DNA methyltransferase as a promising target for the treatment of temozolomide-resistant gliomas. Cell Death and Disease. 2013.
63. Hegi ME, Liu L, Herman JG, Stupp R, Wick W, Weller M, Mehta MP, Gilbert MR. Correlation of O6-methylguanine methyltransferase (MGMT) promoter methylation with clinical outcomes in glioblastoma and clinical strategies to modulate MGMT activity. Journal of Clinical Oncology. 2008.
64. Nakagawachi T, Soejima H, Urano T, Zhao W, Higashimoto K, Satoh Y, Matsukura S, Kudo S, Kitajima Y, Harada H, Furukawa K, Matsuzaki H, Emi M, et al. Silencing effect of CpG island hypermethylation and histone modifications on O6-methylguanine-DNA methyltransferase (MGMT) gene expression in human cancer. Oncogene. 2003; 22.
65. Mellai M, Monzeglio O, Piazzi A, Caldera V, Annovazzi L, Cassoni P, Valente G, Cordera S, Mocellini C, Schiffer D. MGMT promoter hypermethylation and its associations with genetic alterations in a series of 350 brain tumors. J Neurooncol. 2012; 107.
66. Tateishi K, Wakimoto H, Cahill DP. IDH1 Mutation and World Health Organization 2016 Diagnostic Criteria for Adult Diffuse Gliomas: Advances in Surgical Strategy. Clinical Neurosurgery. 2017.
67. TAMIMI AF, JUWEID M. Epidemiology and Outcome of Glioblastoma. Glioblastoma. 2017.
68. Cambruzzi E. The role of IDH1/2 mutations in the pathogenesis of secondary glioblastomas. Jornal Brasileiro de Patologia e Medicina Laboratorial. 2017.
69. Reifenberger G, Wirsching HG, Knobbe-Thomsen CB, Weller M. Advances in the molecular genetics of gliomas-implications for classification and therapy. Nature Reviews Clinical Oncology. 2017.
70. G. Linkous A, M. Yazlovitskaya E. Angiogenesis in Glioblastoma Multiforme: Navigating the Maze. Anticancer Agents Med Chem. 2012; 11.
71. Urbanska K, Sokolowska J, Szmidt M, Sysa P. Glioblastoma multiforme - An overview. Wspolczesna Onkologia. 2014.
72. Yung WKA. PATHOLOGY AND GENETICS OF TUMOURS OF THE NERVOUS SYSTEM. Neuro Oncol. 2002; 4.
73. Brada M. Pathology and Genetics of Tumours of the Nervous

System. Br J Cancer. 2001; 84.
74. Rong Y, Durden DL, Van Meir EG, Brat DJ. "Pseudopalisading" necrosis in glioblastoma: A familiar morphologic feature that links vascular pathology, hypoxia, and angiogenesis. Journal of Neuropathology and Experimental Neurology. 2006.
75. Ramakrishnan S, Anand V, Roy S. Vascular endothelial growth factor signaling in hypoxia and inflammation. Journal of Neuroimmune Pharmacology. 2014.
76. Brat DJ. Glioblastoma: Biology, Genetics, and Behavior. Am Soc Clin Oncol Educ B. 2012; .
77. Rahman R, Smith S, Rahman C, Grundy R. Antiangiogenic therapy and mechanisms of tumor resistance in malignant glioma. Journal of Oncology. 2010.
78. Onishi M, Kurozumi K, Ichikawa T, Date I. Mechanisms of tumor development and anti-angiogenic therapy in glioblastoma multiforme. Neurol Med Chir (Tokyo). 2013; 53.
79. Saman H, Raza SS, Uddin S, Rasul K. Inducing angiogenesis, a key step in cancer vascularization, and treatment approaches. Cancers. 2020.
80. Wong MLH, Prawira A, Kaye AH, Hovens CM. Tumour angiogenesis: Its mechanism and therapeutic implications in malignant gliomas. Journal of Clinical Neuroscience. 2009.
81. Hicklin DJ, Ellis LM. Role of the vascular endothelial growth factor pathway in tumor growth and angiogenesis. Journal of Clinical Oncology. 2005.
82. Niu G, Chen X. Vascular Endothelial Growth Factor as an Anti-Angiogenic Target for Cancer Therapy. Curr Drug Targets. 2010; 11.
83. Haibe Y, Kreidieh M, El Hajj H, Khalifeh I, Mukherji D, Temraz S, Shamseddine A. Resistance Mechanisms to Anti-angiogenic Therapies in Cancer. Frontiers in Oncology. 2020.
84. Sever R, Brugge JS. Signal transduction in cancer. Cold Spring Harb Perspect Med. 2015; 5.
85. Lee EYHP, Muller WJ. Oncogenes and tumor suppressor genes. Cold Spring Harbor perspectives in biology. 2010.
86. Maire CL, Ligon KL. Molecular pathologic diagnosis of epidermal growth factor receptor. Neuro-Oncology. 2014.
87. Hill VK, Kim JS, James CD, Waldman T. Correction of PTEN mutations in glioblastoma cell lines via AAV-mediated gene editing. PLoS One. 2017; 12.

88. Cheng Y, Ng HK, Ding M, Zhang SF, Pang JCS, Lo KW. Molecular analysis of microdissected de novo glioblastomas and paired astrocytic tumors. J Neuropathol Exp Neurol. 1999; 58.
89. Crespo I, Vital AL, Gonzalez-Tablas M, Patino MDC, Otero A, Lopes MC, De Oliveira C, Domingues P, Orfao A, Tabernero MD. Molecular and Genomic Alterations in Glioblastoma Multiforme. American Journal of Pathology. 2015.
90. Reitman ZJ, Yan H. Isocitrate dehydrogenase 1 and 2 mutations in cancer: Alterations at a crossroads of cellular metabolism. Journal of the National Cancer Institute. 2010.
91. Al-Khallaf H. Isocitrate dehydrogenases in physiology and cancer: Biochemical and molecular insight. Cell Biosci. 2017; 7.
92. Waitkus MS, Diplas BH, Yan H. Biological Role and Therapeutic Potential of IDH Mutations in Cancer. Cancer Cell. 2018.
93. Yan H, Parsons DW, Jin G, McLendon R, Rasheed BA, Yuan W, Kos I, Batinic-Haberle I, Jones S, Riggins GJ, Friedman H, Friedman A, Reardon D, et al. IDH1 and IDH2 Mutations in Gliomas . N Engl J Med. 2009; 360.
94. Yan H, Bigner DD, Velculescu V, Parsons DW. Mutant metabolic enzymes are at the origin of gliomas. Cancer Research. 2009.
95. Waitkus MS, Diplas BH, Yan H. Isocitrate dehydrogenase mutations in gliomas. Neuro-Oncology. 2016.
96. Stein EM. Molecular pathways: IDH2 mutations-co-opting cellular metabolism for malignant transformation. Clin Cancer Res. 2016; 22.
97. Esteller M, Herman JG. Generating mutations but providing chemosensitivity: The role of O 6-methylguanine DNA methyltransferase in human cancer. Oncogene. 2004.
98. Esteller M. CpG island hypermethylation and tumor suppressor genes: A booming present, a brighter future. Oncogene. 2002.
99. Pedraza-Fariña LG. Mechanisms of oncogenic cooperation in cancer initiation and metastasis. Yale Journal of Biology and Medicine. 2006.
100. Lodish H, Berk A, Zipursky SL, Matsudaira P, Baltimore D, Darnell J. Section 24.2, Proto-Oncogenes and Tumor-

Suppressor Genes. Molecular Cell Biology. 2000.
101. Harvey L, Arnold B, S Lawrence Z, Pau l M, David B, James D. Molecular Cell Biology. 4th edition. Journal of the American Society for Mass Spectrometry. 2000.
102. Ohgaki H, Dessen P, Jourde B, Horstmann S, Nishikawa T, Di Patre PL, Burkhard C, Schüler D, Probst-Hensch NM, Maiorka PC, Baeza N, Pisani P, Yonekawa Y, et al. Genetic pathways to glioblastoma: A population-based study. Cancer Res. 2004; 64.
103. Stephens P, Hunter C, Bignell G, Edkins S, Davies H, Teague J, Stevens C, O'Meara S, Smith R, Parker A, Barthorpe A, Blow M, Brackenbury L, et al. Lung cancer: intragenic ERBB2 kinase mutations in tumours. Nature. 2004; 431.
104. Zhang Y, Dube C, Gibert M, Cruickshanks N, Wang B, Coughlan M, Yang Y, Setiady I, Deveau C, Saoud K, Grello C, Oxford M, Yuan F, et al. The p53 pathway in glioblastoma. Cancers. 2018.
105. Fridman JS, Lowe SW. Control of apoptosis by p53. Oncogene. 2003.
106. Louis DN, Ohgaki H, Wiestler OD, Cavenee WK, Burger PC, Jouvet A, Scheithauer BW, Kleihues P. The 2007 WHO classification of tumours of the central nervous system. Acta Neuropathologica. 2007.
107. Miller CR, Perry A. Glioblastoma: Morphologic and molecular genetic diversity. Archives of Pathology and Laboratory Medicine. 2007.
108. Lobbous M, Bernstock JD, Coffee E, Friedman GK, Metrock LK, Chagoya G, Elsayed G, Nakano I, Hackney JR, Korf BR, Nabors LB. An update on neurofibromatosis type 1-associated gliomas. Cancers. 2020.
109. Gottfried ON, Viskochil DH, Couldwell WT. Neurofibromatosis Type 1 and tumorigenesis: Molecular mechanisms and therapeutic implications. Neurosurgical Focus. 2010.
110. Bergoug M, Doudeau M, Godin F, Mosrin C, Vallée B, Bénédetti H. Neurofibromin Structure, Functions and Regulation. Cells. 2020.
111. Davis ME. Glioblastoma: Overview of disease and treatment. Clin J Oncol Nurs. 2016; 20.
112. IJzerman-Korevaar M, Snijders TJ, de Graeff A, Teunissen SCCM, de Vos FYF. Prevalence of symptoms in glioma patients

throughout the disease trajectory: a systematic review. Journal of Neuro-Oncology. 2018.
113. Posti JP, Bori M, Kauko T, Sankinen M, Nordberg J, Rahi M, Frantzén J, Vuorinen V, Sipilä JOT. Presenting symptoms of glioma in adults. Acta Neurol Scand. 2015; 131.
114. D'Alessio A, Proietti G, Sica G, Scicchitano BM. Pathological and molecular features of glioblastoma and its peritumoral tissue. Cancers. 2019.
115. Pacifici GM, Franchi M, Bencini C, Repetti F, Di Lascio N, Muraro GB. Tissue distribution of drug-metabolizing enzymes in humans. Xenobiotica. 1988; 18.
116. Orringer DA, Pandian B, Niknafs YS, Hollon TC, Boyle J, Lewis S, Garrard M, Hervey-Jumper SL, Garton HJL, Maher CO, Heth JA, Sagher O, Wilkinson DA, et al. Rapid intraoperative histology of unprocessed surgical specimens via fibre-laser-based stimulated Raman scattering microscopy. Nat Biomed Eng. 2017; 1.
117. Russell SM, Elliott R, Forshaw D, Golfinos JG, Nelson PK, Kelly PJ. Glioma vascularity correlates with reduced patient survival and increased malignancy. Surg Neurol. 2009; 72.
118. Folkman J. Role of angiogenesis in tumor growth and metastasis. Seminars in oncology. 2002.
119. Mabray MC, Barajas RF, Cha S. Modern Brain Tumor Imaging. Brain Tumor Res Treat. 2015; 3.
120. Weller M, Cloughesy T, Perry JR, Wick W. Standards of care for treatment of recurrent glioblastoma-are we there yet? Neuro-Oncology. 2013.
121. Taal W, Jacoline E C Bromberg MJ van den B. Chemotherapy in glioma. CNS Oncol. 2015; .
122. Tan AC, Ashley DM, López GY, Malinzak M, Friedman HS, Khasraw M. Management of glioblastoma: State of the art and future directions. CA Cancer J Clin. 2020; 70.
123. Minniti G, Lombardi G, Paolini S. Glioblastoma in elderly patients: Current management and future perspectives. Cancers (Basel). 2019; 11.
124. Wilson TA, Karajannis MA, Harter DH. Glioblastoma multiforme: State of the art and future therapeutics. Surg Neurol Int. 2014; 5.
125. Newton HB. Overview of Pathology and Treatment of Primary Brain Tumors. Handbook of Neuro-Oncology Neuroimaging:

Second Edition. 2016.
126. Liu EK, Sulman EP, Wen PY, Kurz SC. Novel Therapies for Glioblastoma. Current Neurology and Neuroscience Reports. 2020.
127. Young RM, Jamshidi A, Davis G, Sherman JH. Current trends in the surgical management and treatment of adult glioblastoma. Annals of Translational Medicine. 2015.
128. Mann J, Ramakrishna R, Magge R, Wernicke AG. Advances in radiotherapy for glioblastoma. Frontiers in Neurology. 2018.
129. Hingorani M, Colley WP, Dixit S, Beavis AM. Hypofractionated radiotherapy for glioblastoma: Strategy for poor-risk patients or hope for the future? British Journal of Radiology. 2012.
130. Wick W, Platten M, Meisner C, Felsberg J, Tabatabai G, Simon M, Nikkhah G, Papsdorf K, Steinbach JP, Sabel M, Combs SE, Vesper J, Braun C, et al. Temozolomide chemotherapy alone versus radiotherapy alone for malignant astrocytoma in the elderly: The NOA-08 randomised, phase 3 trial. Lancet Oncol. 2012; 13.
131. Dresemann G. Temozolomide in malignant glioma. OncoTargets and Therapy. 2010.
132. Zhang J, F.G. Stevens M, D. Bradshaw T. Temozolomide: Mechanisms of Action, Repair and Resistance. Curr Mol Pharmacol. 2011; 5.
133. Birol Sarica F, Tufan K, Cekinmez M, Sen O, Cem Onal H, Mertsoylu H, Topkan E, Pehlivan B, Erdogan B, Nur Altinors MN. Effectiveness of temozolomide treatment used at the same time with radiotherapy and adjuvant temozolomide. Concomitant therapy of glioblastoma multiforme: Multivariate analysis and other prognostic factors. J Neurosurg Sci. 2010; 54.
134. Stupp R, Mason WP, Van Den Bent MJ, Weller M, Fisher B, Taphoorn MJB, Belanger K, Brandes AA, Marosi C, Bogdahn U, Curschmann J, Janzer RC, Ludwin SK, et al. Radiotherapy plus concomitant and adjuvant temozolomide for glioblastoma. N Engl J Med. 2005; .
135. Stupp R, Hegi ME, van den Bent MJ, Mason WP, Weller M, Mirimanoff RO, Cairncross JG. Changing paradigms--an update on the multidisciplinary management of malignant glioma. Oncologist. 2006; 11.
136. Clarke J, Butowski N, Chang S. Recent advances in therapy for

glioblastoma. Archives of Neurology. 2010.
137. Hass R, von der Ohe J, Ungefroren H. Impact of the tumor microenvironment on tumor heterogeneity and consequences for cancer cell plasticity and stemness. Cancers. 2020.
138. Gupta S, Roy A, Dwarakanath BS. Metabolic cooperation and competition in the tumor microenvironment: Implications for therapy. Front Oncol. 2017; 7.
139. Whiteside TL. The tumor microenvironment and its role in promoting tumor growth. Oncogene. 2008.
140. Balkwill FR, Capasso M, Hagemann T. The tumor microenvironment at a glance. J Cell Sci. 2012; 125.
141. Osipov A, Murphy A, Zheng L. From immune checkpoints to vaccines: The past, present and future of cancer immunotherapy. Advances in Cancer Research. 2019.
142. Allegrezza MJ, Conejo-Garcia JR. Targeted Therapy and Immunosuppression in the Tumor Microenvironment. Trends in Cancer. 2017.
143. Landskron G, De La Fuente M, Thuwajit P, Thuwajit C, Hermoso MA. Chronic inflammation and cytokines in the tumor microenvironment. Journal of Immunology Research. 2014.
144. De Palma M, Lewis CE. Macrophage regulation of tumor responses to anticancer therapies. Cancer Cell. 2013.
145. Kiss M, Van Gassen S, Movahedi K, Saeys Y, Laoui D. Myeloid cell heterogeneity in cancer: not a single cell alike. Cellular Immunology. 2018.
146. Coussens LM, Pollard JW. Leukocytes in mammary development and cancer. Cold Spring Harb Perspect Biol. 2011; 3.
147. Engblom C, Pfirschke C, Pittet MJ. The role of myeloid cells in cancer therapies. Nature Reviews Cancer. 2016.
148. Lee N, Zakka LR, Mihm MC, Schatton T. Tumour-infiltrating lymphocytes in melanoma prognosis and cancer immunotherapy. Pathology. 2016; 48.
149. Zheng X, Song X, Shao Y, Xu B, Hu W, Zhou Q, Chen L, Zhang D, Wu C, Jiang J. Prognostic role of tumor-infiltrating lymphocytes in esophagus cancer: A meta-analysis. Cell Physiol Biochem. 2018; 45.
150. Noy R, Pollard JW. Tumor-Associated Macrophages: From

Mechanisms to Therapy. Immunity. 2014.
151. Rodriguez PC, Quiceno DG, Ochoa AC. L-arginine availability regulates T-lymphocyte cell-cycle progression. Blood. 2007; 109.
152. Tsai CS, Chen FH, Wang CC, Huang HL, Jung SM, Wu CJ, Lee CC, McBride WH, Chiang CS, Hong JH. Macrophages From Irradiated Tumors Express Higher Levels of iNOS, Arginase-I and COX-2, and Promote Tumor Growth. Int J Radiat Oncol Biol Phys. 2007; 68.
153. Carvalho Da Fonseca AC, Badie B. Microglia and macrophages in malignant gliomas: Recent discoveries and implications for promising therapies. Clinical and Developmental Immunology. 2013.
154. Antunes ARP, Scheyltjens I, Duerinck J, Neyns B, Movahedi K, Van Ginderachter JA. Understanding the glioblastoma immune microenvironment as basis for the development of new immunotherapeutic strategies. Elife. 2020; 9.
155. Hambardzumyan D, Gutmann DH, Kettenmann H. The role of microglia and macrophages in glioma maintenance and progression. Nature Neuroscience. 2015.
156. Sasaki A. Microglia and brain macrophages: An update. Neuropathology. 2017; 37.
157. Prionisti I, Bühler LH, Walker PR, Jolivet RB. Harnessing microglia and macrophages for the treatment of glioblastoma. Frontiers in Pharmacology. 2019.
158. Wolf SA, Boddeke HWGM, Kettenmann H. Microglia in Physiology and Disease. Annual Review of Physiology. 2017.
159. Hussain SF, Yang D, Suki D, Aldape K, Grimm E, Heimberger AB. The role of human glioma-infiltrating microglia/macrophages in mediating antitumor immune responses. Neuro Oncol. 2006; .
160. Gieryng A, Pszczolkowska D, Walentynowicz KA, Rajan WD, Kaminska B. Immune microenvironment of gliomas. Laboratory Investigation. 2017.
161. Szulzewsky F, Pelz A, Feng X, Synowitz M, Markovic D, Langmann T, Holtman IR, Wang X, Eggen BJL, Boddeke HWGM, Hambardzumyan D, Wolf SA, Kettenmann H. Glioma-associated microglia/macrophages display an expression profile different from M1 and M2 polarization and highly express Gpnmb and Spp1. PLoS One. 2015; 10.

162. Borisov KE, Sakaeva DD. The immunosuppressive microenvironment of malignant gliomas. Arkh Patol. 2015; 77.
163. Cole AP, Hoffmeyer E, Chetty SL, Cruz-Cruz J, Hamrick F, Youssef O, Cheshier S, Mitra SS. Microglia in the Brain Tumor Microenvironment. Advances in Experimental Medicine and Biology. 2020.
164. Bowman RL, Klemm F, Akkari L, Pyonteck SM, Sevenich L, Quail DF, Dhara S, Simpson K, Gardner EE, Iacobuzio-Donahue CA, Brennan CW, Tabar V, Gutin PH, et al. Macrophage Ontogeny Underlies Differences in Tumor-Specific Education in Brain Malignancies. Cell Rep. 2016; 17.
165. Li Q, Barres BA. Microglia and macrophages in brain homeostasis and disease. Nature Reviews Immunology. 2018.
166. Gabrusiewicz K, Ellert-Miklaszewska A, Lipko M, Sielska M, Frankowska M, Kaminska B. Characteristics of the alternative phenotype of microglia/macrophages and its modulation in experimental gliomas. PLoS One. 2011; 6.
167. Li W, Graeber MB. The molecular profile of microglia under the influence of glioma. Neuro-Oncology. 2012.
168. Xavier AL, Menezes JRL, Goldman SA, Nedergaard M. Fine-tuning the central nervous system: Microglial modelling of cells and synapses. Philosophical Transactions of the Royal Society B: Biological Sciences. 2014.
169. Li F, Jiang D, Samuel MA. Microglia in the developing retina. Neural Development. 2019.
170. Harry GJ, Kraft AD. Microglia in the developing brain: A potential target with lifetime effects. NeuroToxicology. 2012.
171. Bachiller S, Jiménez-Ferrer I, Paulus A, Yang Y, Swanberg M, Deierborg T, Boza-Serrano A. Microglia in neurological diseases: A road map to brain-disease dependent-inflammatory response. Frontiers in Cellular Neuroscience. 2018.
172. Davis BM, Salinas-Navarro M, Cordeiro MF, Moons L, Groef L De. Characterizing microglia activation: A spatial statistics approach to maximize information extraction. Sci Rep. 2017; 7.
173. Orihuela R, McPherson CA, Harry GJ. Microglial M1/M2 polarization and metabolic states. British Journal of Pharmacology. 2016.

174. Jurga AM, Paleczna M, Kuter KZ. Overview of General and Discriminating Markers of Differential Microglia Phenotypes. Front Cell Neurosci. 2020; 14.
175. Yin J, Valin KL, Dixon ML, Leavenworth JW. The Role of Microglia and Macrophages in CNS Homeostasis, Autoimmunity, and Cancer. Journal of Immunology Research. 2017.
176. Butturini E, Boriero D, Carcereri de Prati A, Mariotto S. STAT1 drives M1 microglia activation and neuroinflammation under hypoxia. Arch Biochem Biophys. 2019; 669.
177. Wei J, Gabrusiewicz K, Heimberger A. The controversial role of microglia in malignant gliomas. Clinical and Developmental Immunology. 2013.
178. Yang L, Zhang Y. Tumor-associated macrophages: from basic research to clinical application. Journal of hematology & oncology. 2017.
179. Böttcher C, Schlickeiser S, Sneeboer MAM, Kunkel D, Knop A, Paza E, Fidzinski P, Kraus L, Snijders GJL, Kahn RS, Schulz AR, Mei HE, Hol EM, et al. Human microglia regional heterogeneity and phenotypes determined by multiplexed single-cell mass cytometry. Nat Neurosci. 2019; 22.
180. Komohara Y, Horlad H, Ohnishi K, Ohta K, Makino K, Hondo H, Yamanaka R, Kajiwara K, Saito T, Kuratsu J ichi, Takeya M. M2 macrophage/microglial cells induce activation of Stat3 in primary central nervous system lymphoma. J Clin Exp Hematop. 2011; 51.
181. Pollard JW. Tumour-educated macrophages promote tumour progression and metastasis. Nature Reviews Cancer. 2004.
182. Murray PJ, Allen JE, Biswas SK, Fisher EA, Gilroy DW, Goerdt S, Gordon S, Hamilton JA, Ivashkiv LB, Lawrence T, Locati M, Mantovani A, Martinez FO, et al. Macrophage Activation and Polarization: Nomenclature and Experimental Guidelines. Immunity. 2014.
183. Quirino IEP, Cardoso VN, Santos RDGC Dos, Evangelista WP, Arantes RME, Fiúza JA, Glória MBA, Alvarez-Leite JI, Batista MA, Correia MITD. The role of L-arginine and inducible nitric oxide synthase in intestinal permeability and bacterial translocation. J Parenter Enter Nutr. 2013; 37.
184. Banati RB. Neuropathological imaging: in vivo detection of glial activation as a measure of disease and adaptive change

in the brain. British Medical Bulletin. 2003.
185. Tu H, Chu H, Guan S, Hao F, Xu N, Zhao Z, Liang Y. The role of the M1/M2 microglia in the process from cancer pain to morphine tolerance. Tissue and Cell. 2021.
186. Zheng ZV, Wong KCG. Microglial activation and polarization after subarachnoid hemorrhage. Neuroimmunol Neuroinflammation. 2019; 2019.
187. Bach JP, Deuster O, Balzer-Geldsetzer M, Meyer B, Dodel R, Bacher M. The role of macrophage inhibitory factor in tumorigenesis and central nervous system tumors. Cancer. 2009.
188. Zhang L, Handel M Van, Schartner JM, Hagar A, Allen G, Curet M, Badie B. Regulation of IL-10 expression by upstream stimulating factor (USF-1) in glioma-associated microglia. J Neuroimmunol. 2007; 184.
189. Charles NA, Holland EC, Gilbertson R, Glass R, Kettenmann H. The brain tumor microenvironment. Glia. 2012; .
190. Wu A, Wei J, Kong LY, Wang Y, Priebe W, Qiao W, Sawaya R, Heimberger AB. Glioma cancer stem cells induce immunosuppressive macrophages/microglia. Neuro Oncol. 2010; 12.
191. Sica A, Schioppa T, Mantovani A, Allavena P. Tumour-associated macrophages are a distinct M2 polarised population promoting tumour progression: Potential targets of anti-cancer therapy. Eur J Cancer. 2006; 42.
192. Matias D, Balça-Silva J, da Graça GC, Wanjiru CM, Macharia LW, Nascimento CP, Roque NR, Coelho-Aguiar JM, Pereira CM, Dos Santos MF, Pessoa LS, Lima FRS, Schanaider A, et al. Microglia/astrocytes–glioblastoma crosstalk: Crucial molecular mechanisms and microenvironmental factors. Frontiers in Cellular Neuroscience. 2018.
193. Peng Y, Chen F, Li S, Liu X, Wang C, Yu C, Li W. Tumor-associated macrophages as treatment targets in glioma. Brain Sci Adv. 2020; 6.
194. Markovic DS, Vinnakota K, Chirasani S, Synowitz M, Raguet H, Stock K, Sliwa M, Lehmann S, Kälin R, Van Rooijen N, Holmbeck K, Heppner FL, Kiwit J, et al. Gliomas induce and exploit microglial MT1-MMP expression for tumor expansion. Proc Natl Acad Sci U S A. 2009; 106.
195. Held-Feindt J, Hattermann K, Müerköster SS, Wedderkopp H,

Knerlich-Lukoschus F, Ungefroren H, Mehdorn HM, Mentlein R. CX3CR1 promotes recruitment of human glioma-infiltrating microglia/macrophages (GIMs). Exp Cell Res. 2010; 316.
196. da Fonseca ACC, Romão L, Amaral RF, Assad Kahn S, Lobo D, Martins S, Marcondes de Souza J, Moura-Neto V, Lima FRS. Microglial stress inducible protein 1 promotes proliferation and migration in human glioblastoma cells. Neuroscience. 2012; 200.
197. Ma J, Chen CC, Li M. Macrophages/microglia in the glioblastoma tumor microenvironment. International Journal of Molecular Sciences. 2021.
198. Wang CY, Hsieh YT, Fang KM, Yang CS, Tzeng SF. Reduction of CD200 expression in glioma cells enhances microglia activation and tumor growth. J Neurosci Res. 2016; 94.
199. Felsenstein M, Blank A, Bungert AD, Mueller A, Ghori A, Kremenetskaia I, Rung O, Broggini T, Turkowski K, Scherschinski L, Raggatz J, Vajkoczy P, Brandenburg S. CCR2 of tumor microenvironmental cells is a relevant modulator of glioma biology. Cancers (Basel). 2020; 12.
200. Shi Y, Ping YF, Zhou W, He ZC, Chen C, Bian BSJ, Zhang L, Chen L, Lan X, Zhang XC, Zhou K, Liu Q, Long H, et al. Tumour-associated macrophages secrete pleiotrophin to promote PTPRZ1 signalling in glioblastoma stem cells for tumour growth. Nat Commun. 2017; 8.
201. Caponegro MD, Moffitt RA, Tsirka SE. Expression of neuropilin-1 is linked to glioma associated microglia and macrophages and correlates with unfavorable prognosis in high grade gliomas. Oncotarget. 2018; 9.
202. Doucette TA, Kong LY, Yang Y, Ferguson SD, Yang J, Wei J, Qiao W, Fuller GN, Bhat KP, Aldape K, Priebe W, Bögler O, Heimberger AB, et al. Signal transducer and activator of transcription 3 promotes angiogenesis and drives malignant progression in glioma. Neuro Oncol. 2012; 14.
203. Bezzi P, Domercq M, Brambilla L, Galli R, Schols D, Clercq E De, Vescovi A, Bagetta G, Kollias G, Meldolesi J, Volterra A. CXCR4-activated astrocyte glutamate release via TNF. Nat Neurosci. 2001; 4.
204. de la Cruz-López KG, Castro-Muñoz LJ, Reyes-Hernández DO, García-Carrancá A, Manzo-Merino J. Lactate in the Regulation

of Tumor Microenvironment and Therapeutic Approaches. Frontiers in Oncology. 2019.
205. Castracani CC, Longhitano L, Distefano A, Anfuso D, Kalampoka S, La Spina E, Astuto M, Avola R, Caruso M, Nicolosi D, Giallongo C, Tibullo D. Role of 17 β -Estradiol on Cell Proliferation and Mitochondrial Fitness in Glioblastoma Cells. J Oncol. 2020; .
206. De Leo A, Ugolini A, Veglia F. Myeloid Cells in Glioblastoma Microenvironment. Cells. 2020.
207. Won W-J, Deshane JS, Leavenworth JW, Oliva CR, Griguer CE. Metabolic and functional reprogramming of myeloid-derived suppressor cells and their therapeutic control in glioblastoma. Cell Stress. 2019; .
208. Watters JJ, Schartner JM, Badie B. Microglia function in brain tumors. Journal of Neuroscience Research. 2005.
209. Zhai H, Heppner FL, Tsirka SE. Microglia/macrophages promote glioma progression. Glia. 2011; .
210. Miranda-Gonçalves V, Granja S, Martinho O, Honavar M, Pojo M, Costa BM, Pires MM, Pinheiro C, Cordeiro M, Bebiano G, Costa P, Reis RM, Baltazar F. Hypoxia-mediated upregulation of MCT1 expression supports the glycolytic phenotype of glioblastomas. Oncotarget. 2016; .
211. Duan K, Liu Z jian, Hu S qiong, Huo H yu, Xu Z ru, Ruan J fei, Sun Y, Dai L ping, Yan C bao, Xiong W, Cui Q hua, Yu H jing, Yu M, et al. Lactic acid induces lactate transport and glycolysis/OXPHOS interconversion in glioblastoma. Biochem Biophys Res Commun. 2018; .
212. Walenta S, Mueller-Klieser WF. Lactate: Mirror and motor of tumor malignancy. Semin Radiat Oncol. 2004; .
213. Brizel DM, Schroeder T, Scher RL, Walenta S, Clough RW, Dewhirst MW, Mueller-Klieser W. Elevated tumor lactate concentrations predict for an increased risk of metastases in head-and-neck cancer. Int J Radiat Oncol Biol Phys. 2001; .
214. Ferguson BS, Rogatzki MJ, Goodwin ML, Kane DA, Rightmire Z, Gladden LB. Lactate metabolism: historical context, prior misinterpretations, and current understanding. European Journal of Applied Physiology. 2018.
215. Gladden LB. Lactate metabolism: A new paradigm for the third millennium. Journal of Physiology. 2004.
216. Goodwin ML, Gladden LB, Nijsten MWN, Jones KB. Lactate

and Cancer: Revisiting the Warburg Effect in an Era of Lactate Shuttling. Front Nutr. 2015; 1.
217. Schurr A, West CA, Rigor BM. Lactate-supported synaptic function in the rat hippocampal slice preparation. Sci Sci. 1988; 240.
218. Palsson-Mcdermott EM, O'Neill LAJ. The Warburg effect then and now: From cancer to inflammatory diseases. BioEssays. 2013; 35.
219. Goetze K, Walenta S, Ksiazkiewicz M, Kunz-Schughart LA, Mueller-Klieser W. Lactate enhances motility of tumor cells and inhibits monocyte migration and cytokine release. Int J Oncol. 2011; .
220. Colegio OR, Chu NQ, Szabo AL, Chu T, Rhebergen AM, Jairam V, Cyrus N, Brokowski CE, Eisenbarth SC, Phillips GM, Cline GW, Phillips AJ, Medzhitov R. Functional polarization of tumour-associated macrophages by tumour-derived lactic acid. Nature. 2014; 513.
221. Ratter JM, Rooijackers HMM, Hooiveld GJ, Hijmans AGM, de Galan BE, Tack CJ, Stienstra R. In vitro and in vivo Effects of Lactate on Metabolism and Cytokine Production of Human Primary PBMCs and Monocytes. Front Immunol. 2018; 9.
222. Liberti M V., Locasale JW. The Warburg Effect: How Does it Benefit Cancer Cells? Trends in Biochemical Sciences. 2016.
223. Heiden MGV, Cantley LC, Thompson CB. Understanding the warburg effect: The metabolic requirements of cell proliferation. Science. 2009.
224. Koppenol WH, Bounds PL, Dang C V. Otto Warburg's contributions to current concepts of cancer metabolism. Nature Reviews Cancer. 2011.
225. Doherty JR, Cleveland JL. Targeting lactate metabolism for cancer therapeutics. Journal of Clinical Investigation. 2013.
226. Williams NC, O'Neill LAJ. A role for the krebs cycle intermediate citrate in metabolic reprogramming in innate immunity and inflammation. Frontiers in Immunology. 2018.
227. Yang L, Venneti S, Nagrath D. Glutaminolysis: A Hallmark of Cancer Metabolism. Annu Rev Biomed Eng. 2017; 19.
228. Jensen M V., Joseph JW, Ronnebaum SM, Burgess SC, Sherry AD, Newgard CB. Metabolic cycling in control of glucose-stimulated insulin secretion. American Journal of Physiology - Endocrinology and Metabolism. 2008.

229. Son J, Lyssiotis CA, Ying H, Wang X, Hua S, Ligorio M, Perera RM, Ferrone CR, Mullarky E, Shyh-Chang N, Kang Y, Fleming JB, Bardeesy N, et al. Glutamine supports pancreatic cancer growth through a KRAS-regulated metabolic pathway. Nature. 2013; 496.
230. Urbańska K, Orzechowski A. Unappreciated role of LDHA and LDHB to control apoptosis and autophagy in tumor cells. International Journal of Molecular Sciences. 2019.
231. Ždralević M, Brand A, Ianni L Di, Dettmer K, Reinders J, Singer K, Peter K, Schnell A, Bruss C, Decking SM, Koehl G, Felipe-Abrio B, Durivault J, et al. Double genetic disruption of lactate dehydrogenases A and B is required to ablate the "Warburg effect" restricting tumor growth to oxidative metabolism. J Biol Chem. 2018; 293.
232. Valvona CJ, Fillmore HL, Nunn PB, Pilkington GJ. The Regulation and Function of Lactate Dehydrogenase A: Therapeutic Potential in Brain Tumor. Brain Pathology. 2016.
233. Peng M, Yin N, Chhangawala S, Xu K, Leslie CS, Li MO. Aerobic glycolysis promotes T helper 1 cell differentiation through an epigenetic mechanism. Science (80-). 2016; 354.
234. Seth P, Csizmadia E, Hedblom A, Vuerich M, Xie H, Li M, Longhi MS, Wegiel B. Deletion of lactate dehydrogenase-A in myeloid cells triggers antitumor immunity. Cancer Res. 2017; 77.
235. Jones RS, Morris ME. Monocarboxylate Transporters: Therapeutic Targets and Prognostic Factors in Disease. Clin Pharmacol Ther. 2016; .
236. Garcia CK, Goldstein JL, Pathak RK, Anderson RGW, Brown MS. Molecular characterization of a membrane transporter for lactate, pyruvate, and other monocarboxylates: Implications for the Cori cycle. Cell. 1994; 76.
237. Halestrap AP, Price NT. The proton-linked monocarboxylate transporter (MCT) family: Structure, function and regulation. Biochemical Journal. 1999.
238. Halestrap AP, Meredith D. The SLC16 gene family - From monocarboxylate transporters (MCTs) to aromatic amino acid transporters and beyond. Pflugers Archiv European Journal of Physiology. 2004.
239. Meredith D, Christian HC. The SLC16 monocaboxylate transporter family. Xenobiotica. 2008.

240. Spencer TL, Lehninger AL. L-lactate transport in Ehrlich ascites-tumour cells. Biochem J. 1976; 154.
241. Pinheiro C, Garcia EA, Morais-Santos F, Scapulatempo-Neto C, Mafra A, Steenbergen RDM, Boccardo E, Villa LL, Baltazar F, Longatto-Filho A. Lactate transporters and vascular factors in HPV-induced squamous cell carcinoma of the uterine cervix. BMC Cancer. 2014; 14.
242. Fang J, Quinones QJ, Holman TL, Morowitz MJ, Wang Q, Zhao H, Sivo F, Maris JM, Wahl ML. The H+-linked monocarboxylate transporter (MCT1/SLC16A1): A potential therapeutic target for high-risk neuroblastoma. Mol Pharmacol. 2006; 70.
243. Curry JM, Tuluc M, Whitaker-Menezes D, Ames JA, Anantharaman A, Butera A, Leiby B, Cognetti DM, Sotgia F, Lisanti MP, Martinez-Outschoorn UE. Cancer metabolism, stemness and tumor recurrence : MCT1 and MCT4 are functional biomarkers of metabolic symbiosis in head and neck cancer. Cell Cycle. 2013; 12.
244. Ullah MS, Davies AJ, Halestrap AP. The plasma membrane lactate transporter MCT4, but not MCT1, is up-regulated by hypoxia through a HIF-1α-dependent mechanism. J Biol Chem. 2006; 281.
245. Sprowl-Tanio S, Habowski AN, Pate KT, McQuade MM, Wang K, Edwards RA, Grun F, Lyou Y, Waterman ML. Lactate/pyruvate transporter MCT-1 is a direct Wnt target that confers sensitivity to 3-bromopyruvate in colon cancer. Cancer Metab. 2016; 4.
246. Boidot R, Veǵran F, Meulle A, Le Breton A, Dessy C, Sonveaux P, Lizard-Nacol S, Feron O. Regulation of monocarboxylate transporter MCT1 expression by p53 mediates inward and outward lactate fluxes in tumors. Cancer Res. 2012; 72.
247. Ho J, de Moura MB, Lin Y, Vincent G, Thorne S, Duncan LM, Hui-Min L, Kirkwood JM, Becker D, Van Houten B, Moschos SJ. Importance of glycolysis and oxidative phosphorylation in advanced melanoma. Mol Cancer. 2012; 11.
248. Pisarsky L, Bill R, Fagiani E, Dimeloe S, Goosen RW, Hagmann J, Hess C, Christofori G. Targeting Metabolic Symbiosis to Overcome Resistance to Anti-angiogenic Therapy. Cell Rep. 2016; 15.
249. Faubert B, Li KY, Cai L, Hensley CT, Kim J, Zacharias LG, Yang C, Do QN, Doucette S, Burguete D, Li H, Huet G, Yuan Q, et al.

Lactate Metabolism in Human Lung Tumors. Cell. 2017; 171.
250. Sonveaux P, Végran F, Schroeder T, Wergin MC, Verrax J, Rabbani ZN, De Saedeleer CJ, Kennedy KM, Diepart C, Jordan BF, Kelley MJ, Gallez B, Wahl ML, et al. Targeting lactate-fueled respiration selectively kills hypoxic tumor cells in mice. J Clin Invest. 2008; 118.
251. Semenza GL. Tumor metabolism: Cancer cells give and take lactate. Journal of Clinical Investigation. 2008.
252. Van Hée VF, Pérez-Escuredo J, Cacace A, Copetti T, Sonveaux P. Lactate does not activate NF-κB in oxidative tumor cells. Front Pharmacol. 2015; 6.
253. Hashimoto T, Hussien R, Oommen S, Gohil K, Brooks GA. Lactate sensitive transcription factor network in L6 cells: activation of MCT1 and mitochondrial biogenesis . FASEB J. 2007; 21.
254. Liu C, Wu J, Zhu J, Kuei C, Yu J, Shelton J, Sutton SW, Li X, Su JY, Mirzadegan T, Mazur C, Kamme F, Lovenberg TW. Lactate inhibits lipolysis in fat cells through activation of an orphan G-protein-coupled receptor, GPR81. J Biol Chem. 2009; 284.
255. Pérez-Escuredo J, Van Hée VF, Sboarina M, Falces J, Payen VL, Pellerin L, Sonveaux P. Monocarboxylate transporters in the brain and in cancer. Biochim Biophys Acta - Mol Cell Res. 2016; 1863.
256. Pérez-Tomás R, Pérez-Guillén I. Lactate in the tumor microenvironment: An essential molecule in cancer progression and treatment. Cancers. 2020.
257. Offermanns S, Colletti SL, Lovenberg TW, Semple G, Wise A, Ijzerman AP. International union of basic and clinical pharmacology. LXXXII: Nomenclature and classification of hydroxy-carboxylic acid receptors (GPR81, GPR109A, and GPR109B). Pharmacol Rev. 2011; 63.
258. Ge H, Weiszmann J, Reagan JD, Gupte J, Baribault H, Gyuris T, Chen JL, Tian H, Li Y. Elucidation of signaling and functional activities of an orphan GPCR, GPR81. J Lipid Res. 2008; 49.
259. Lauritzen KH, Morland C, Puchades M, Holm-Hansen S, Hagelin EM, Lauritzen F, Attramadal H, Storm-Mathisen J, Gjedde A, Bergersen LH. Lactate receptor sites link neurotransmission, neurovascular coupling, and brain energy metabolism. Cereb Cortex. 2014; 24.
260. Cai TQ, Ren N, Jin L, Cheng K, Kash S, Chen R, Wright SD,

Taggart AKP, Waters MG. Role of GPR81 in lactate-mediated reduction of adipose lipolysis. Biochem Biophys Res Commun. 2008; 377.
261. Kuei C, Yu J, Zhu J, Wu J, Zhang L, Shih A, Mirzadegan T, Lovenberg T, Liu C. Study of GPR81, the lactate receptor, from distant species identifies residues and motifs critical for GPR81 functions. Mol Pharmacol. 2011; 80.
262. Brown TP, Ganapathy V. Lactate/GPR81 signaling and proton motive force in cancer: Role in angiogenesis, immune escape, nutrition, and Warburg phenomenon. Pharmacology and Therapeutics. 2020.
263. Wallenius K, Thalén P, Björkman J-A, Johannesson P, Wiseman J, Böttcher G, Fjellström O, Oakes ND. Involvement of the metabolic sensor GPR81 in cardiovascular control. JCI Insight. 2017; 2.
264. Sun S, Li H, Chen J, Qian Q. Lactic acid: No longer an inert and end-product of glycolysis. Physiology. 2017.
265. Marbaniang C, Kma L. Dysregulation of glucose metabolism by oncogenes and tumor suppressors in cancer cells. Asian Pacific Journal of Cancer Prevention. 2018.
266. Wegiel B, Vuerich M, Daneshmandi S, Seth P. Metabolic switch in the tumor microenvironment determines immune responses to anti-cancer therapy. Frontiers in Oncology. 2018.
267. Warburg O. On the origin of cancer cells. Science (80-). 1956; 123.
268. Maldonado EN, Lemasters JJ. Warburg revisited: Regulation of mitochondrial metabolism by voltage-dependent anion channels in cancer cells. Journal of Pharmacology and Experimental Therapeutics. 2012.
269. Hanahan D, Weinberg RA. Hallmarks of cancer: The next generation. Cell. 2011.
270. Nieman KM, Kenny HA, Penicka C V., Ladanyi A, Buell-Gutbrod R, Zillhardt MR, Romero IL, Carey MS, Mills GB, Hotamisligil GS, Yamada SD, Peter ME, Gwin K, et al. Adipocytes promote ovarian cancer metastasis and provide energy for rapid tumor growth. Nat Med. 2011; 17.
271. Locasale JW, Grassian AR, Melman T, Lyssiotis CA, Mattaini KR, Bass AJ, Heffron G, Metallo CM, Muranen T, Sharfi H, Sasaki AT, Anastasiou D, Mullarky E, et al. Phosphoglycerate

dehydrogenase diverts glycolytic flux and contributes to oncogenesis. Nat Genet. 2011; 43.
272. Buzzai M, Bauer DE, Jones RG, DeBerardinis RJ, Hatzivassiliou G, Elstrom RL, Thompson CB. The glucose dependence of Akt-transformed cells can be reversed by pharmacologic activation of fatty acid β-oxidation. Oncogene. 2005; 24.
273. Plas DR, Thompson CB. Akt-dependent transformation: There is more to growth than just surviving. Oncogene. 2005.
274. Shim H, Dolde C, Lewis BC, Wu CS, Dang G, Jungmann RA, Dalla-Favera R, Dang C V. c-Myc transactivation of LDH-A: Implications for tumor metabolism and growth. Proc Natl Acad Sci U S A. 1997; 94.
275. San-Millán I, Brooks GA. Reexamining cancer metabolism: Lactate production for carcinogenesis could be the purpose and explanation of the Warburg Effect. Carcinogenesis. 2017.
276. DeBerardinis RJ, Lum JJ, Hatzivassiliou G, Thompson CB. The Biology of Cancer: Metabolic Reprogramming Fuels Cell Growth and Proliferation. Cell Metabolism. 2008.
277. Levine AJ, Puzio-Kuter AM. The control of the metabolic switch in cancers by oncogenes and tumor suppressor genes. Science. 2010.
278. Hirschhaeuser F, Sattler UGA, Mueller-Klieser W. Lactate: A metabolic key player in cancer. Cancer Research. 2011.
279. DeBerardinis RJ. Is cancer a disease of abnormal cellular metabolism? New angles on an old idea. Genetics in Medicine. 2008.
280. Xia AL, Xu Y, Lu XJ. Cancer immunotherapy: Challenges and clinical applications. Journal of Medical Genetics. 2019.
281. Zou W. Immunosuppressive networks in the tumour environment and their therapeutic relevance. Nature Reviews Cancer. 2005.
282. Rabinovich GA, Gabrilovich D, Sotomayor EM. Immunosuppressive strategies that are mediated by tumor cells. Annual Review of Immunology. 2007.
283. Romero-Garcia S, Moreno-Altamirano MMB, Prado-Garcia H, Sánchez-García FJ. Lactate contribution to the tumor microenvironment: Mechanisms, effects on immune cells and therapeutic relevance. Frontiers in Immunology. 2016.
284. Fischer K, Hoffmann P, Voelkl S, Meidenbauer N, Ammer J, Edinger M, Gottfried E, Schwarz S, Rothe G, Hoves S, Renner

K, Timischl B, Mackensen A, et al. Inhibitory effect of tumor cell-derived lactic acid on human T cells. Blood. 2007; 109.
285. Gottfried E, Kunz-Schughart LA, Ebner S, Mueller-Klieser W, Hoves S, Andreesen R, Mackensen A, Kreutz M. Tumor-derived lactic acid modulates dendritic cell activation and antigen expression. Blood. 2006; 107.
286. Puig-Kröger A, Muñiz-Pello O, Selgas R, Criado G, Bajo M-A, Sánchez-Tomero JA, Alvarez V, del Peso G, Sánchez-Mateos P, Holmes C, Faict D, López-Cabrera M, Madrenas J, et al. Peritoneal dialysis solutions inhibit the differentiation and maturation of human monocyte-derived dendritic cells: effect of lactate and glucose-degradation products. J Leukoc Biol. 2003; 73.
287. Harmon C, Robinson MW, Hand F, Almuaili D, Mentor K, Houlihan DD, Hoti E, Lynch L, Geoghegan J, O'Farrelly C. Lactate-mediated acidification of tumor microenvironment induces apoptosis of liver-resident NK cells in colorectal liver metastasis. Cancer Immunol Res. 2019; 7.
288. Kumar A, Pyaram K, Yarosz EL, Hong H, Lyssiotis CA, Giri S, Chang CH. Enhanced oxidative phosphorylation in NKT cells is essential for their survival and function. Proc Natl Acad Sci U S A. 2019; 116.
289. Nasi A, Fekete T, Krishnamurthy A, Snowden S, Rajnavölgyi E, Catrina AI, Wheelock CE, Vivar N, Rethi B. Dendritic Cell Reprogramming by Endogenously Produced Lactic Acid. J Immunol. 2013; 191.
290. Zhao S, Wu D, Wu P, Wang Z, Huang J, Gao JX. Serum IL-10 predicts worse outcome in cancer patients: A meta-analysis. PLoS One. 2015; 10.
291. Bronte V. Tumor cells hijack macrophages via lactic acid. Immunology and Cell Biology. 2014.
292. Annunziata M, Granata R, Ghigo E. The IGF system. Acta Diabetologica. 2011.
293. Brahmkhatri VP, Prasanna C, Atreya HS. Insulin-like growth factor system in cancer: Novel targeted therapies. BioMed Research International. 2015.
294. Laron Z. Insulin-like growth factor 1 (IGF-1): A growth hormone. J Clin Pathol - Mol Pathol. 2001; 54.
295. Boisclair YR, Rhoads RP, Ueki I, Wang J, Ooi GT. The acid-labile subunit (ALS) of the 150 kDa IGF-binding protein

complex: An important but forgotten component of the circulating IGF system. Journal of Endocrinology. 2001.
296. Li J, Choi E, Yu H, Bai X chen. Structural basis of the activation of type 1 insulin-like growth factor receptor. Nat Commun. 2019; 10.
297. Sun Y, Sun X, Shen B. Molecular Imaging of IGF-1R in Cancer. Molecular Imaging. 2017.
298. Gombos A, Metzger-Filho O, Lago LD, Awada-Hussein A. Clinical development of insulin-like growth factor receptor-1 (IGF-1R) inhibitors: At the crossroad? Investigational New Drugs. 2012.
299. Bach LA, Fu P, Yang Z. Insulin-like growth factor-binding protein-6 and cancer. Clinical Science. 2013.
300. Ding H, Wu T. Insulin-like growth factor binding proteins in autoimmune diseases. Frontiers in Endocrinology. 2018.
301. Bach LA. What happened to the IGF binding proteins? Endocrinology. 2018.
302. Allard JB, Duan C. IGF-binding proteins: Why do they exist and why are there so many? Frontiers in Endocrinology. 2018.
303. Firth SM, Baxter RC. Cellular actions of the insulin-like growth factor binding proteins. Endocrine Reviews. 2002.
304. Holly JMP, Biernacka K, Perks CM. Systemic metabolism, its regulators, and cancer: Past mistakes and future potential. Frontiers in Endocrinology. 2019.
305. Baxter RC. Inhibition of the insulin-like growth factor (IGF)-IGF-binding protein interaction. Hormone Research. 2001.
306. Duan C, Xu Q. Roles of insulin-like growth factor (IGF) binding proteins in regulating IGF actions. General and Comparative Endocrinology. 2005.
307. Mohan S, Baylink DJ. IGF-binding proteins are multifunctional and act via IGF-dependent and -independent mechanisms. J Endocrinol. 2002; 175.
308. Bach LA, Headey SJ, Norton RS. IGF-binding proteins - The pieces are falling into place. Trends in Endocrinology and Metabolism. 2005.
309. Bach LA. Current ideas on the biology of IGFBP-6: More than an IGF-II inhibitor? Growth Hormone and IGF Research. 2016.
310. Van Doorn J, Ringeling AM, Shmueli SS, Kuijpers MC, Hokken-

Koelega ACS, Van Buul-Offers SC, Jansen M. Circulating levels of human insulin-like growth factor binding protein- 6 (IGFBP-6) in health and disease as determined by radioimmunoassay. Clin Endocrinol (Oxf). 1999; 50.
311. Chandrashekaran IR, Yao S, Wang CC, Bansal PS, Alewood PF, Forbes BE, Wallace JC, Bach LA, Norton RS. The N-terminal subdomain of insulin-like growth factor (IGF) binding protein 6. Structure and interaction with IGFs. Biochemistry. 2007; 46.
312. Bach LA. Recent insights into the actions of IGFBP-6. J Cell Commun Signal. 2015; 9.
313. Jeon HJ, Park J, Shin JH, Chang MS. Insulin-like growth factor binding protein-6 released from human mesenchymal stem cells confers neuronal protection through IGF-1R-mediated signaling. Int J Mol Med. 2017; 40.
314. Oh YS, Kim EJ, Schaffer BS, Kang YH, Binderup L, MacDonald RG, Park JHY. Synthetic low-calcaemic vitamin D3 analogues inhibit secretion of insulin-like growth factor II and stimulate production of insulin-like growth factor-binding protein-6 in conjunction with growth suppression of HT-29 colon cancer cells. Mol Cell Endocrinol. 2001; 183.
315. Conese M, Pace L, Pignataro N, Catucci L, Ambrosi A, Di Gioia S, Tartaglia N, Liso A. Insulin-like growth factor binding protein 6 is secreted in extracellular vesicles upon hyperthermia and oxidative stress in dendritic cells but not in monocytes. Int J Mol Sci. 2020; 21.
316. Liso A, Capitanio N, Gerli R, Conese M. From fever to immunity: A new role for IGFBP-6? Journal of Cellular and Molecular Medicine. 2018.
317. Iosef C, Vilk G, Gkourasas T, Lee KJ, Chen BPC, Fu P, Bach LA, Lajoie G, Gupta MB, Li SSC, Han VK. Insulin-like growth factor binding protein-6 (IGFBP-6) interacts with DNA-end binding protein Ku80 to regulate cell fate. Cell Signal. 2010; 22.
318. Fell VL, Schild-Poulter C. The Ku heterodimer: Function in DNA repair and beyond. Mutation Research - Reviews in Mutation Research. 2015.
319. Fu P, Yang Z, Bach LA. Prohibitin-2 binding modulates insulin-like growth factor-binding protein-6 (IGFBP-6)-induced rhabdomyosarcoma cell migration. J Biol Chem. 2013; 288.

320. Mishra S, Ande SR, Nyomba BLG. The role of prohibitin in cell signaling. FEBS Journal. 2010.
321. Baxter RC. IGF binding proteins in cancer: Mechanistic and clinical insights. Nature Reviews Cancer. 2014.
322. Lee YJ, Shin KJ, Park SA, Park KS, Park S, Heo K, Seo YK, Noh DY, Ryu SH, Suh PG. G-protein-coupled receptor 81 promotes a malignant phenotype in breast cancer through angiogenic factor secretion. Oncotarget. 2016; 7.
323. Brown TP, Bhattacharjee P, Ramachandran S, Sivaprakasam S, Ristic B, Sikder MOF, Ganapathy V. The lactate receptor GPR81 promotes breast cancer growth via a paracrine mechanism involving antigen-presenting cells in the tumor microenvironment. Oncogene. 2020; 39.
324. Miranda-Gonçalves V, Honavar M, Pinheiro C, Martinho O, Pires MM, Pinheiro C, Cordeiro M, Bebiano G, Costa P, Palmeirim I, Reis RM, Baltazar F. Monocarboxylate transporters (MCTs) in gliomas: Expression and exploitation as therapeutic targets. Neuro Oncol. 2013; .
325. Froberg MK, Gerhart DZ, Enerson BE, Manivel C, Guzman-Paz M, Seacotte N, Drewes LR. Expression of monocarboxylate transporter MCT1 in normal and neoplastic human CNS tissues. Neuroreport. 2001; 12.
326. Zhao Y, Li M, Yao X, Fei Y, Lin Z, Li Z, Cai K, Zhao Y, Luo Z. HCAR1/MCT1 Regulates Tumor Ferroptosis through the Lactate-Mediated AMPK-SCD1 Activity and Its Therapeutic Implications. Cell Rep. 2020; 33.
327. Cormio A, Guerra F, Cormio G, Pesce V, Fracasso F, Loizzi V, Resta L, Putignano G, Cantatore P, Selvaggi LE, Gadaleta MN. Mitochondrial DNA content and mass increase in progression from normal to hyperplastic to cancer endometrium. BMC Res Notes. 2012; 5.
328. Lebleu VS, O'Connell JT, Gonzalez Herrera KN, Wikman H, Pantel K, Haigis MC, De Carvalho FM, Damascena A, Domingos Chinen LT, Rocha RM, Asara JM, Kalluri R. PGC-1α mediates mitochondrial biogenesis and oxidative phosphorylation in cancer cells to promote metastasis. Nat Cell Biol. 2014; 16.
329. Tian L, Cao W, Yue R, Yuan Y, Guo X, Qin D, Xing J, Wang X. Pretreatment with Tilianin improves mitochondrial energy metabolism and oxidative stress in rats with myocardial ischemia/reperfusion injury via AMPK/SIRT1/PGC-1 alpha

signaling pathway. J Pharmacol Sci. 2019; 139.
330. Rius-Pérez S, Torres-Cuevas I, Millán I, Ortega ÁL, Pérez S, Sandhu MA. PGC-1 α, Inflammation, and Oxidative Stress: An Integrative View in Metabolism. Oxid Med Cell Longev. 2020; 2020.
331. Brenmoehl J, Hoeflich A. Dual control of mitochondrial biogenesis by sirtuin 1 and sirtuin 3. Mitochondrion. 2013.
332. Li W, Wei Z, Liu Y, Li H, Ren R, Tang Y. Increased 18F-FDG uptake and expression of Glut1 in the EMT transformed breast cancer cells induced by TGF-β. Neoplasma. 2010; 57.
333. Li J, Dong L, Wei D, Wang X, Zhang S, Li H. Fatty acid synthase mediates the epithelial-mesenchymal transition of breast cancer cells. Int J Biol Sci. 2014; 10.
334. Jiang L, Xiao L, Sugiura H, Huang X, Ali A, Kuro-O M, DeBerardinis RJ, Boothman DA. Metabolic reprogramming during TGFβ1-induced epithelial-to-mesenchymal transition. Oncogene. 2015; 34.
335. Böhme I, Bosserhoff AK. Acidic tumor microenvironment in human melanoma. Pigment Cell and Melanoma Research. 2016.
336. Brandenburg S, Müller A, Turkowski K, Radev YT, Rot S, Schmidt C, Bungert AD, Acker G, Schorr A, Hippe A, Miller K, Heppner FL, Homey B, et al. Resident microglia rather than peripheral macrophages promote vascularization in brain tumors and are source of alternative pro-angiogenic factors. Acta Neuropathol. 2016; 131.
337. Beauchamp M-C, Yasmeen A, Knafo A, Gotlieb WH. Targeting Insulin and Insulin-Like Growth Factor Pathways in Epithelial Ovarian Cancer. J Oncol. 2010; 2010.
338. Oliva CR, Halloran B, Hjelmeland AB, Vazquez A, Bailey SM, Sarkaria JN, Griguer CE. IGFBP6 controls the expansion of chemoresistant glioblastoma through paracrine IGF2/IGF-1R signaling. Cell Commun Signal. 2018; 16.
339. Aboalola D, Han VKM. Insulin-Like Growth Factor Binding Protein-6 Promotes the Differentiation of Placental Mesenchymal Stem Cells into Skeletal Muscle Independent of Insulin-Like Growth Factor Receptor-1 and Insulin Receptor. Stem Cells Int. 2019; 2019.
340. Fu P, Thompson JA, Bach LA. Promotion of cancer cell migration: An insulin-like growth factor (IGF)-independent

action of IGF-binding protein-6. J Biol Chem. 2007; 282.
341. Fu P, Liang GJ, Khot SS, Phan R, Bach LA. Cross-talk between MAP kinase pathways is involved in IGF-independent, IGFBP-6-induced Rh30 rhabdomyosarcoma cell migration. J Cell Physiol. 2010; 224.
342. Yang Z, Bach LA. Differential effects of insulin-like growth factor binding protein-6 (IGFBP-6) on migration of two ovarian cancer cell lines. Front Endocrinol (Lausanne). 2014; 5.
343. Lauro C, Chece G, Monaco L, Antonangeli F, Peruzzi G, Rinaldo S, Paone A, Cutruzzolà F, Limatola C. Fractalkine Modulates Microglia Metabolism in Brain Ischemia. Front Cell Neurosci. 2019; 13.
344. Cherry JD, Olschowka JA, O'Banion MK. Neuroinflammation and M2 microglia: The good, the bad, and the inflamed. Journal of Neuroinflammation. 2014.
345. Mu X, Shi W, Xu Y, Xu C, Zhao T, Geng B, Yang J, Pan J, Hu S, Zhang C, Zhang J, Wang C, Shen J, et al. Tumor-derived lactate induces M2 macrophage polarization via the activation of the ERK/STAT3 signaling pathway in breast cancer. Cell Cycle. 2018; 17.
346. Allen E, Miéville P, Warren CM, Saghafinia S, Li L, Peng MW, Hanahan D. Metabolic Symbiosis Enables Adaptive Resistance to Anti-angiogenic Therapy that Is Dependent on mTOR Signaling. Cell Rep. 2016; 15.
347. Liu N, Luo J, Kuang D, Xu S, Duan Y, Xia Y, Wei Z, Xie X, Yin B, Chen F, Luo S, Liu H, Wang J, et al. Lactate inhibits ATP6V0d2 expression in tumor-associated macrophages to promote HIF-2α–mediated tumor progression. J Clin Invest. 2019; 129.
348. Cuasnicu PS, Bedford JM. The effect of moderate epididymal aging on the kinetics of the acrosome reaction and fertilizing ability of hamster spermatozoa. Biol Reprod. 1989; 40.
349. Zhang A, Xu Y, Xu H, Ren J, Meng T, Ni Y, Zhu Q, Zhang WB, Pan YB, Jin J, Bi Y, Wu ZB, Lin S, et al. Lactate-induced M2 polarization of tumor-associated macrophages promotes the invasion of pituitary adenoma by secreting CCL17. Theranostics. 2021; 11.
350. Clemmons DR. Modifying IGF1 activity: An approach to treat endocrine disorders, atherosclerosis and cancer. Nature Reviews Drug Discovery. 2007.

351. Chesik D, Glazenburg K, Wilczak N, Geeraedts F, De Keyser J. Insulin-like growth factor binding protein-1-6 expression in activated microglia. Neuroreport. 2004; 15.
352. Alunno A, Bistoni O, Manetti M, Cafaro G, Valentini V, Bartoloni E, Gerli R, Liso A. Insulin-like growth factor binding protein 6 in rheumatoid arthritis: A possible novel chemotactic factor? Front Immunol. 2017; 8.
353. Gonzalez MM. The insulin-like growth factor-binding protein (IGFBP) family and its role in obesity and cancer. Biomed J Sci Tech Res. 2019; 13.